DIAGENETIC CHANGES IN A CAMBRIAN SHALE AS A FUNCTION OF BURIAL DEPTH

A THESIS

Presented to

The Faculty of the Division of Graduate Studies

by

Bradley Robert Broekstra

In Partial Fulfillment

of the Requirements for the Degree

Master of Science in Geophysical Sciences

Georgia Institute of Technology

March, 1978

DIAGENETIC CHANGES IN A CAMBRIAN
SHALE AS A FUNCTION OF BURIAL DEPTH

Approved:

C. E. Weaver, Chairman

J. M. Wampler

E. V. Eslinger

Date approved by Chairman 4/17/78

ACKNOWLEDGEMENTS

I would like to thank my thesis advisor Dr. Weaver for proposing the initial topic, and for the many suggestions that he has made during the research and writing of this thesis. Suggestions and comments from Dr. Wampler and Dr. Eslinger are also appreciated. Dr. Wampler also deserves special note for helping to repair the many mechanical failures which occurred during research procedures. Dr. Pollard was very helpful in his suggestions concerning the petrography and the photography which have gone into the thesis. Dianne Clark deserves special thanks for the innumerable help which she has given me during my stay here at Tech.

All of my friends who have helped me while at Tech are too numerous to mention but special thanks are devoted to Bob Sedivy and Bill Volz for helping with the computer program, to Jack Carpenter who helped out with size fractionations, to Mike Fridell who helped supply maps and information about northwest Georgia, and to Gary Cooke who gave me many suggestions in the initial phases of the thesis.

A special space must be reserved to thank Nick VerHey for proof reading, and helping me keep my sanity during times of personal problems.

This thesis is dedicated to my mother and father who have loved and supported me from the beginning.

TABLE OF CONTENTS

LIST OF TABLES

LIST OF TABLES (Continued)

LIST OF ILLUSTRATIONS

LIST OF ILLUSTRATIONS (Continued)

LIST OF ILLUSTRATIONS (Continued)

LIST OF ILLUSTRATIONS (Continued)

LIST OF ILLUSTRATIONS (Continued)

SUMMARY

Samples of the Conasauga Shale were collected in Northwest Georgia, Alabama, and Tennessee. Several size fractions were studied in order to obtain a better understanding of burial diagenesis. Stratigraphic thicknesses are much greater in the southeastern Valley and Ridge Province than in Alabama, extreme north Georgia, and Tennessee. Thicknesses range from a few thousand meters to greater than 10,000 meters.

Minerals present in the Conasauga Shale are illite, mixed-layer illite-montmorillonite, chlorite, kaolinite, paragonite, quartz, Na-feldspar, K-feldspar, calcite, and dolomite. The presence and abundance of these minerals are geographically, and diagenitically related. Illite abundance decreases with increasing grain size yielding to chlorite and sometimes kaolinite. Mixed-layer material increases with decreasing grain size, and is considerably more abundant in western, and northern areas. K_2O percentages decrease with increased mixed-layer material, and also increase with increased illite content.

Paragonite is only present in samples very close to the Cartersville Fault. Paragonite bearing samples contain larger percentages of Na_2O in the finer fractions. Sodium from Na-feldspars in larger size fractions migrate to the smaller fractions, and is utilized in the formation of paragonite. High stress created during the thrust movement of the Cartersville Fault is the critical factor in the formation of paragonite, although these samples are not the ones which have undergone the greatest diagenetic changes.

The amount of 1 Md illite decreases and the percentage of 2M illite increases with increasing grain size and depth of burial.

Sharpness ratios increase with increasing grain size, and decrease with increasing distance from OW1 (maximum depth of burial). Samples in the southeastern portion of the Valley and Ridge in Georgia fit into the category of low-grade metamorphism proposed by Weaver (1961), and the category of metagenesis or anchizone proposed by Foscolas and Stott (1975). Samples in extreme northwestern Georgia and in Alabama, and Tennessee fall into categories of early, middle, and late diagenesis.

Crystallinity indices decrease with increasing grain size. Values increase from southeast to north and west. Mean crystallinity indices from Tennessee are considerably larger than those from Georgia. Weight percentages of the <.2μm, and .2-2μm fractions increase from southeast to north and west. Weight percentage of the 2-44μm fraction decrease slightly from southeast to north and west.

Illite reflection intensity ratios (002/001) increase from north and west towards the southeast in the <.2μm and .2-2μm fractions but remain fairly constant in the 2-44μm fraction. The ratio increase is due to a decrease in Fe and/or increase in K.

Thin section studies indicate mineral foliation increases towards the southeast. The clay flakes show less preferred orientation in the northern samples.

The depth of burial of the Conasauga shale increases towards the southeast. Correlation coefficient values indicate most of the measured mineral parameters change systematically with distance from the area of maximum burial.

The parameters which best reflect the increase in depth of burial (temperature) are: sharpness ratios, crystallinity indices, 2m polymorph percentages, and size fraction percentages.

CHAPTER I

INTRODUCTION

Weaver (1961a) postulated that the sharpness ratio of illite (001) showed a good correspondence between the degree of metamorphism determined by X-ray diffraction and the degree of metamorphism determined by petrographical evidence. Kubler (1966) used a crystallinity index to prove similar trends in the degree of diagenesis in argillaceous sediments. Several other authors (Dunoyer De Segonac, 1970; Frey, 1970; Gavish and Reynolds, 1970; Weber, 1972; Foscolos and Kodama, 1973; Foscolos and Stott, 1975; and Gill *et al.*, 1977) have used these methods to help resolve diagenetic histories of Paleozoic and younger sediments. Other parameters such as polymorphic structures of dioctahedral micas (Velde and Hower, 1963; Maxwell and Hower, 1967; and van Moort, 1971), mineralogical and chemical changes (Burst, 1959, 1969; Reynolds and Hower, 1970; Weaver and Wampler, 1970; Weaver *et al.*, 1971; and Hower *et al.*, 1976), and the intensity ratio (002/001) of illite basal reflections (Frey, 1970, and Gill *et al.*, 1977) have similarly been used to help define burial diagenesis.

In this study all of the previously mentioned parameters have been utilized, plus others including relative grain size percentages and petrographic evidence, to show diagenetic effects which have occurred since sediment deposition. In order to obtain a better understanding of the diagenetic changes and to develop criteria that can

be used to estimate burial temperatures, samples were fractionated into several size ranges: <.2μm, .2-2μm, ≤2μm, ≤4μm, and 2-44μm.

Formerly, diagenetic trends have been studied by examining samples at different depth intervals in cores, or by using a variety of formations having different lithologic characteristics over an extensive area. In this case a single formation was selected for study which had been buried to maximum depths ranging from a few thousand meters, to nearly 10,000 meters. The formation selected for study was the middle to Upper Cambrian Conasauga Shale from the Southern Appalachian Basin.

Different depositional or environmental trends in the Southern Appalachians produced unexpected results which made it desirable to split the thesis area into two sections; specifically a Georgia-Alabama area, and a Tennessee area.

CHAPTER II

GEOLOGIC SETTING

The thesis area includes northwestern Georgia, eastern Alabama, and the East Tennessee Valley. The Conasauga formation outcrops extensively in the Valley and Ridge Province of these three states extending from the Cartersville Fault (Great Smoky Fault in Tennessee) to the eastern boundary of the Cumberland Plateau. The Cartersville Thrust Fault separates the Piedmont, comprised of meta-igneous and meta-sedimentary rocks, from unmetamorphosed Paleozoic sediments in the Valley and Ridge.

There are two main thrust faults which cut the Valley and Ridge Province in Georgia, namely the previously mentioned Cartersville Fault, and the Rome Fault. Butts and Gildersleeve (1948) suggested the Cartersville Fault is a result of the thrusting of low-grade metamorphic rocks of the Talladega belt northwest at least 24 km (15 miles) over unmetamorphosed rocks of the Valley and Ridge. The Rome Fault divides the Valley and Ridge into two distinct parts (Chowns, 1977). Northwest of the fault the rocks are mainly of Ordovician to Pennsylvanian age. Resistant sandstones in the Silurian and Pennsylvanian systems give rise to linear ridges which trend northeast-southwest. These ridges are separated by valleys underlain by limestones of Middle Ordovician and Mississippian age. South and East of the Rome Thrust Fault, outcrops are comprised largely of Cambrian and Ordovician limestones and shales.

Resistant ridge formers in this section are dolomite and limestones of the Knox and Conasauga Formations.

> "Silurian through Pennsylvanian rocks are absent in this locale; Mississippian and Pennsylvanian systems have been removed from the top of the section, and the Silurian was either never deposited or removed prior to Devonian times" (Chowns, 1977, p. 1).

Figure 1 shows Conasauga outcrop locales. The source of the sediments that fill the Appalachian Basin has been disputed for a long time. Petrographical and paleocurrent evidence suggests that sediments younger than Cambrian age were derived from an eastern source (Colton, 1970); although both southeastern and northeastern (Hadley and Goldsmith, 1963) sources have been suggested.

The Paleozoic column in the Appalachian Basin is remarkably complete from Cambrian to lower Permian (Table 1). Sediment thicknesses increase towards the southeast (Fisher, et al. ed., 1970; Epstein, et al., 1976). A shallow northwest transgressing Cambrian sea is believed to have deposited the Conasauga Formation. Conasauga sediments are in a wedge shaped mass, and are thicker along eastern basin boundaries where rocks are predominantly older, than along the western boundary where rocks are progressively younger. In the Conasauga Formation, shales are more abundant in the eastern part of the basin. The limestone content generally increases to the west.

Three primary shale and limestone members comprise the Conasauga Formation. In Georgia and Alabama, the limestones and shales are differentiated into lower, middle, and upper units. In Tennessee the Conasauga formation is differentiated into the Maryville, and

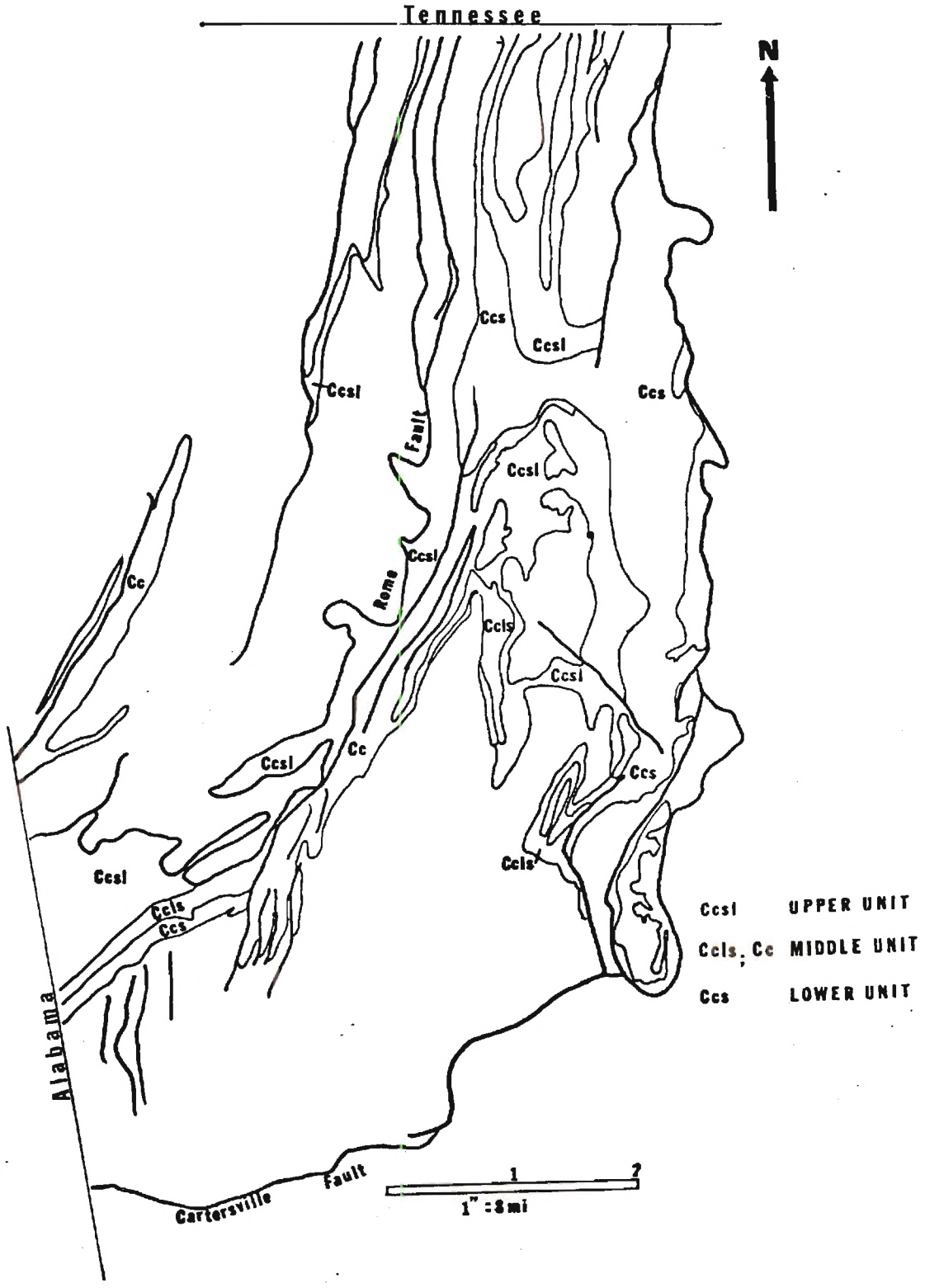

Figure 1. Location of Conasauga Formation Outcrops in Northwestern Georgia.

Table 1. Stratigraphy of the Valley and Ridge Province (From G.G.S. Guidebook #11, Chowns 1972).

System	Stratigraphic Units	Sedimentary Environments
Pennsylvanian	Crab Orchard Mountains Fm.	Humid, terrigeneous, tidal marsh, lagoon and barrier island sediments
	Grizzard Fm.	
Mississippian	Pennington Fm. Bangor Limestone Hartselle Fm. Monteagle Limestone Tuscumbia Limestone Fort Payne Fm.	Shallow marine shell and semi-arid tidal flat carbonates with pro-molasse terrigeneous wedges
		Arid tidal flat, carbonate deposits passing upwards into shallow marine shelf carbonate sediments. Terrigeneous promolasse sediments to the south and east.
Devonian	Chattanooga Shale	Terrigeneous shallow, euxinic sea.
Silurian	Red Mountain Fm.	Terrigeneous, promolasse slope and platform deposits with barrier islands and lagoons.
Ordovician	Sequatichie Fm. Chickamauga Limestone	Shallow marine carbonates passing eastwards into terrigeneous tidal flat and alluvial deposits (molasse facies).
Cambro-Ordovician	Knox Group	Shallow marine and tidal flat carbonates.

Table 1 (Continued)

System	Stratigraphic Units	Sedimentary Environments
Cambrian	Conasauga, Rome, Shady, and Weisner Fms.	Terrigeneous wedges, and shallow marine carbonates.

Maynardville Limestones, and the Pumpkin Valley, Rogersville, and Nolichucky Shales.

Typical lithologic descriptions of the Conasauga in Georgia described by Butts and Gildersleeve (1948), Cressler (1970, 1974), and Chowns (1977), are as follows:

Lower dolostone unit: Thin-to-massive bedded, light-to-medium-gray dolostone, commonly with distinctive reddened bedding and joint surfaces. Locally oolitic and cherty. Weathers to produce a siliceous residuum with many hard gray fragments of jasperoid. Possibly equivalent to the Honaker Dolomite of Tennessee (Chowns, 1977).

Lower shale unit: Light green, olive-green, and silver-gray when fresh with local limestone lenses. It contains some silty lenses, and weathers to a pale pinkish red. The lower unit is probably equivalent to either the Pumpkin Valley or Rogersville Shale in Tennessee.

Middle limestone unit: Massive, blue-gray limestone with irregular layers of silty dolostone.

Middle shale unit: Light green to olive-green, and yellowish clay shale containing thin layers and lenses of blue limestone. Some silty layers are also present, and it usually weathers to an orange-yellow color.

Upper carbonate unit: Thinly to massively bedded dolostone, interbedded with clayey limestone. Contains abundant black chert beds, and nodules at the top, which are quite distinct from the light gray cherts derived from the overlying Knox Group. Unit is probably equivalent to the Maynardville Limestone of Tennessee.

Upper shale unit: Consists of olive-green, and gray shales interbedded with thin layers of limestone and calcareous siltstone. "Further to the

west it has a dominant lithology of dark olive-gray, somewhat silty, shale containing abundant mica flakes" (Cressler, 1970).

CHAPTER III

METHODS, PROCEDURES, AND INSTRUMENTATION

Field Methods

Accuracy of results from data obtained required that fresh samples be collected. This was done whenever possible, but in some instances weathered samples were the only ones available. If this was the case data components affected by weathering, such as chlorite contents, were omitted from final results. The general practice was to collect samples from quarries, well cuttings, cores, and fresh road cuts. Sample locations for Georgia-Alabama, and Tennessee are shown in Figures 2 and 3. Sample descriptions are in the Appendix.

References and geological maps consulted were those of Butts and Gildersleeve (1948); Cressler (1964, 1970, 1974); and Pickering et al. (1976). In Cressler's descriptions of the geology and ground-water resources of various counties in Northwest Georgia, he listed locations of existing and previously worked mines and quarries in the Conasauga Shale and Limestone Formations. These were very helpful, and provided starting points for many collecting trips. Conversations with Northwest Georgia natives aided in finding a few old quarries and open pits. Many samples were located by the seek-and-find method of driving perpendicular to or along strike until a spot was found where the rocks were fresh, and the dogs were tied. Only in-situ samples were collected to be sure of exact locations. Samples were tagged,

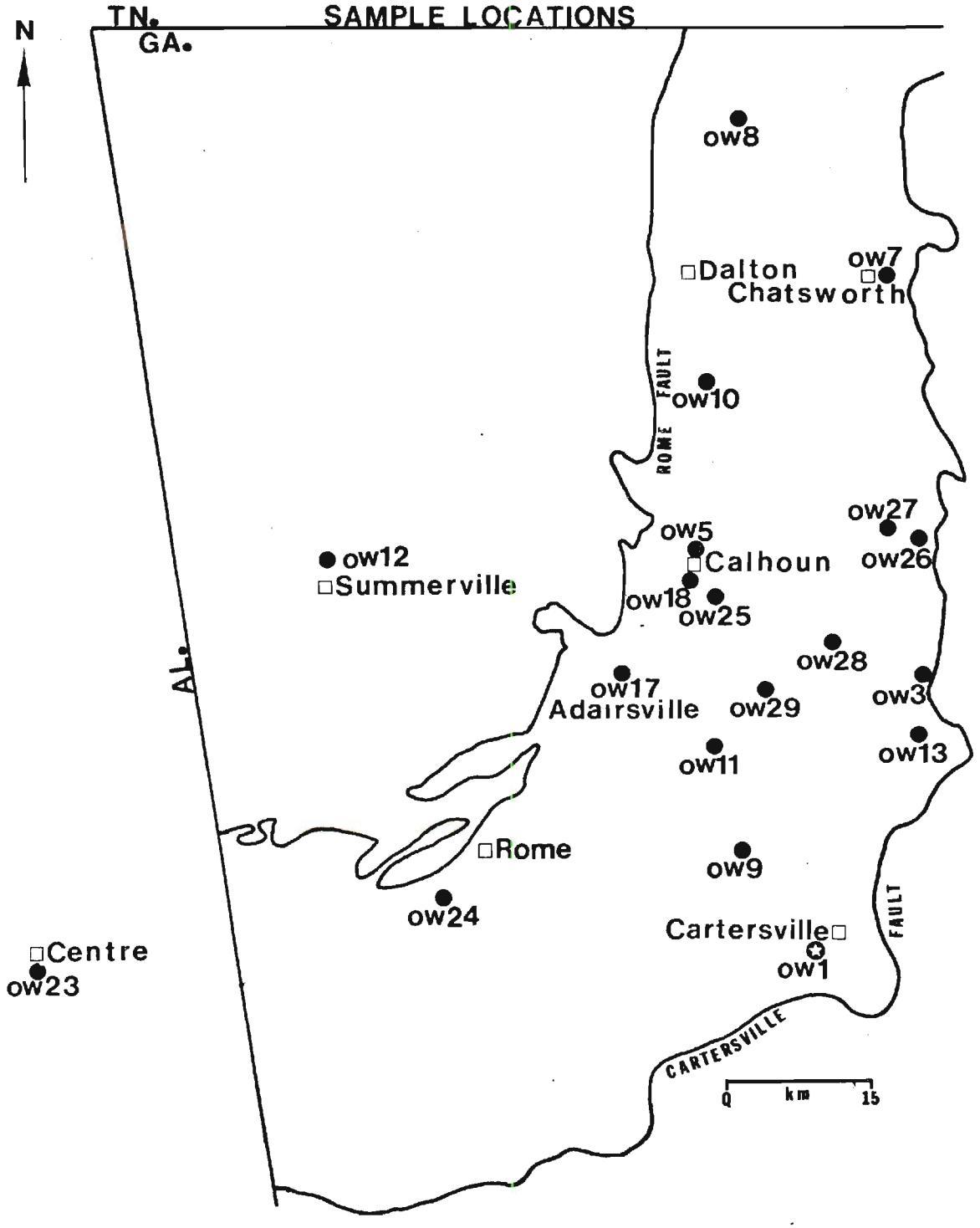

Figure 2. Sample Locations in Northwest Georgia, and Eastern Alabama.

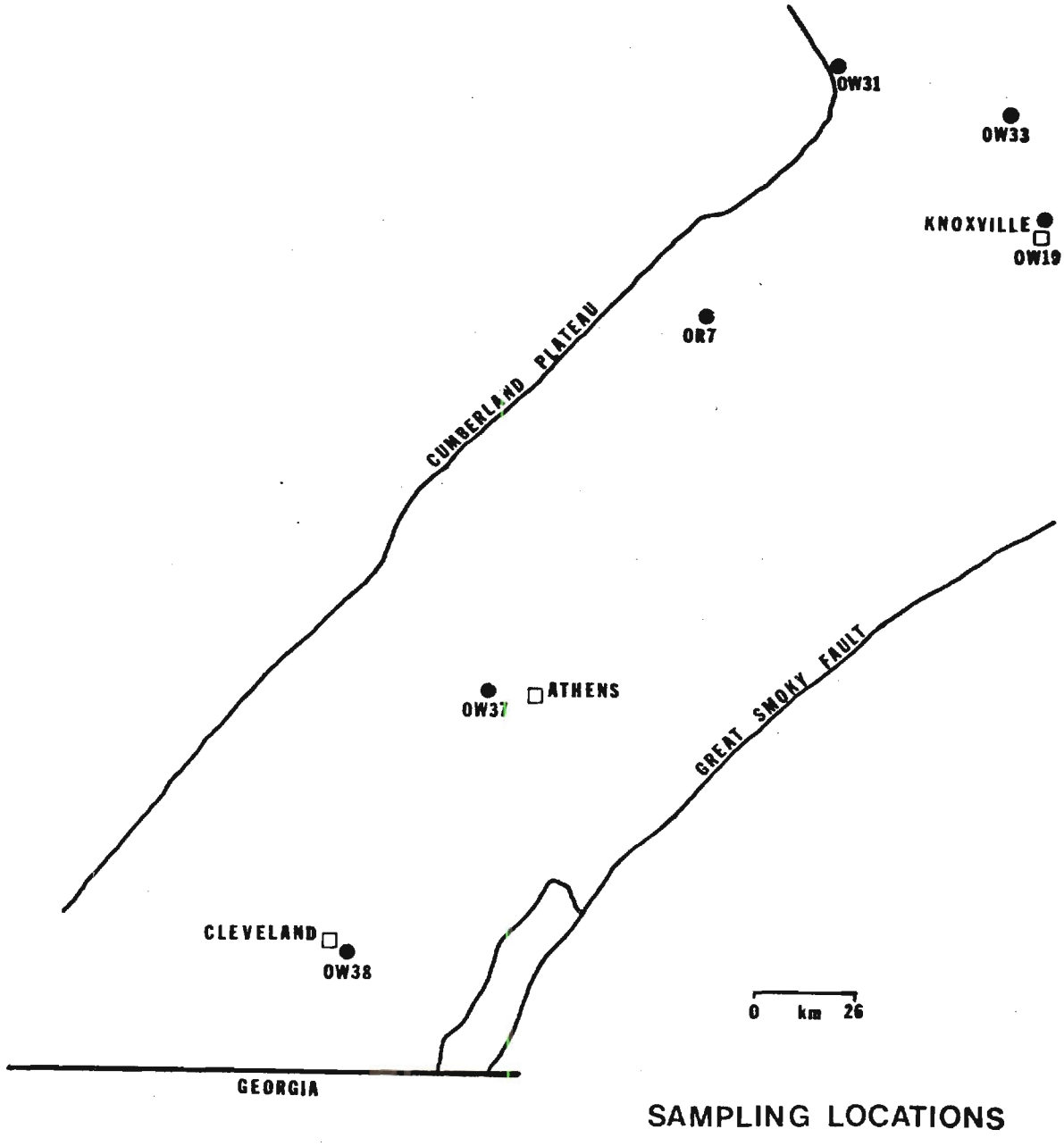

Figure 3. Sample Locations in Tennessee.

identified, described, and placed in zip-lock bags.

Well cuttings were located by asking water well drillers if they had recently drilled a well in a specific area in which samples were needed. Some samples from the Knoxville, Tennessee area were donated by the Tennessee Valley Authority, and the Tennessee Highway Department. In all, 18 samples were gathered from Northwest Georgia, 6 from Tennessee, and 1 from Alabama.

Laboratory Procedures

Preparations for grain size separations included washing samples to remove any extraneous materials, and drying them in a Thelco Precision Model 26 Oven at 110^{o}C for 1 hour. Samples were ground in a Lemaire Instrument Model 150 Jaw Crusher which dissagregated samples into small pea-sized pellets. Pellets were then run through a pulverizer which ground the shale down into a powdered form. If further grinding was necessary it was done with a mortar and pestle using short circular motions. The reason for such severity in grinding procedures was the extreme degree of lithification and cementation present in the Conasauga samples. It is possible that suspicions were aroused to see if grinding procedures mechanically broke down larger mineral grains into smaller ones. The author believes that this was not the case because quartz and feldspar were omnipresent in whole rock samples, but never present in the <.2μm fraction. If mechanical breakdown of grains had occured it would be expected that very small pieces of quartz and feldspar would appear in the fine fraction.

Ground samples were placed on a 230 mesh (63μm) sieve and

and mechanically shaken causing grains smaller than 63μm to fall through sieve openings and into a collecting pan. Approximately 40 grams from the pan were extracted and weighed precisely on a Mettler H15 analytical balance. Grains were placed in a 400 ml beaker with 250 ml of distilled water (DH_2O) and sonified with a Bronwill Biosonic Ultrasonifier for 2 minutes. Clay slurries were wet sieved through a 325 mesh (44μm) screen into a 1 liter beaker. Sonification and wet sieving were repeated until liquids passing through the screen were clear. That portion of the sample remaining on the 44μm sieve was poured off into a pre-weighed beaker, and placed in the oven at 110°C to dry. The >44μm suspension was poured into eight (50 ml polypropylene) centrifuge tubes and spun at 1000 RPM for 3 minutes on an International Centrifuge Model UV with a #240 rotor, which removed from suspension everything larger than 2μm. Centrifugation methods are based on Stoke's Law of gravitational settling and particle sizes are equivalent spherical diameters for quartz. The Supernate was decanted and saved while the remaining settled solid was resuspended in DH_2O using the ultrasonifer and recentrifuged. This procedure was repeated 8-10 times, or until the remaining supernate was relatively clear. The settled solid was removed, dryed, and labelled 2-44μm fraction.

Repeated centrifugation of <2μm suspensions at 3000 RPM for 32 minutes separated .2-2μm fractions from all material <.2μm. Remaining suspension containing the <.2μm fraction were spun at 15,000 RPM for 60 minutes on a Sorvall high speed centrifuge (SS3 with SS34 head). The solid collected was dryed at 110°C, and weighed along with the previously described fractions.

If carbonate was detected in any size fraction of a sample, a portion of that fraction was repeatedly treated with 0.1N HCl until all carbonate was destroyed. Because of the low normality of HCl used in this procedure no deterioration or degradation of silicate mineral grains appears to have occurred. HCl treated samples were rinsed with DH_2O twice and dried at 110°C.

Oriented samples were prepared by suspending 0.1 gm of sample in 4 ml of 2% calgon dispersant solution in small glass vials. Suspensions were sonified to redisperse any aggregates which might have formed during drying. An eye dropper was used to cover (9.7 cm^2) glass slides with the slurries. Slides were covered so no dust contamination would occur, and were allowed to air dry for 10-12 hours. Natural sedimentation of grains in this manner promotes preferred orientation of the C-axis in platy minerals which produces well developed basal reflections (001) in X-ray diffraction patterns. X-rays were produced on a Philips X-ray Diffractometer Model 72A using CuKα radiation with a scan speed of 1° 2θ/min, chart speed of 0.6 cm/min. (¼ in/min.), using 45 Kilovolts, 20 Milliamperes, a time constant of 2 seconds, and a window slit of 2.5 mm. All X-ray patterns were scanned from 2° to 40° which encompasses all major clay mineral peaks. In order to determine the degree of mixed layering present, samples were treated with ethylene glycol for 12-24 hours and then x-rayed from 2° to 20° 2θ immediately after removal from the glycol tub. The position of the $(001)_{10}/(002)_{17}$ peak was checked for evidence of mixed layering (Perry and Hower, 1970). The samples were then heated at 300°C for 1.5 hours and again x-rayed from 2° to 20° to check for the amount of expanded layers which had reverted back to

10 Å. This was done for the <.2μm, .2-2μm and 2-44μm fractions.

The relative amounts of the dioctahedral illite polytypes were determined using the method of Maxwell and Hower (1967). Portions of size fractions (<.2μm and .2-2μm) were boiled in 2N HCl for 30 minutes, rinsed with 2% $NaCO_3$ twince, and rinsed with DH_2O twice to remove chlorite and biotite. Both minerals are soluble in HCl, and hence interference can be avoided when determining illite polymorphic structures. To procure unoriented specimens for mineral polytype indentification, Aℓ cavity powder packs were made. (C. E. Weaver, personal communication).

Percentages of the 2m polymorph were determined from the curve constructed by Maxwell and Hower (1967), which uses the ratio of the area under the unique 2M 2.80 Å peak ($11\bar{6}$) and the 2.58 Å peak which includes the 2M ($13\bar{1}$), (116), ($20\bar{2}$) reflections and the 1M and 1Md ($13\bar{1}$) and (130) reflections (Figure 4).

The crystallinity index of the illite (001) was determined using the method of Kubler (1966) which is a measurement of the width of the illite (001) peak in mm at half height above background level (Figure 5). Weaver's sharpness ratio (1961a) is defined as the ratio of the height of the (001) illite peak at 10 Å to the height at 10.5 Å (Figure 6). Two phenomena affect both of these measurements. The width at half-height of a symmetric peak decreases with increasing crystallite size and the assymetry of a peak decreases with decreasing montmorillanite layers. During burial metamorphism the expected trend would be both an increase in crystallite size and a decrease in montmorillanite layers. Therefore the numbers representing crystallinity index should decrease and the numbers representing sharpness ratio should increase with increasing

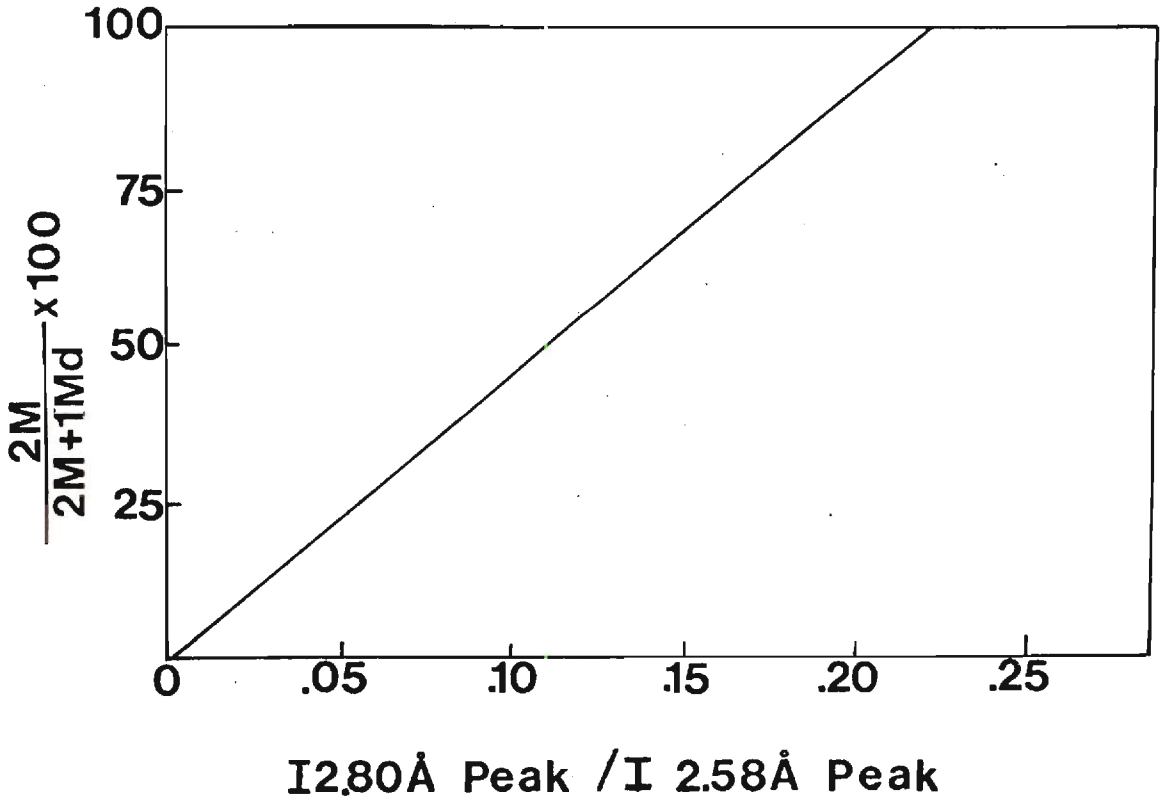

Figure 4. Curve for Determination of Percent 2m Dioctahedral Mica (Maxwell and Hower, 1967).

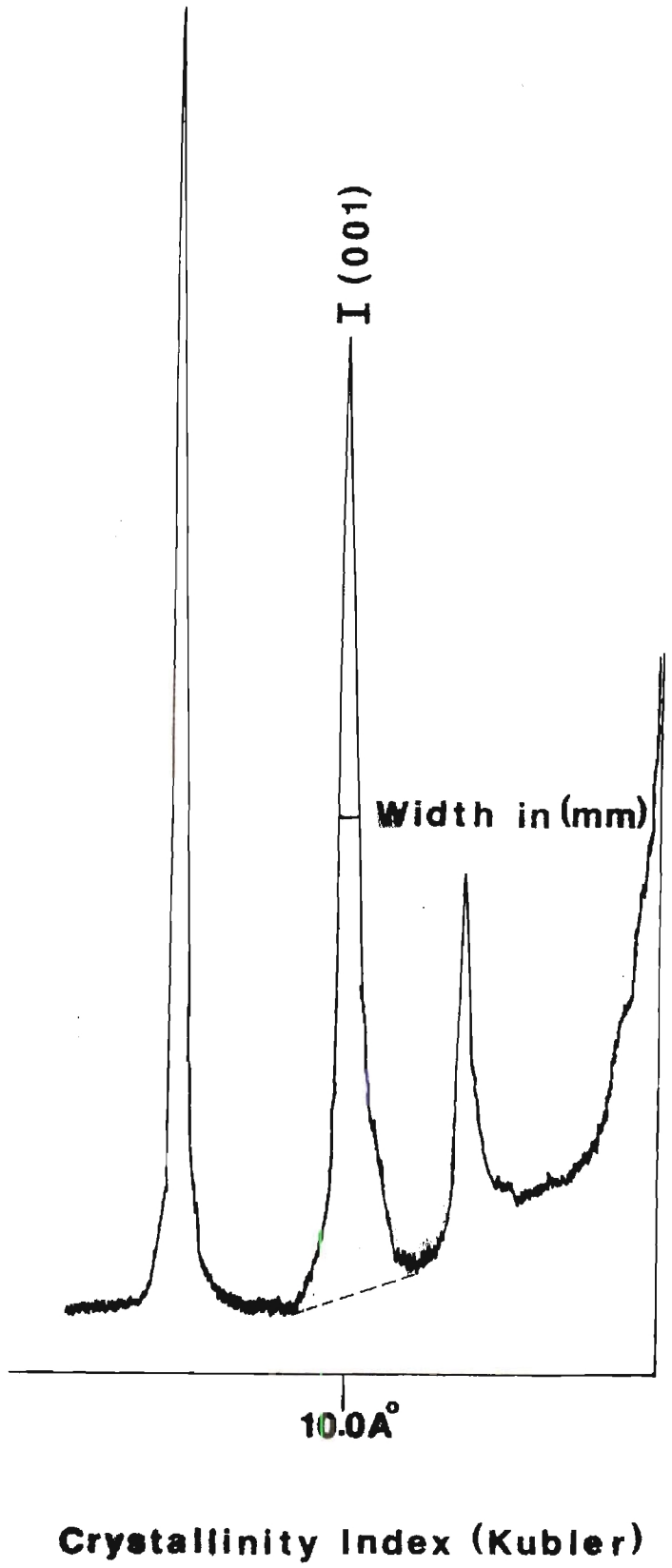

Figure 5. Determination of Crystallinity Index (Kubler, 1966).

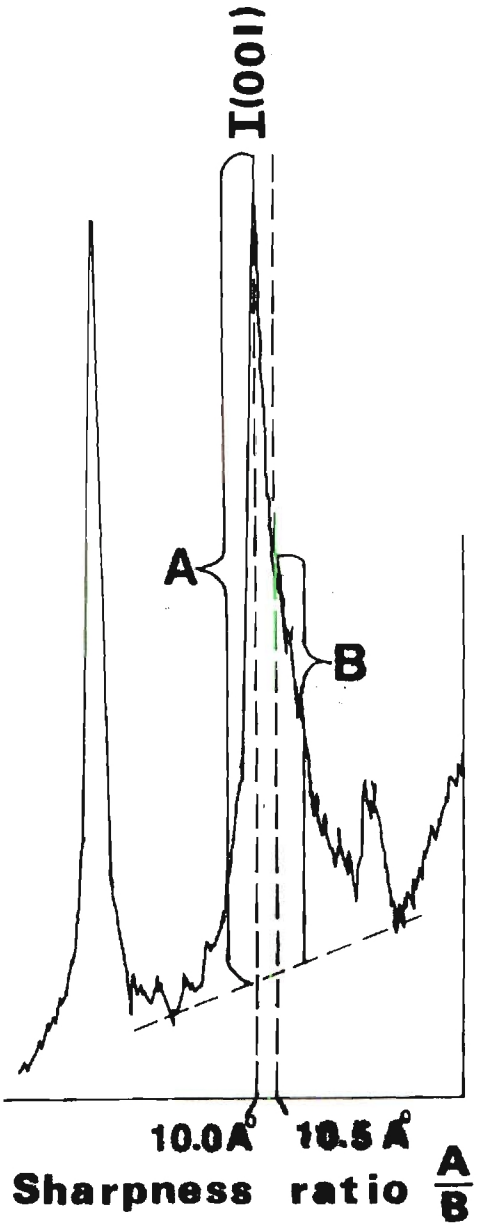

Figure 6. Determination of Sharpness Ratio (Weaver, 1961a).

metamorphic grade.

Percentages of discrete illite, kaolinite, and chlorite were detected by measuring (001) illite and the 12.2 Å (002) chlorite + (001) kaolinite peak intensities of oriented slides in mm, and dividing them by experimentally determined values of 1 for illite, and 2.5 for chlorite and kaolinite (C. E. Weaver, personal communication). Chlorite was distinguished from kaolinite by measuring the (002) kaolinite and (004) chlorite peaks which occur at 3.57 Å , and 3.55 Å respectively and transposing that ratio to the (001) kaolinite and (002) chlorite peak to obtain a semi-quantitative percentage.

The amounts of mixed-layer material present were determined by measuring the 10 Å peak height of the glycolated samples and subtracting that number from the 10 Å peak height of the heated samples. The difference divided by the heated peak height represents the percentage of mixed-layered material contracted down to 10 Å (C. E. Weaver, personal communication).

Petrographic slides were studied using a Carl Zeiss petrographic microscope. Slides were prepared by D. M. Organist Petrographic Laboratory (Newark, DE 19711).

K_2O percentages were determined by Bob Sedivy, using the following technique: A known weight of each shale fraction was dissolved in an 80% hydrofluoric-20% perchloric acid mixture and evaporated to dryness. The residual salts obtained from each solution were then redissolved in a 4% nitric acid solution and the resulting solution was then analyzed for K using atomic absorption spectrophotometry (R. Sedivy, personal communication).

Na_2O percentages were also determined using atomic absorption spectrophotometry. Samples were prepared by the $LiBO_2$ fusion method which consists of placing 0.7 grams of $LiBO_2$ and 0.1 grams of sample in a graphite crucible and heating it at 920°C for 30 minutes. After heating the fused pellet was placed in 100 ml of 5% HNO_3 solution and mechanically stirred for 10 minutes. This solution was then analyzed for Na using U.S.G.S. standards. Samples were compared to a cumulative percentage curve in order to obtain semi-quantitative results.

A computer program was used (with the help of R. Sedivy) to calculate the equation of the least squares line (E.L.S.L.) and a correlation coefficient (C.C.) to search for correlations among the measurements obtained from each of the different size fractions. A table giving the (E.L.S.L.) and (C.C.) of useful correlations found in this study is in the Appendix. Parameters were compared to each other (i.e. % K_2O content vs. % illite) and to distance from reference point OW1 (i.e. distance vs. crystallinity index).

CHAPTER IV

DISCUSSION

Mineralogy

Non-Clay Minerals

The Conasauga Shale contains relatively few accessory non-clay minerals in the <44μm fraction. Quartz is present in all samples, and abundance increases with increasing grain size. Sodium plagioclase, like most other accessory minerals (other than paragonite) is not present in the fine fractions (<.2μm) and is most abundant in the 2-44μm fractions. Potassium feldspar is present in all samples though it is more abundant in the samples from Tennessee than in the samples from Georgia. The sample from Alabama contains only a trace amount of K-feldspar. The reason that K-feldspar is less abundant in the samples from Georgia is probably related to dissolution of K-feldspar during diagenesis (Weaver and Wampler, 197). Hower et al. (1976) have shown that in Gulf Coast sediments K-feldspar, but not Na-plagioclas, disappears at depth and that the K is fixed by illite-montmorillonite mixed-layer clays. Samples from Georgia have been buried more deeply than the samples from Tennessee. Petrographic evidence indicates the presence of muscovite and biotite in some of the northern and western samples. Calcite and dolomite are found in the middle and upper shale and limestone units in Georgia and Alabama, and in all samples from Tennessee.

Clay Minerals

Illite and chlorite are found in all samples. Discrete illite

represents the bulk of the clay mineral fraction in most samples though some contain abundant mixed-layer clays. Illite is predominant in the fine fraction, but decreases in abundance with increasing grain size. Chlorite is the most abundant clay mineral in some of the coarser size fractions (Tables 4 and 7). The relative amounts of the 1 Md, 1M and 2M polymorphic structures of illite vary with depth of burial. These trends will be discussed in detail later in the thesis.

Chlorite is not always present in the <.2μm fraction. It generally decreases in abundance with decreasing grain size. The ratio of peak heights (10 Å/7 Å) is a good indicator of the change in illite and chlorite if no kaolinite is present. Figure 7 shows how the ratio changes as a function of grain size. Interference by peaks from illite and feldspars prevented observations of chlorite polymorphic structures.

Kaolinite is present only in the Tennessee samples. Dunoyer de Segonzac (1970, p. 285) suggested that

> "under certain geochemical conditions kaolinite will become unstable, and even though these factors are not strictly related to regular gradients of temperature and pressure, kaolinite does have a limit of stability which will be reached during some phase of diagenesis".

Kaolinite disappears at depth in the Gulf Coast Sediments (Hower, et al. 1976) and may be absent from the Georgia samples of this study because it has been destroyed during diagenesis. However, since no kaolinite is present in the Alabama sample, which possibly has undergone less diagenetic changes than those in Tennessee, it may be that the presence or absence of kaolinite is merely a function of source area and not burial diagenesis.

Mixed-layer clays are more abundant in the <.2μm fraction and

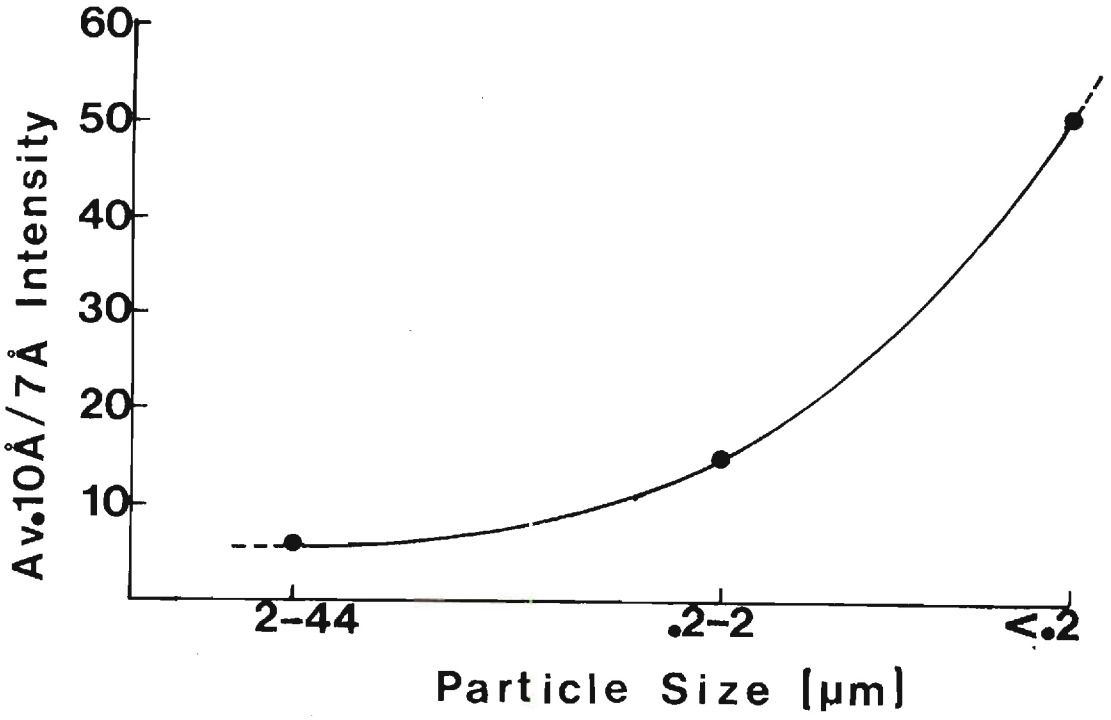

Figure 7. Increase in Mean 10 Å/7 Å Intensity Ratio with Particle Size. No Kaolinite is Present in the Samples.

decrease with increasing grain size (Figure 8). This trend is more prominent in the Georgia-Alabama samples than the Tennessee samples. The percentages of mixed-layer clay increase towards the western and northern boundaries of the thesis area in Georgia and Alabama and show a fairly good trend in the abundance of mixed-layer clays (Figures 9, 10 and 11). Figures 10 and 11 are graphic representations of the amount of mixed-layer material plotted against distance from the OW1 reference point. The choice of sample OW1 is somewhat arbitrary. It was chosen because the illite has the best crystallinity values and because of its location. Stratigraphic data from the literature suggests that sediment thicknesses of the Conasauga and overlying formations increase to the southeast toward a maximum overburden greater than 10,000 meters. OW1 having been buried to the greatest depths has presumably been subjected to the greatest temperatures and pressures and so has undergone the greatest diagenetic alterations. Various point sources and base lines were used to represent the area of maximum diagenesis. The OW1 location appeared to be the best choice. No significant geographical trend is seen in Tennessee (Figures 12, 13 and 14), but the mean mixed-layer clay percentages are considerably higher than those in Georgia (30.0%, 35.2%, 25.2% for the <.2μm, .2-2μm, and 2-44μm fractions, respectively). In Tennessee, mixed-layer percentages do not change drastically with grain size.

In previous studies, authors have determined that if expandable clays are subjected to increased temperature and pressure through burial

> "the proportion of contracted 10 Å layers systematically increases. From about 50°C-100°C the contracted and expanded layers are randomly distributed. At higher

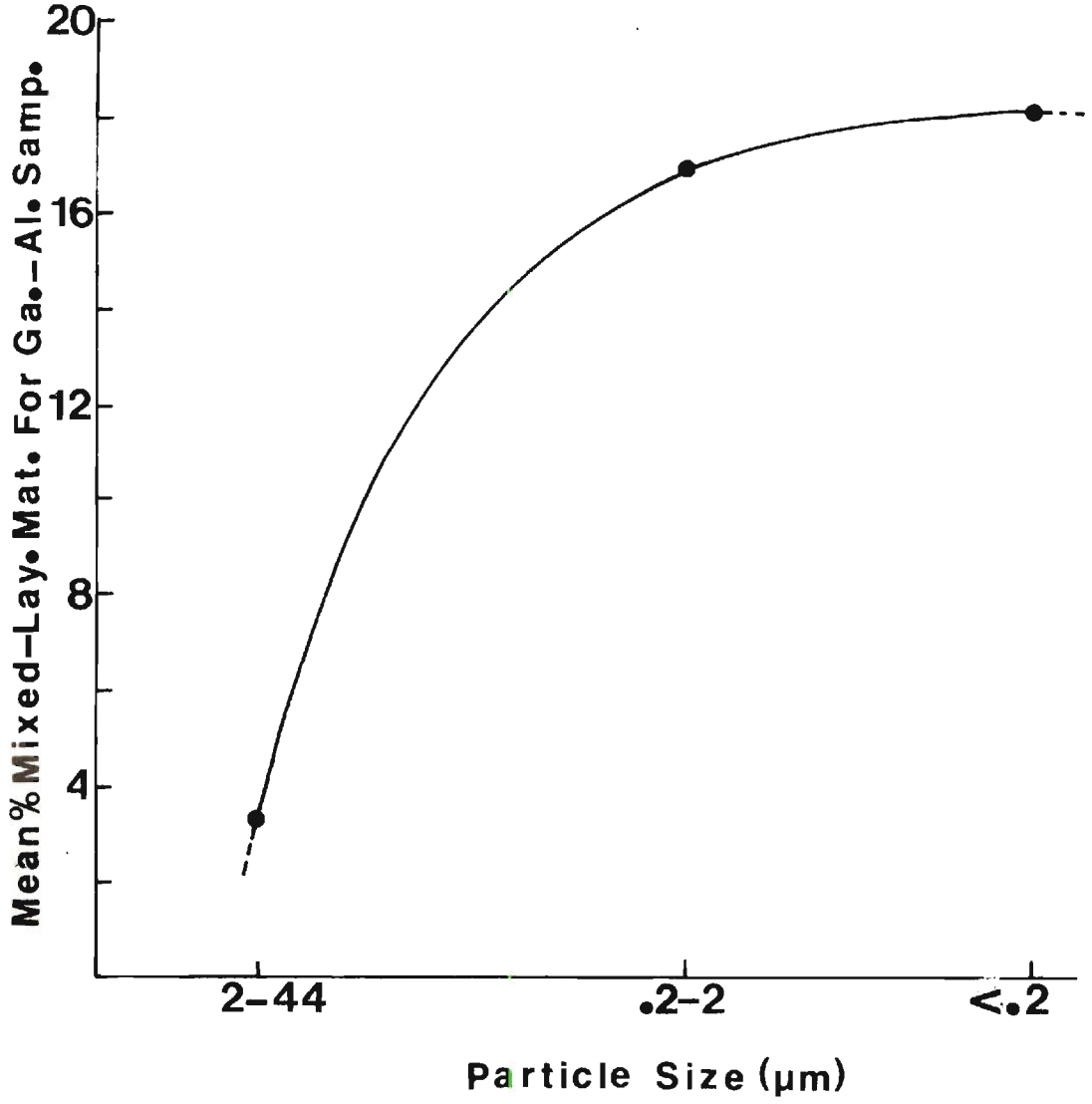

Figure 8. Increase in Mean Percent Mixed-Layered Material for Georgia-Alabama Samples With Particle Size.

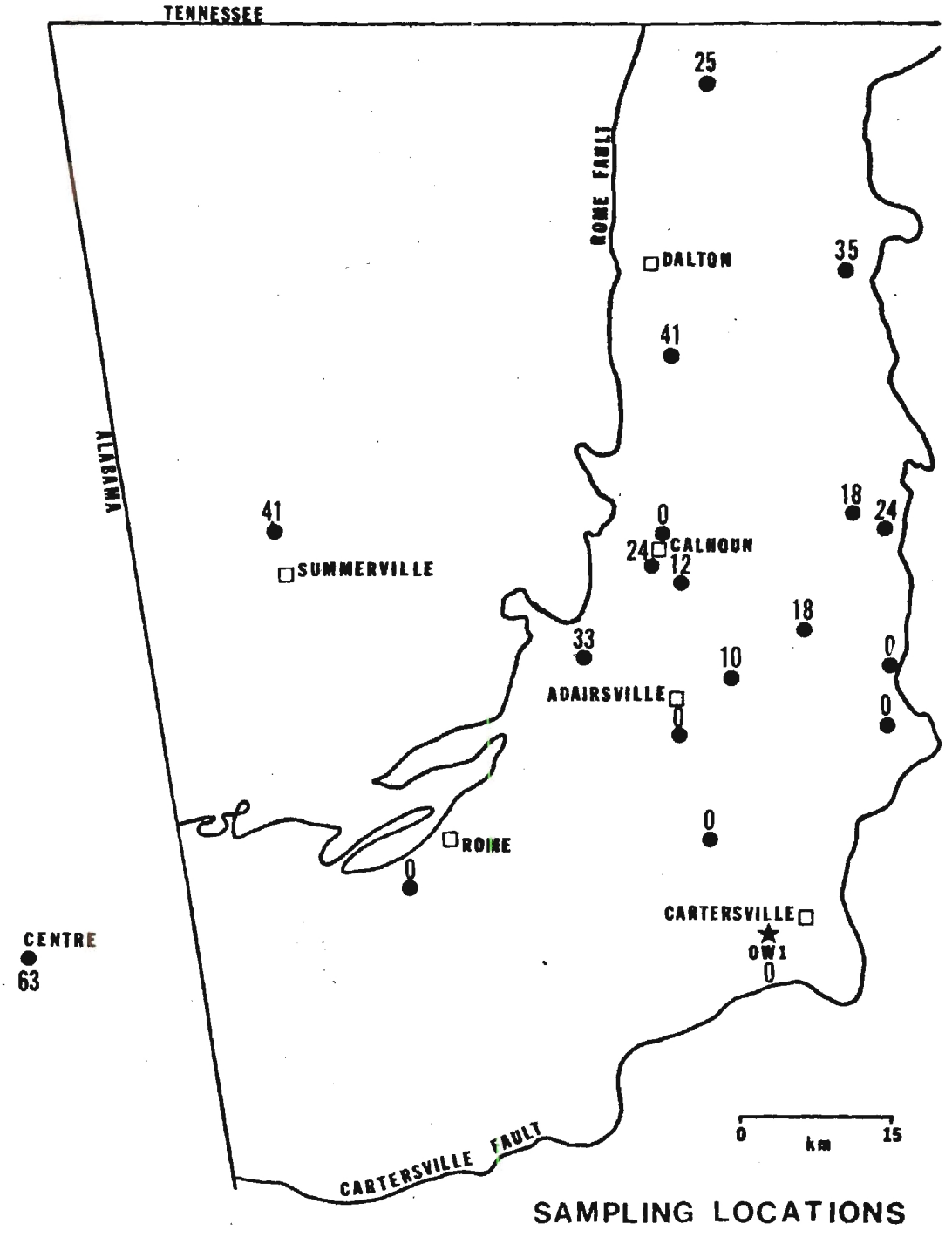

Figure 9. Percent Mixed-Layered Material for the <.2μm Fraction.

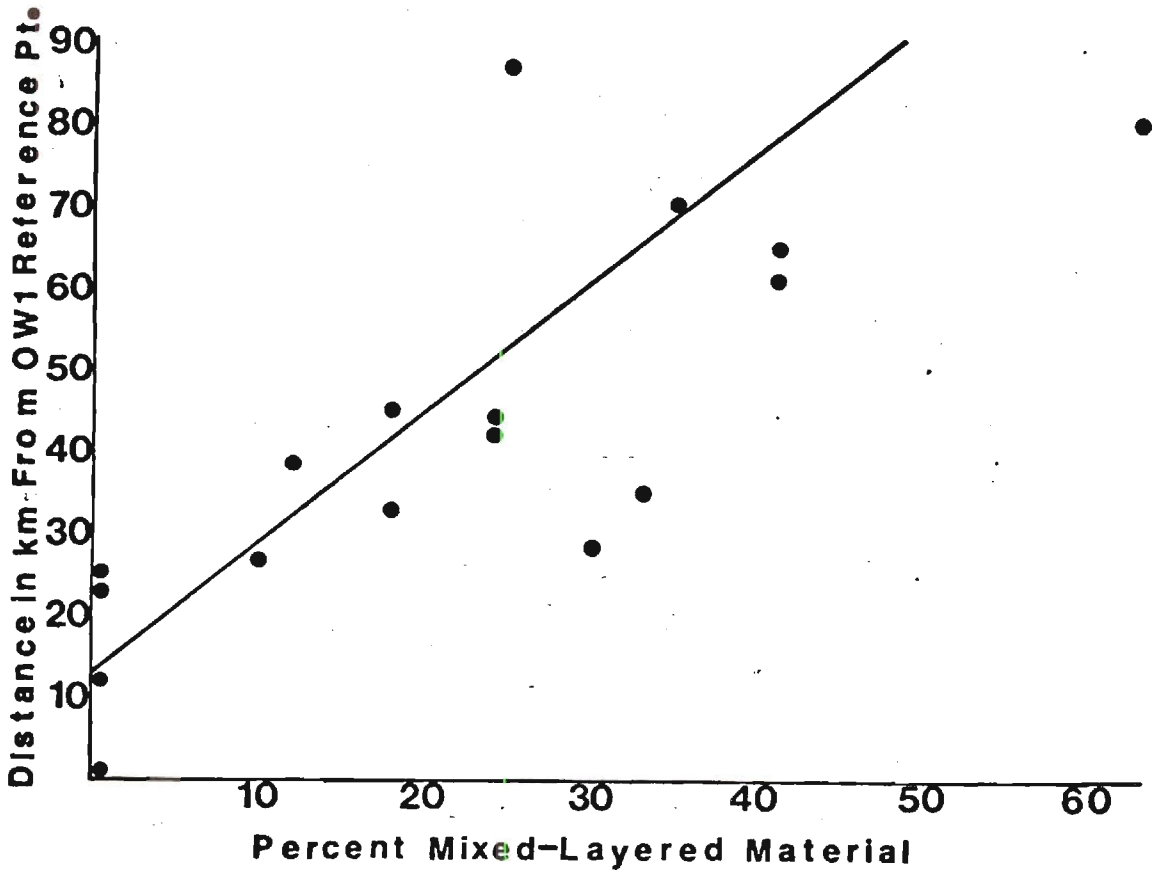

Figure 10. Variation in the <.2μm Fraction Percent Mixed-Layered Material with Increasing Distance from OW1 Reference Point (y = 1.59x + 13.65, C.C. .771).

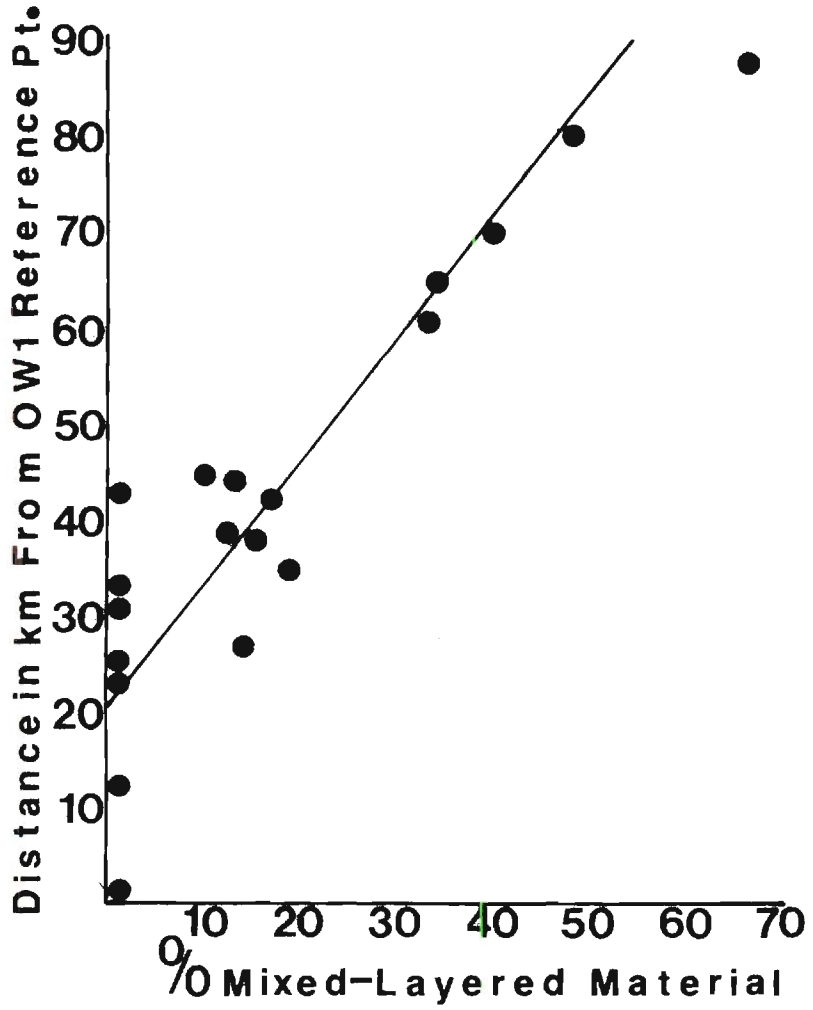

Figure 11. Variation in the .2-2μm Percent Mixed-Layered Material with Increasing Distance from OW1 Reference Point. (y = 1.30x + 20.16, C.C. = .902)

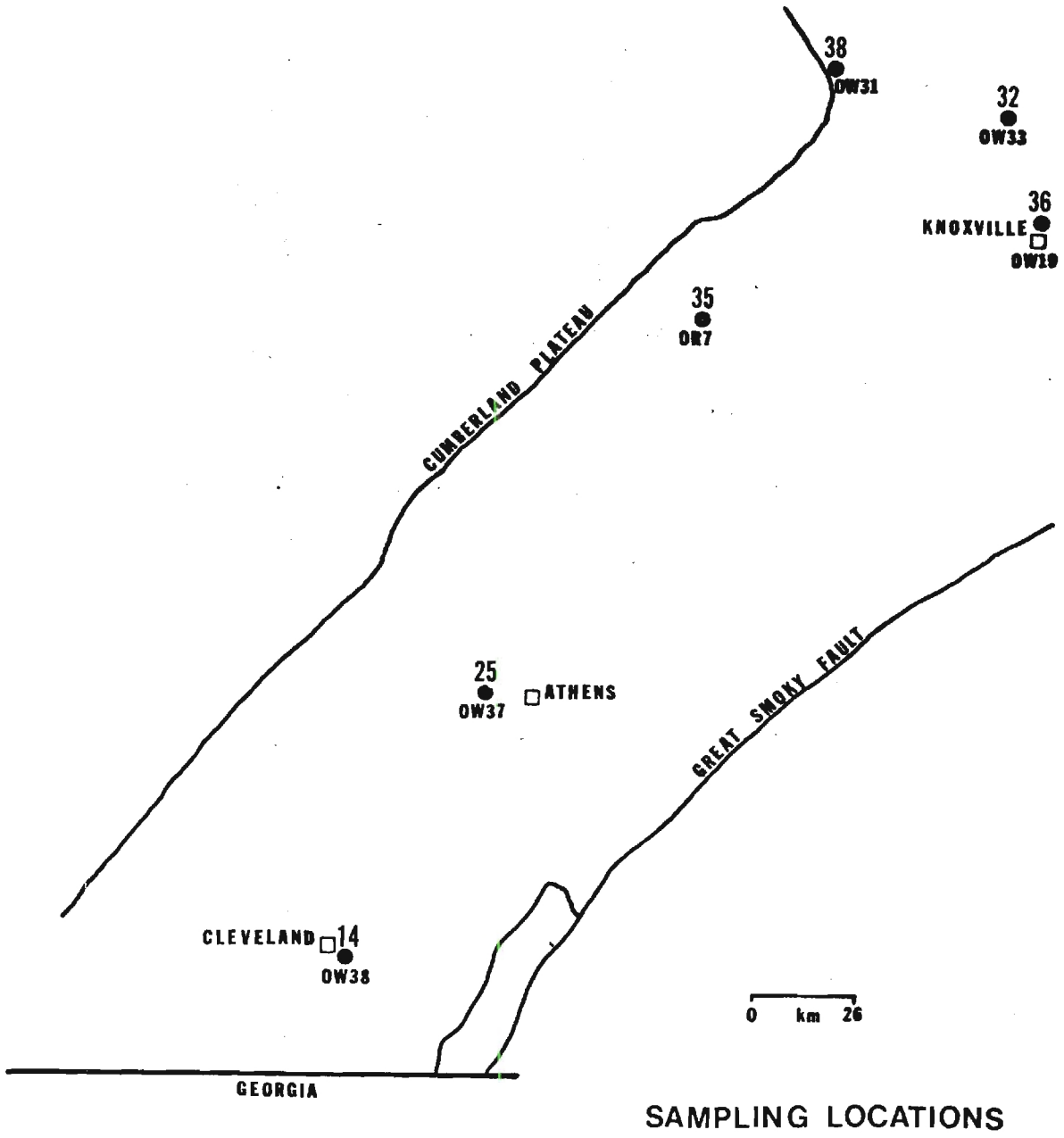

Figure 12. Percent Mixed-Layered Material of the <.2μm Fraction for Tennessee Samples.

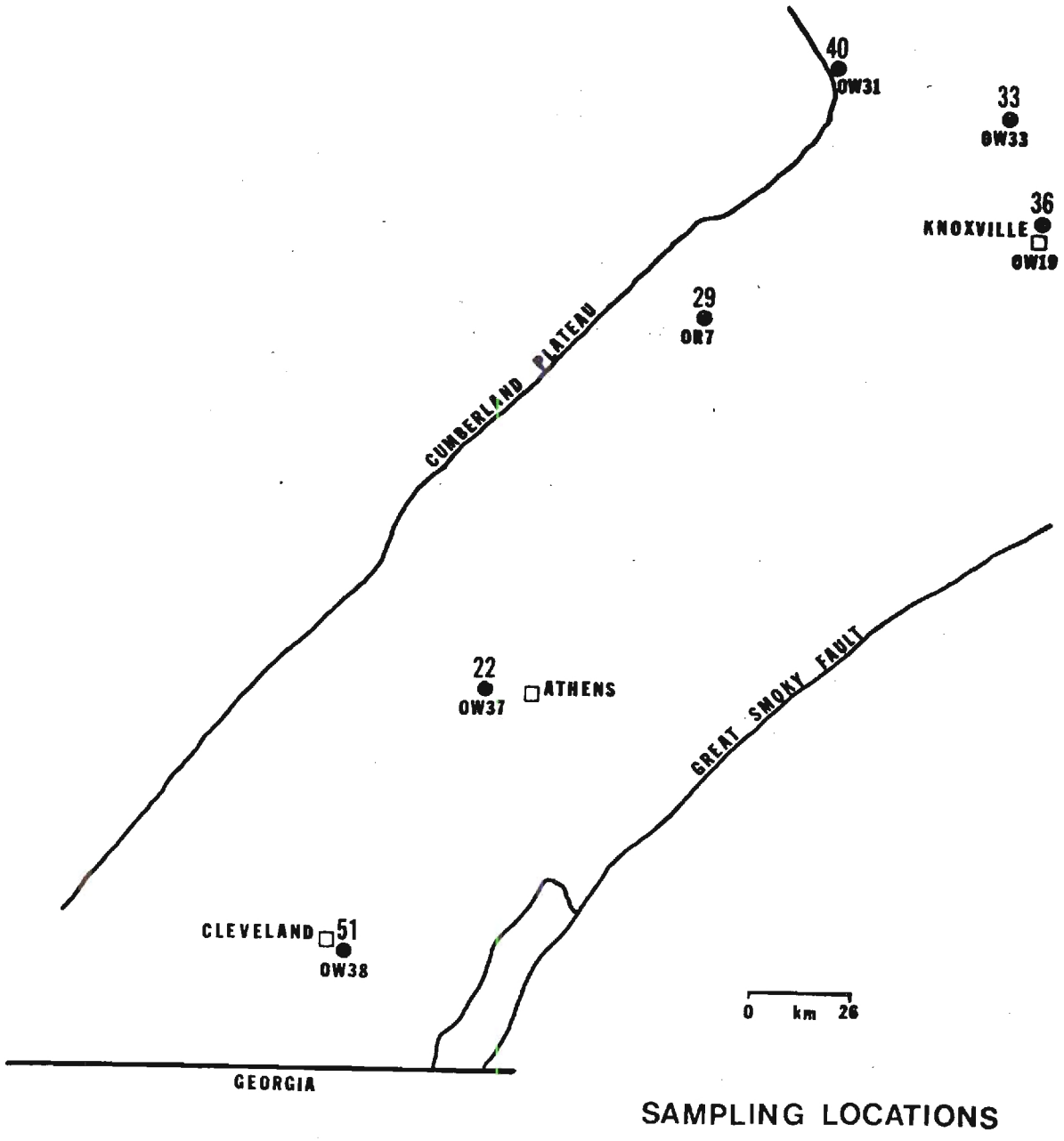

Figure 13. Percent Mixed-Layered Material of the .2-2μm Fraction for Tennessee Samples.

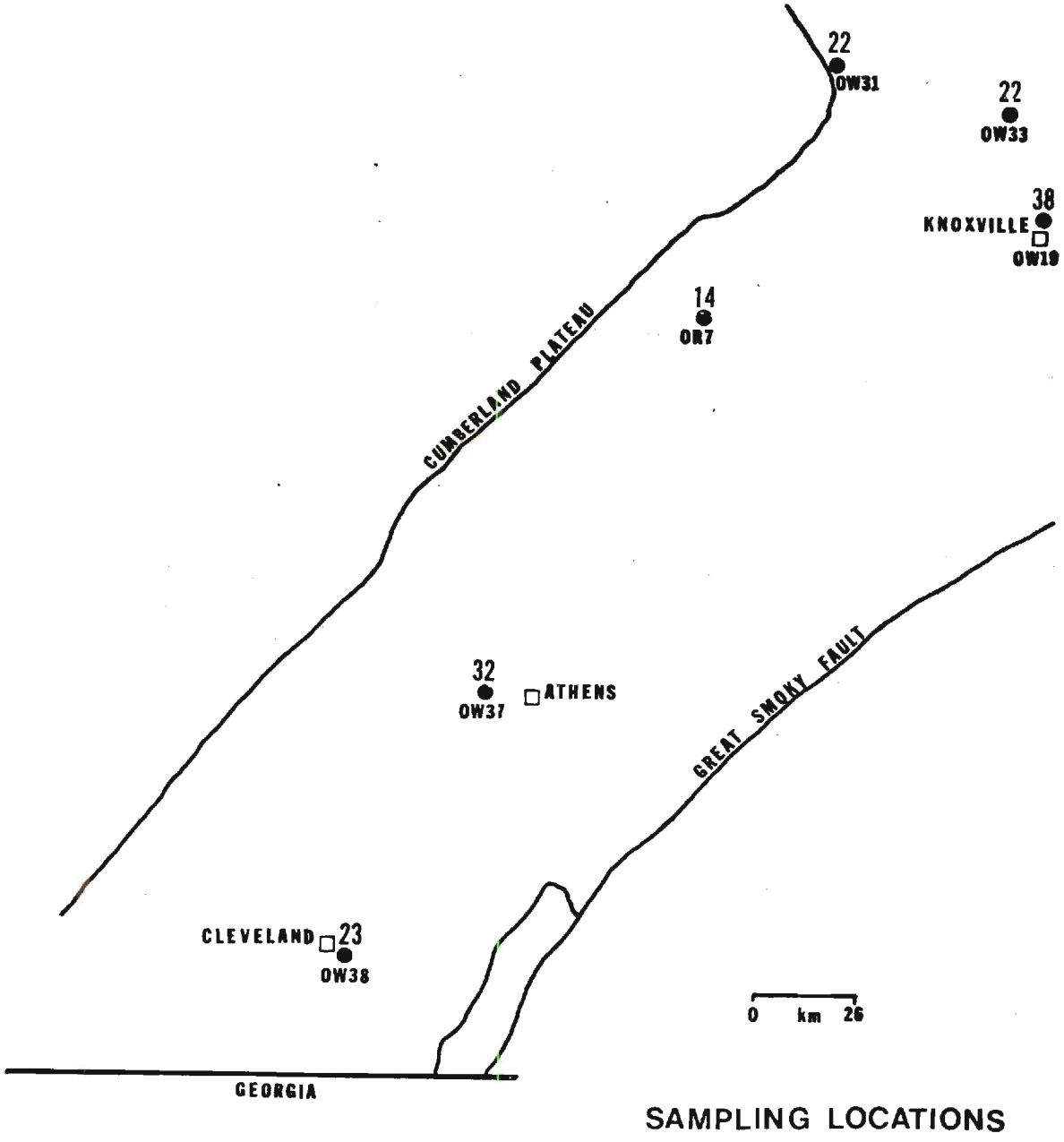

Figure 14. Present Mixed-Layered Material of the 2-44μm Fraction for Tennessee Samples

> temperatures only a few additional layers are randomly distributed. At higher temperatures only a few additional layers are contracted, but the interlayering becomes more ordered. The final product, 7:3, 8:2 (non-expanded/expanded) is relatively stable and persists until temperatures of 200°C-220°C are reached". (Weaver and Pollard, 1973, p. 114).

Using curves of Reynolds and Hower (1970) it was determined that none of the samples containing mixed-layer material have more than 20% expanded layers.

> "At 40% montmorillonite layers, mixed-layer clays almost always have ordered interstratification". (Reynolds and Hower, 1970, p. 25)

Although no low angle (∿30 Å) peak was observed, abiding by this statement, it may be assumed that mixed-layer clays found in this study possess an ordered interstratification.

Weaver and Beck (1971, p. 1) suggested that

> "after burial, K is obtained from K-feldspars and micas. Potassium fixation is accomplished by having the layer charge increased by the reduction of Fe in the octahedral sheet and incorporation of Al, entering through the ditrigonal holes in the basal oxygen plane".

The lack of K-feldspar, the absence of mixed-layer material, and the higher illite percentages in the southeast suggest that most of the K in this area has been fixed in the formation of contracted 10 Å clay. Figure 15a shows a decrease in K_2O percentage with an increase in mixed-layer material in the <.2μm fraction for Georgia-Alabama samples. Unfortunately, only 3 samples could be used to show the trend because others were either contaminated with accessory minerals such as calcite, and paragonite

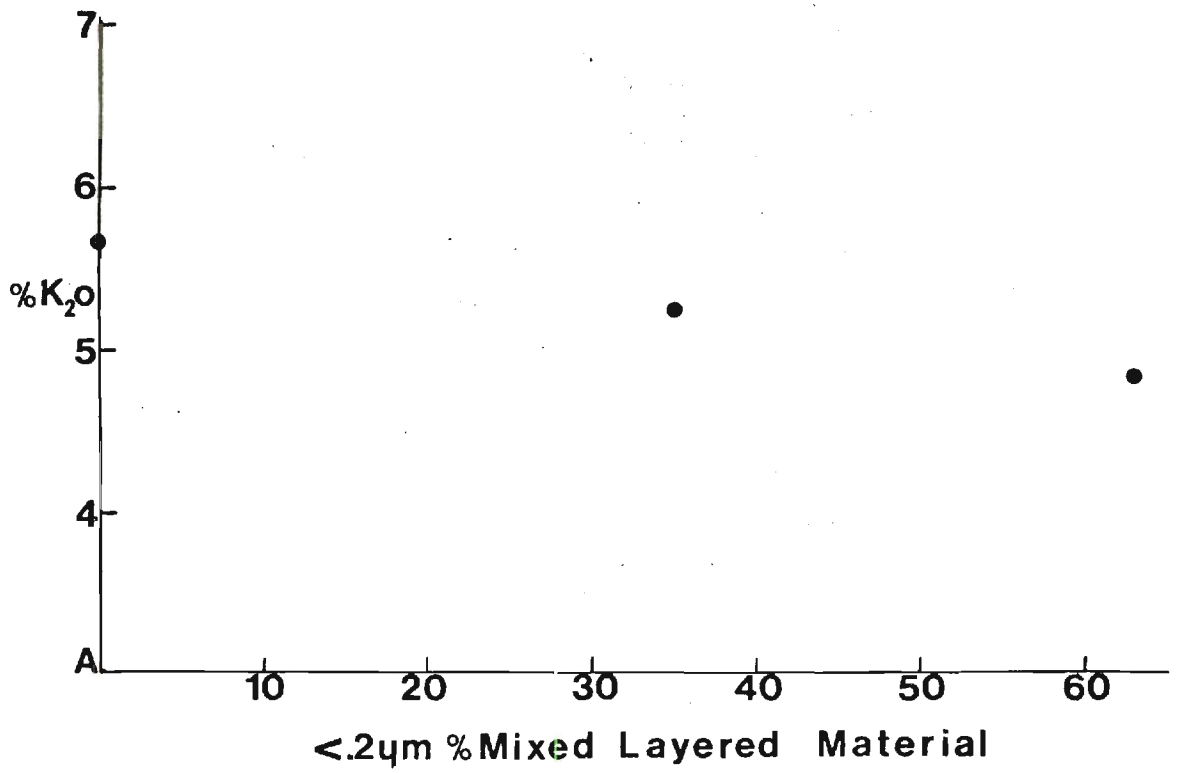

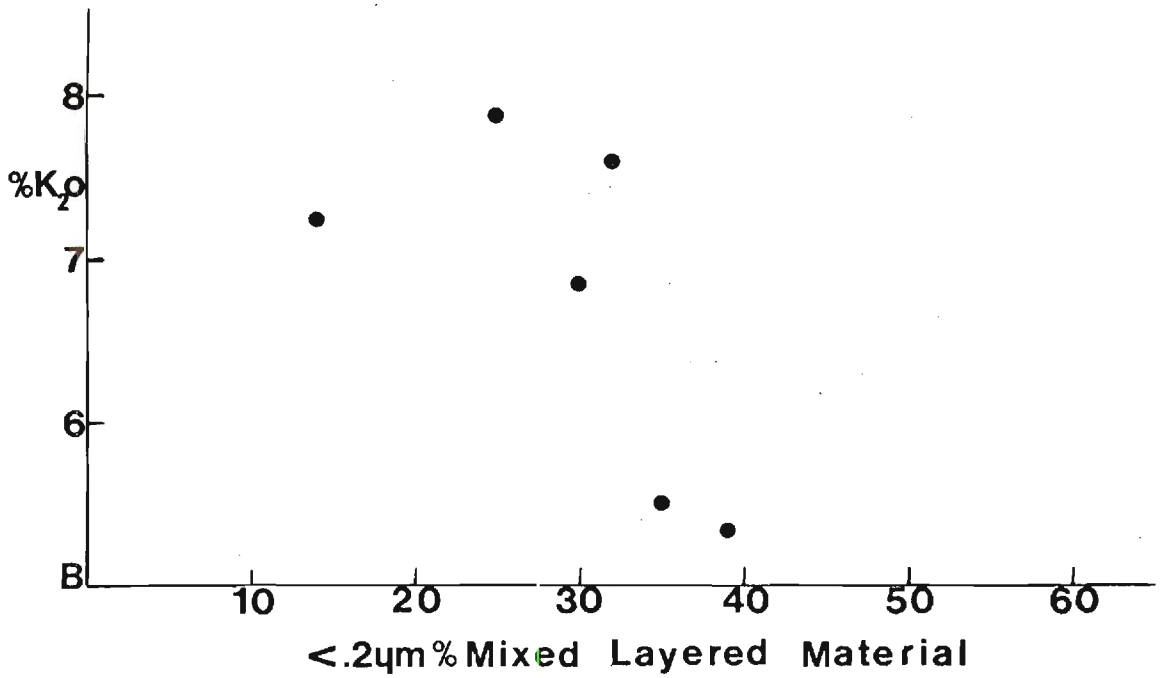

Figure 15a) Variation in <.2μm Percent Mixed-Layered Material with Increase in K_2O Content for Some Georgia Samples.

Figure 15b) Variation in <.2μm Percent Mixed-Layered Material with Increase in K_2O Content for Tennessee Samples.

or not enough <.2μm clay was retrieved during fractionation procedures to be used for chemical analysis. Figure (15b) demonstrates the same relation for Tennessee samples. It would be expected that an increased percentage of illite would occur with an increase in K_2O because of K fixation to form contracted layers in mixed-layer material. Figure 16 shows this trend for samples in Tennessee.

A shift in the illite (001) peak was encountered in samples containing mixed-layer material. The peak shift is intensified in some samples when treated with ethylene glycol. Upon heating to 300°C for 1.5 hours, the illite 001 peak of most samples reverts back to 10 Å. Tables 10-13 exhibit peak positions for all untreated, glycol treated, and heated samples. Most shifts occur in the <.2μm, and .2-2μm fractions, while few 10 Å shifts occur in 2-44μm fractions. This is due partly to increased amounts of mixed-layer material in finer fractions, and partly to particle size effects. Reynolds (1968, p. 320) determined that

> "the diffraction maxima may be displaced from their normal positions by the effects of very fine particle size".

Figure 17a and 17b shows an increase in 10 Å shifts with an increase in the amounts of mixed-layer clay. The clustering that occurs in both figures is partially due to inherent inaccuracies of precisely determining d-spacings from peak positions. Figures 18a and 18b and 19a and 19b display mapped versions of the 10 Å shifts in Georgia-Alabama, and Tennessee samples for <.2μm, and .2-2μm, fractions. Generally, 10 Å shifts increase in a western, and northern direction in Georgia, and indiscriminately in Tennessee. Shifts are related to amounts of expanded

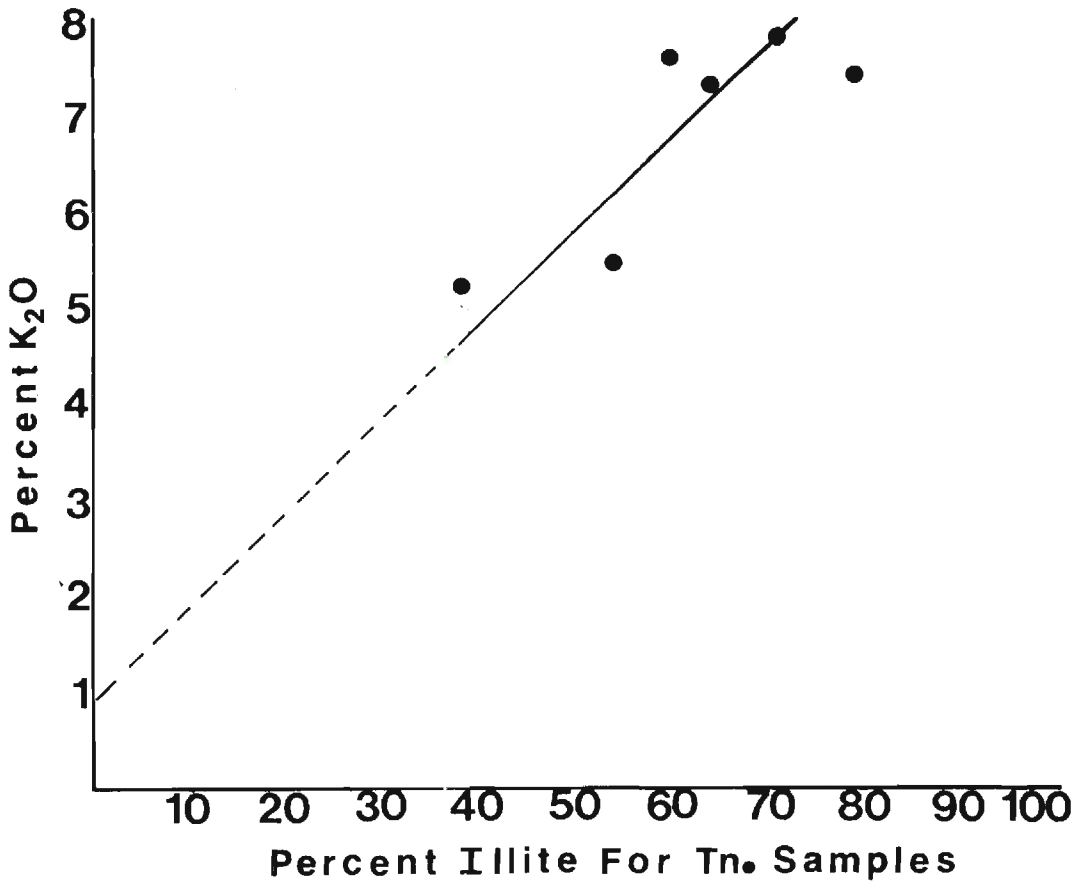

Figure 16. Variation in <.2μm Percent Illite for Tennessee Samples with an Increase in K_2O Percentage.

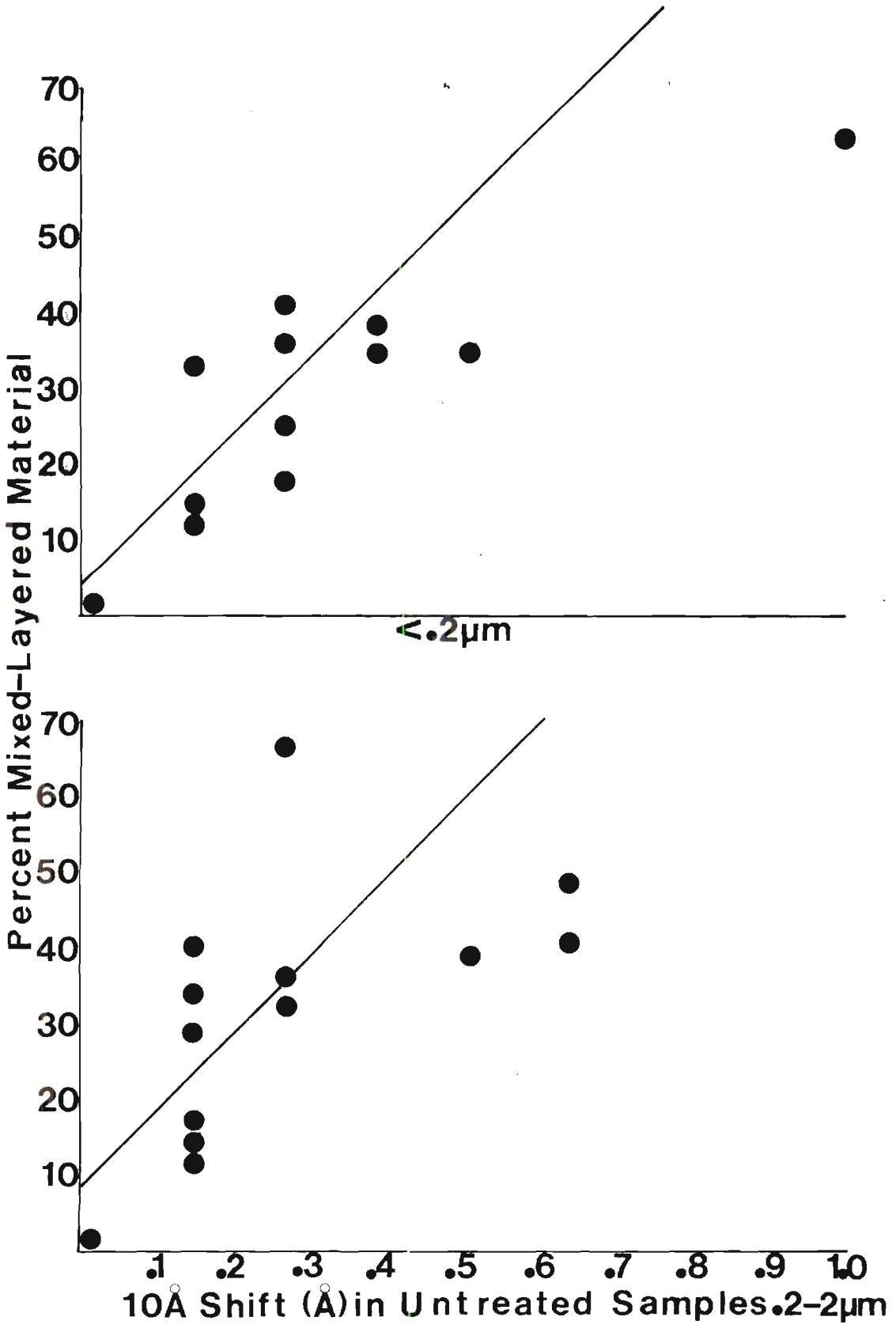

Figure 17 a. and b. Variation in 10 Å Shift in Untreated Samples, a) <.2μm, b) .2-2μm, with an Increase in Percent Mixed-Layered Material. (y = 79.3 + 6.96, C.C. = .645) (y = 60.5 + 10.11, C.C. = .595).

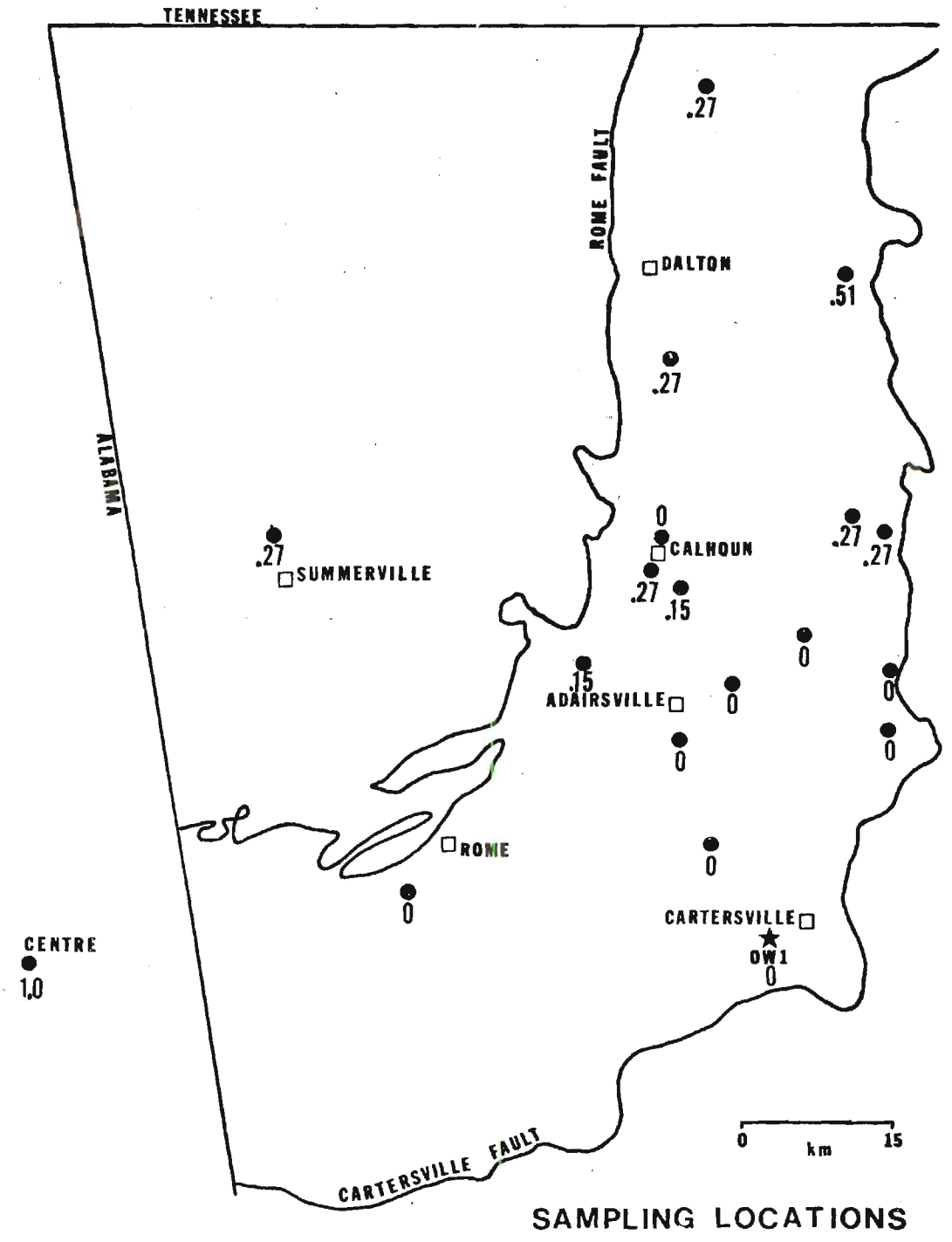

Figure 18a. 10 Å Shift (Å) of the <.2μm Fraction for Georgia-Alabama Samples..

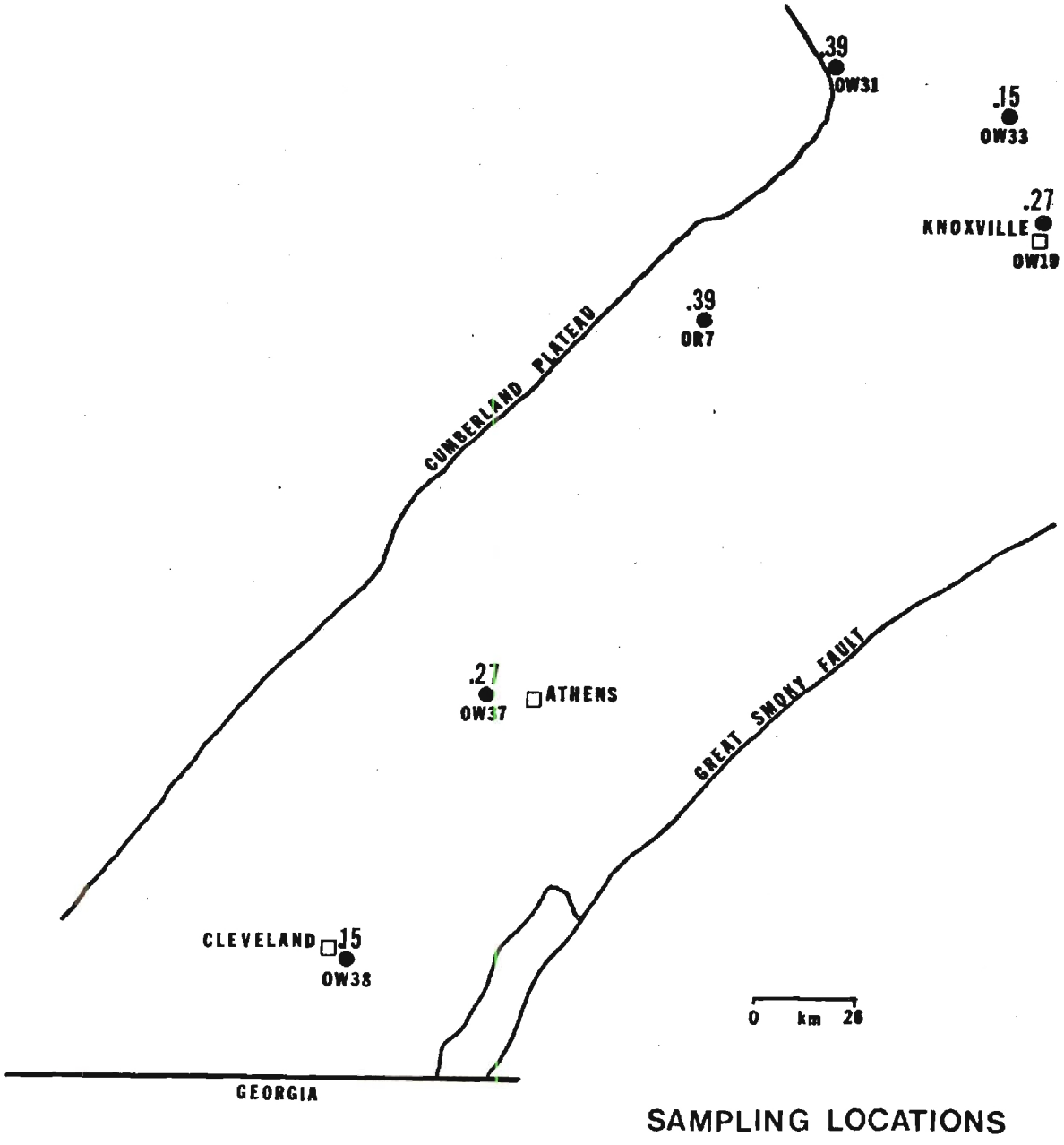

Figure 18b. 10 Å Shift. (A) of the <.2µm Fraction for Tennessee Samples.

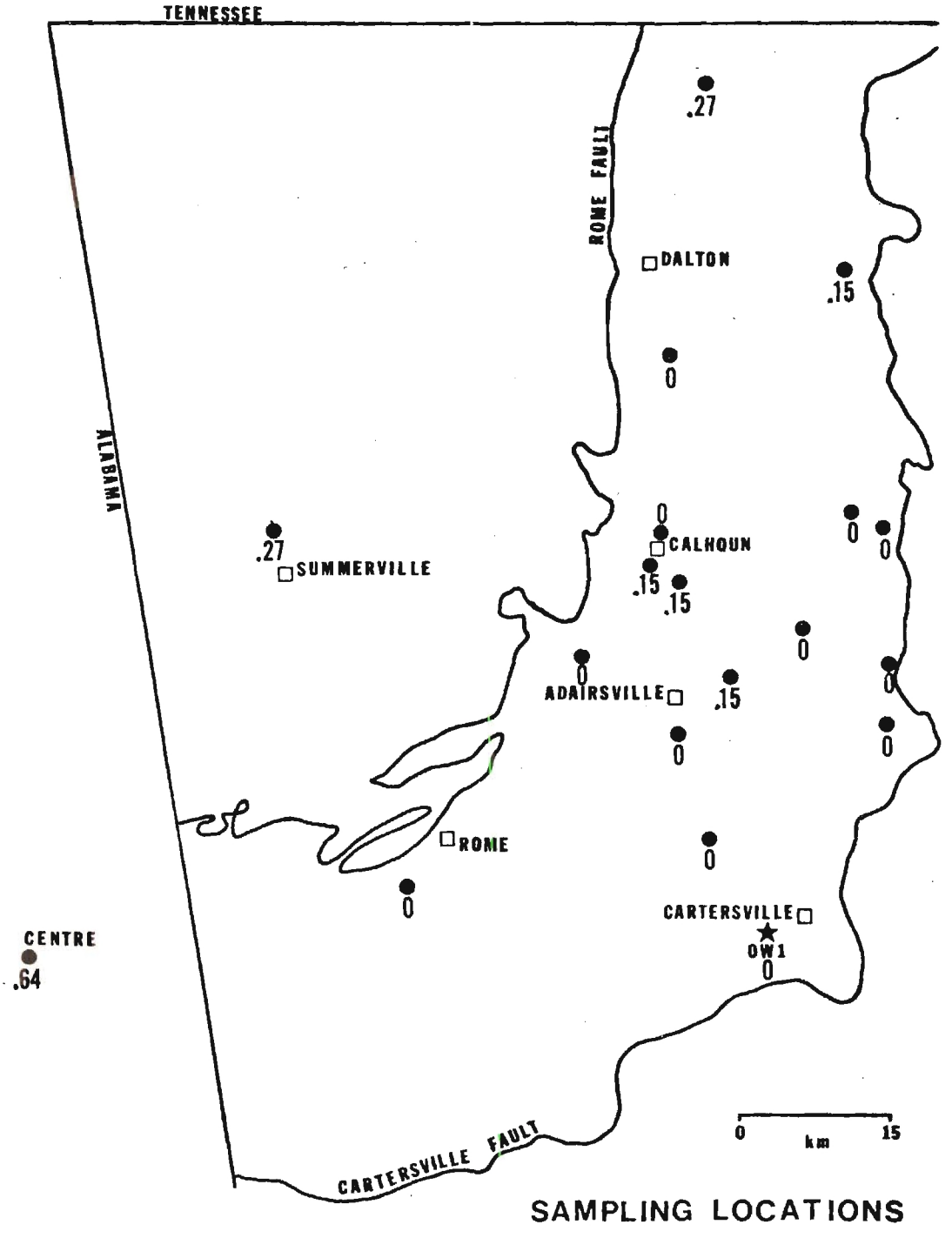

Figure 19a. 10 Å Shift (Å) of the .2-2 μm Fraction for Georgia-Alabama Samples.

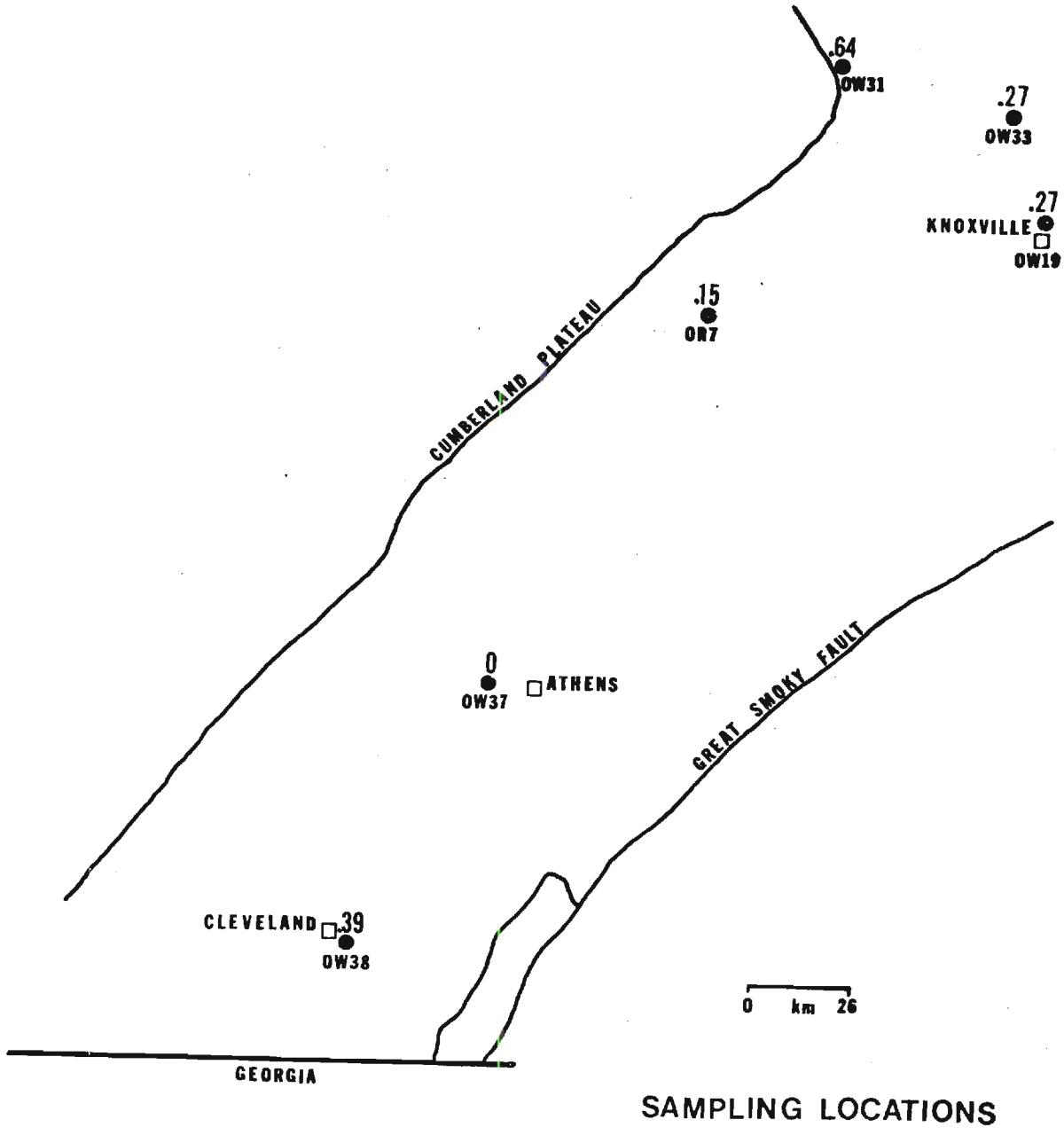

Figure 19b. 10 Å Shift (Å) of the .2-2μm Fraction for Tennessee Samples.

layers, mixed-layer material, and particle size. Since all fine fraction clay should be affected in the same manner, the relative trend appears to demonstrate that there is less mixed-layer material in south-eastern samples, than in western, and northern samples. Figures 20 and 21 show several illite (001) peaks from different locations, and shifts from the 10 Å position. Major shifts occur in western and northern illites (OW23, OW7, OW27), while no shift is seen in OW9.

Paragonite is only found in 3 samples (OW3, OW13, and OW26), (Tables 2-7), which are extremely close to the Cartersville Fault. Paragonite is a sodium-rich mica, and can be identified by its 3 primary basal peaks which give reflections at 9.62 Å (9.2°), 4.81 Å (18.4°) and 3.25 Å (27.4°) (Figure 22). Several reactions have been proposed for the formation of paragonite: Albite + Kaolinite = Paragonite + Quartz + Water (Zen, 1960), and Na-bearing Illite = Paragonite + Phengite + Water (Frey, 1969). Frey (1969) concludes that the mixed-layer paragonite/phengite could be an intermediate phase in the formation of paragonite from Na-bearing illite. He found that mixed-layer paragonite/phengites are frequently found in rocks of low metamorphic grade and that with increasing metamorphic grade paragonite contents increase at the expense of the mixed-layer paragonite/phengite.

In any case Na must be derived from a source, either Na-feldspar, a Na-rich illite, or possibly by metasomatic fluids moving through the fault zone. Na-feldspar is present in all Georgia samples, but only in very small or trace amounts in the 2-44μm fraction of the 3 paragonite bearing samples. Paragonite is associated with high grade diagenetic and low-grade metamorphic rocks but it has never been specified whether

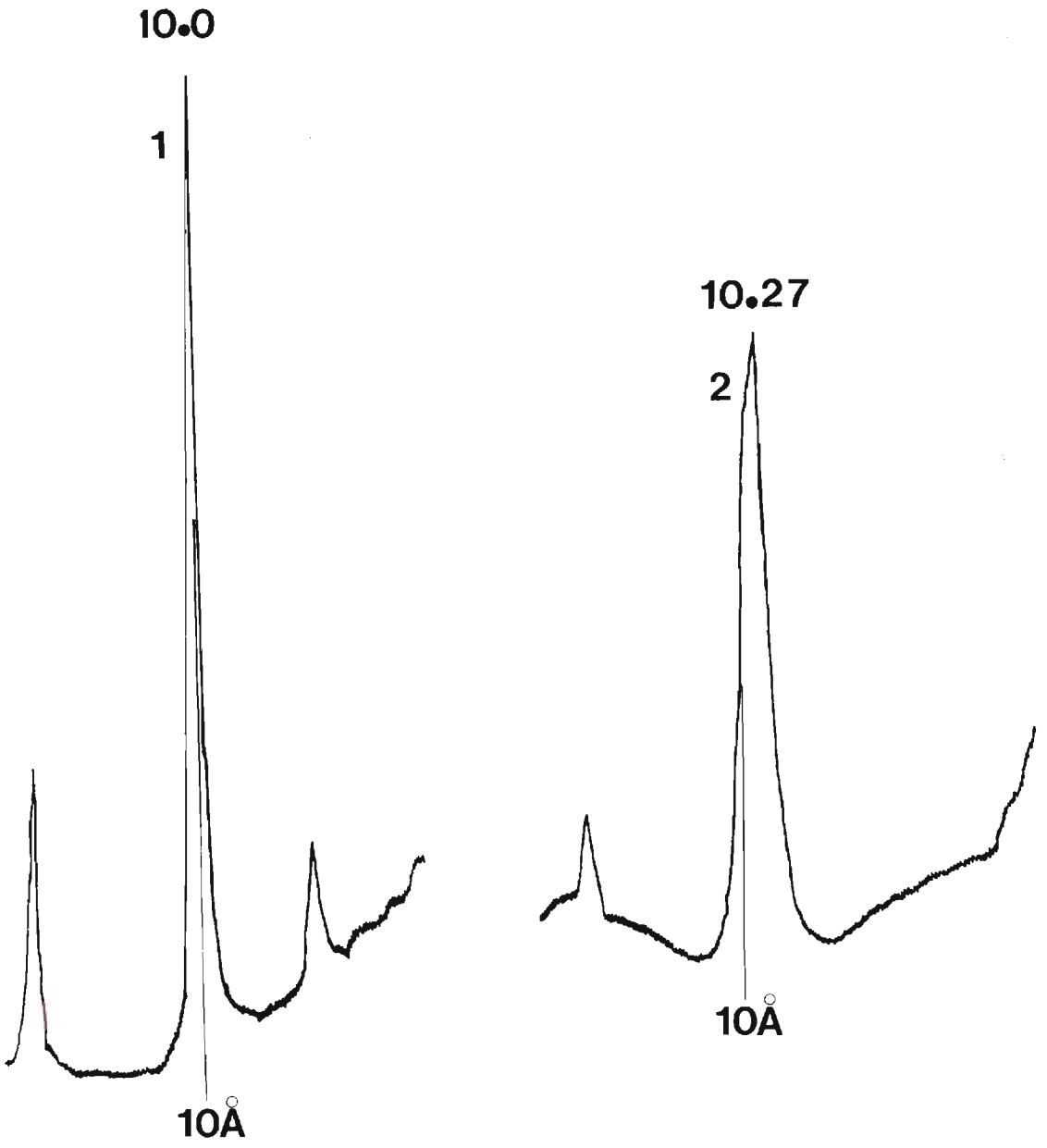

Figure 20. Untreated 10 Å Shift (Å) for OW9(1) and OW27(2) (<.2μm).

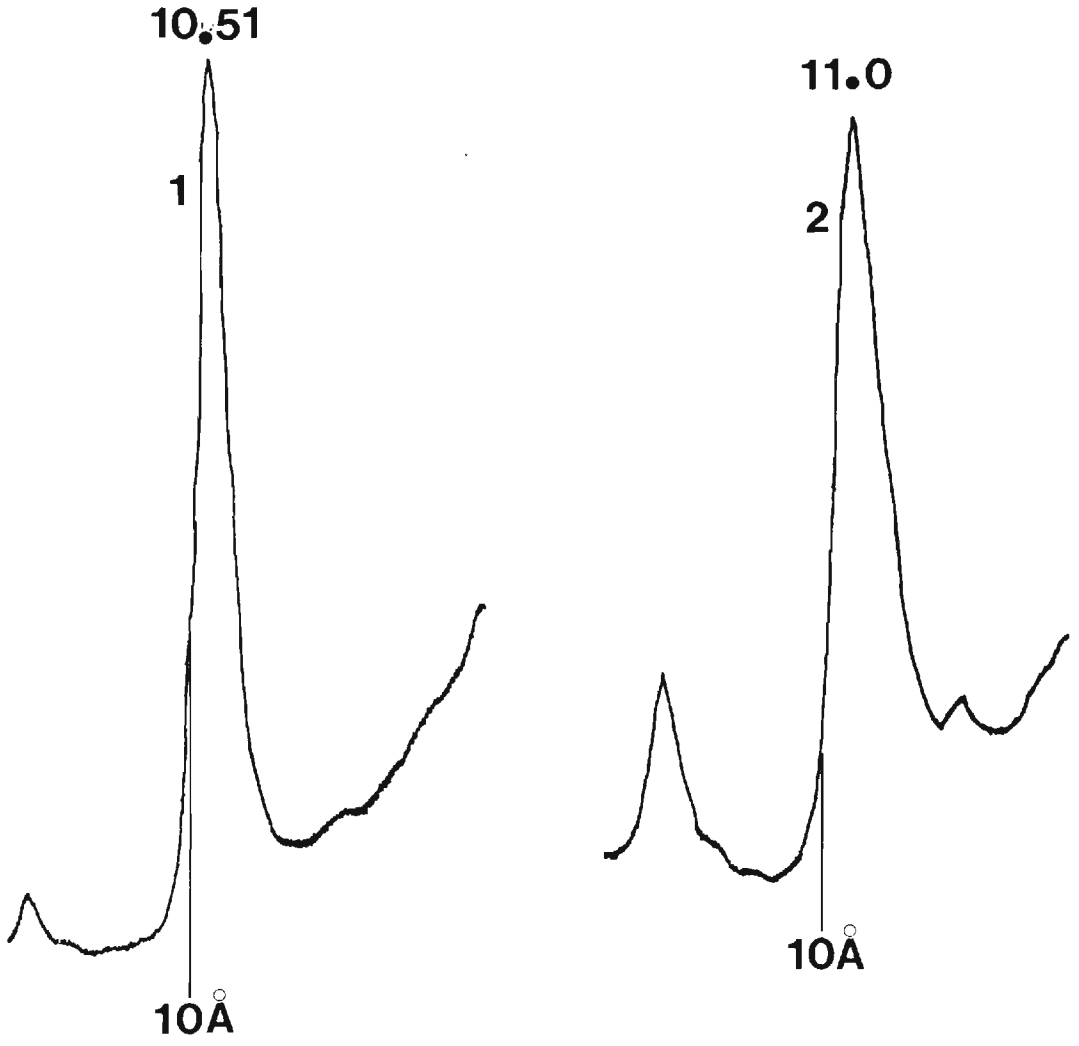

Figure 21. Untreated 10 Å Shift (Å) for OW7(1) and OW23 (2) (<.2μm).

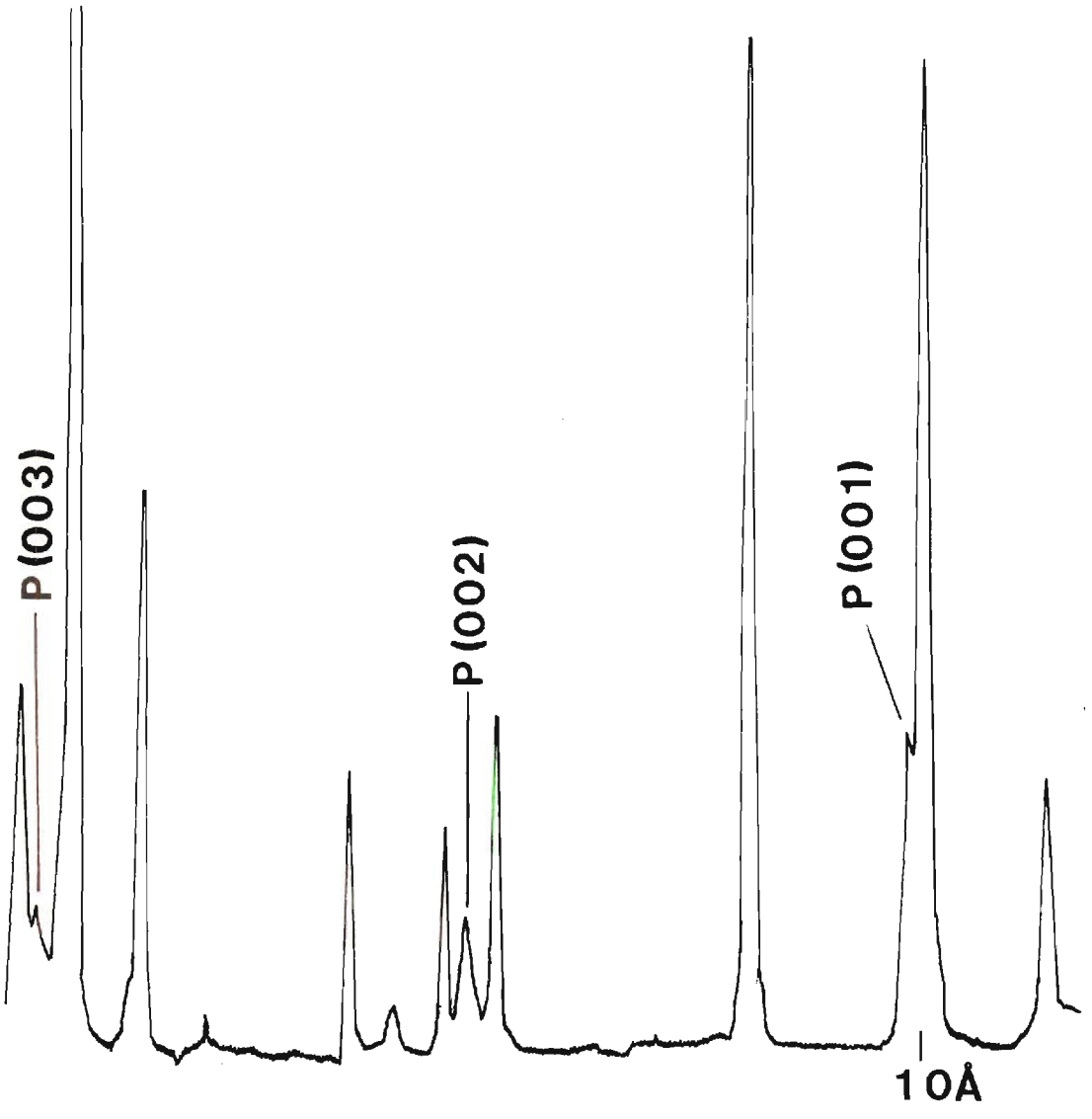

Figure 22. Position of Paragonite's 3 Primary Basal Peaks.

paragonite formation is temperature dependent, pressure dependent, or both. Differential stress caused by thin skinned thrust faults like the Cartersville Fault are responsible different mechanical and chemical effects. Increased horizontal stress causes rotation of mineral lattices, bond breakage, and increased temperature by frictional heating enabling the migration of certain elements such as K and Na. Data from this study suggests that paragonite is more stress dependent because all paragonite bearing samples are very close to the Cartersville Fault, and consequently were subjected to greater horizontal stresses than those samples farther away. Samples in the southeast, but closer to the fault, which have higher mineral crystallinities and 2M polymorph percentages do not show paragonite in their X-ray diffraction patterns.

Chemical data (Table 14) shows that samples located close to the Cartersville Fault containing paragonite have considerably larger amounts of Na_2O in the finer fractions than those located further away from the fault. X-ray patterns of <.2μm fractions reveal no Na-plagioclase in any samples. Chemical data is only available from OW3 the <.2μm fraction (OW13, and OW26 were not prepared and analyzed due to lack of <.2μm material), and its Na_2O percentage is 75% greater than any other sample. It is interesting to note that OW7, OW27, and OW11 which are close to the fault, contain relatively large amounts of Na, but no paragonite is evident in any of the X-ray diffraction patterns. The possibility exists that either paragonite contents are too low to be detected or the transformation or formation of paragonite was never successfully completed. In the .2-2μm fraction concentrations of Na are higher but the same general trend is apparent. Samples (OW3, OW13) are respectively 230%,

and 111% higher in Na_2O concentrations than the highest non-paragonite bearing sample (OW11). Na-plagioclase is not present in either OW3 or OW 13 in .2-2μm fracitons, while in non-paragonite bearing samples it is generally found in these size fractions. Na-plagioclase is present in OW26, but only in trace amounts. Na_2O percentages decrease in abundance in the 2-44μm fraction for samples which contain paragonite (Table 13). Samples which do not contain paragonite show an increase in Na_2O percentages. A higher Na percentage in the 2-44μm fraction seems logical because it is in this fraction where the majority of Na-feldspar is present. In samples which are located very close to the Cartersville fault, Na has apparently migrated from Na-feldspars in the coarser fraction to the finer fractions (<.2μm, and .2-2μm) where it has been utilized in the formation of paragonite. Figure 23 shows the percentage of Na_2O vs. particle size for OW3. Notice that there is an increase in Na from the <.2μm to the .2-2μm fraction, and then a decrease in Na for the 2-44μm fraction. Figures 24, 25 and 26 show Na_2O percentages for some samples in Georgia. The finer fractions of samples close to the Cartersville fault contain considerably more Na_2O than those further away. Al and Si are present in abundance in the form of Al phylosilicates (illite, chlorite), and quartz, and Na in the form of Na-plagioclase. The basic materials for paragonite formation are present, and data from this study suggests that the paragonite in OW3, OW13, and OW26 was formed under high temperatures, and the high pressures created during the thrust movement of the Cartersville Fault. High stress apparently is the critical factor in the formation of paragonite.

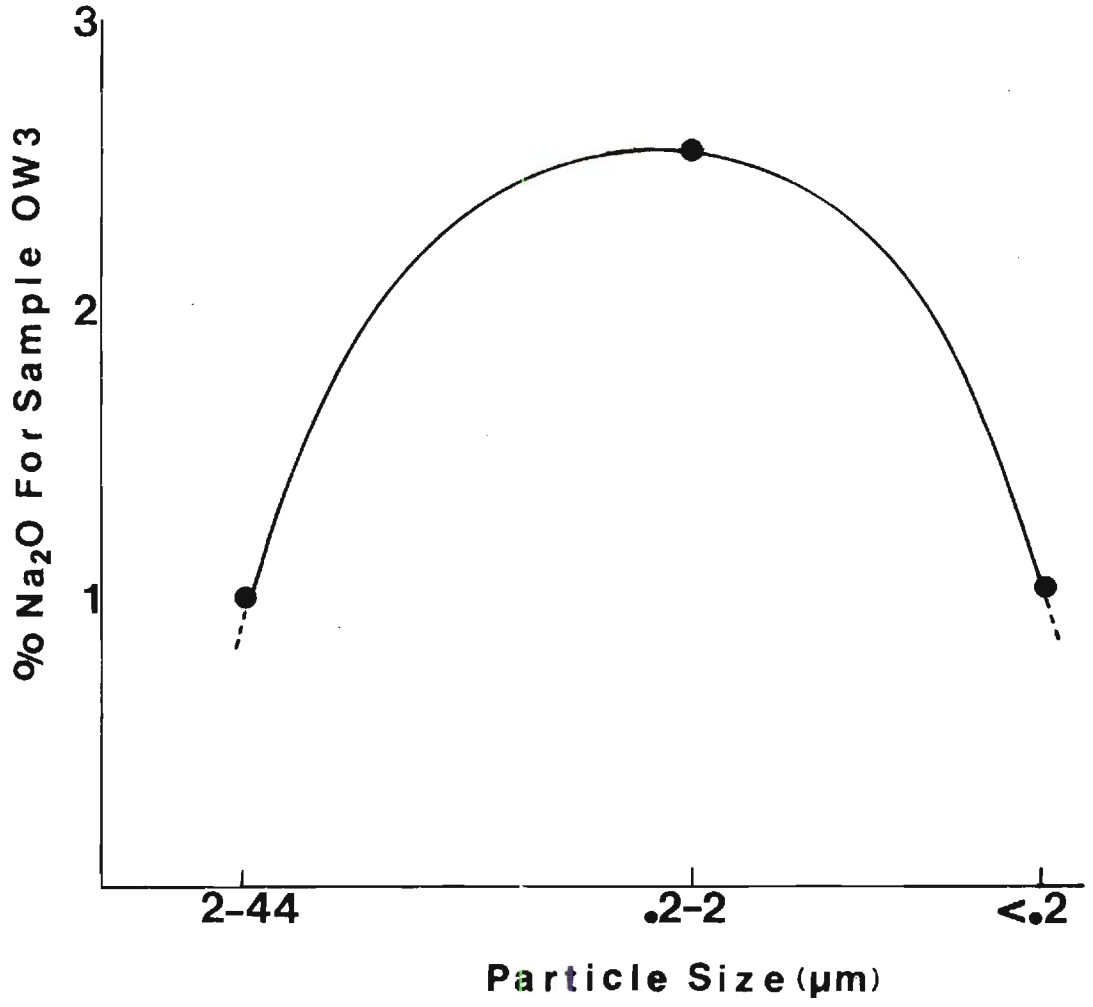

Figure 23. Variation in Percent Na_2O for Sample OW3 with Particle Size.

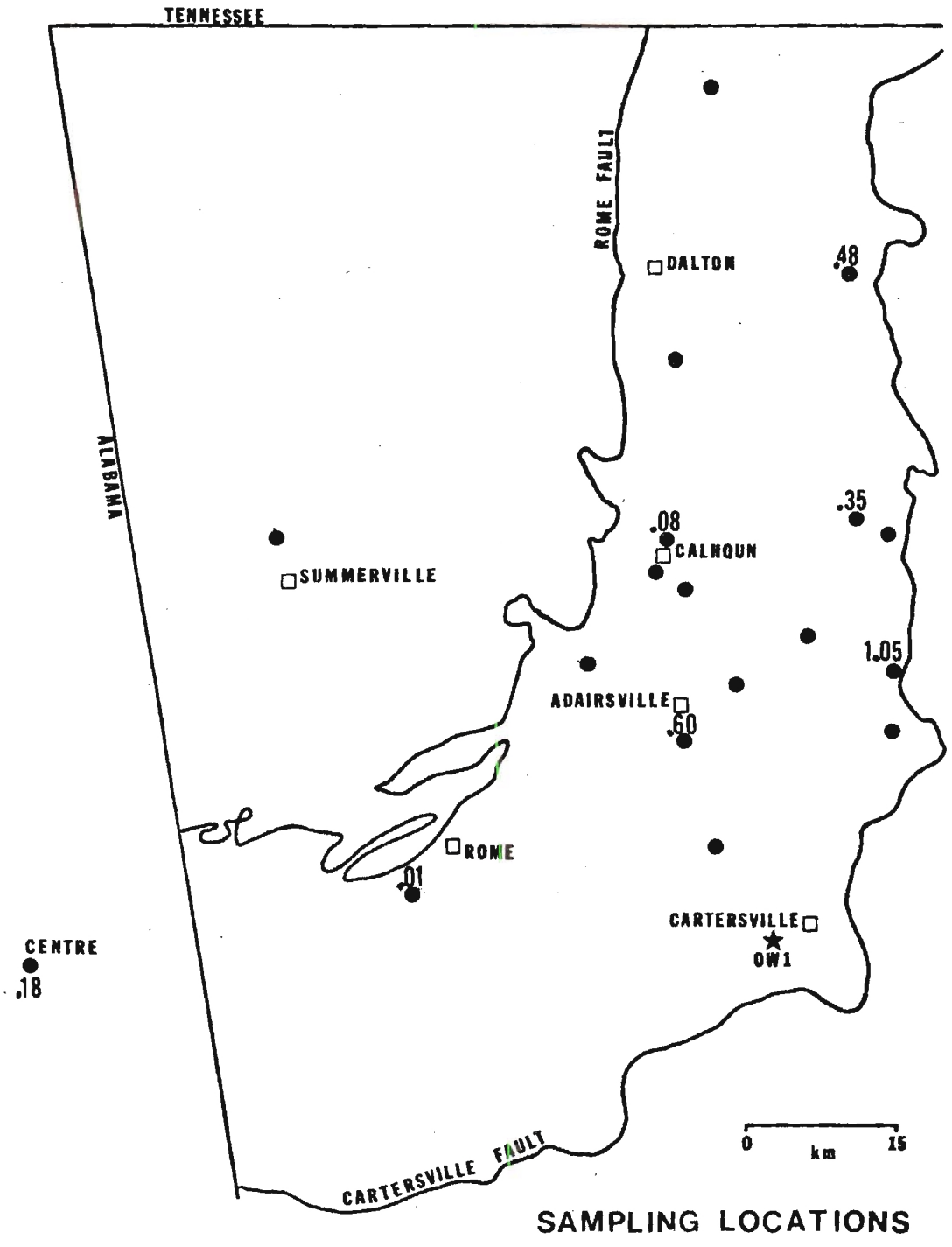

Figure 24. Percent Na_2O for <.2µm Fraction

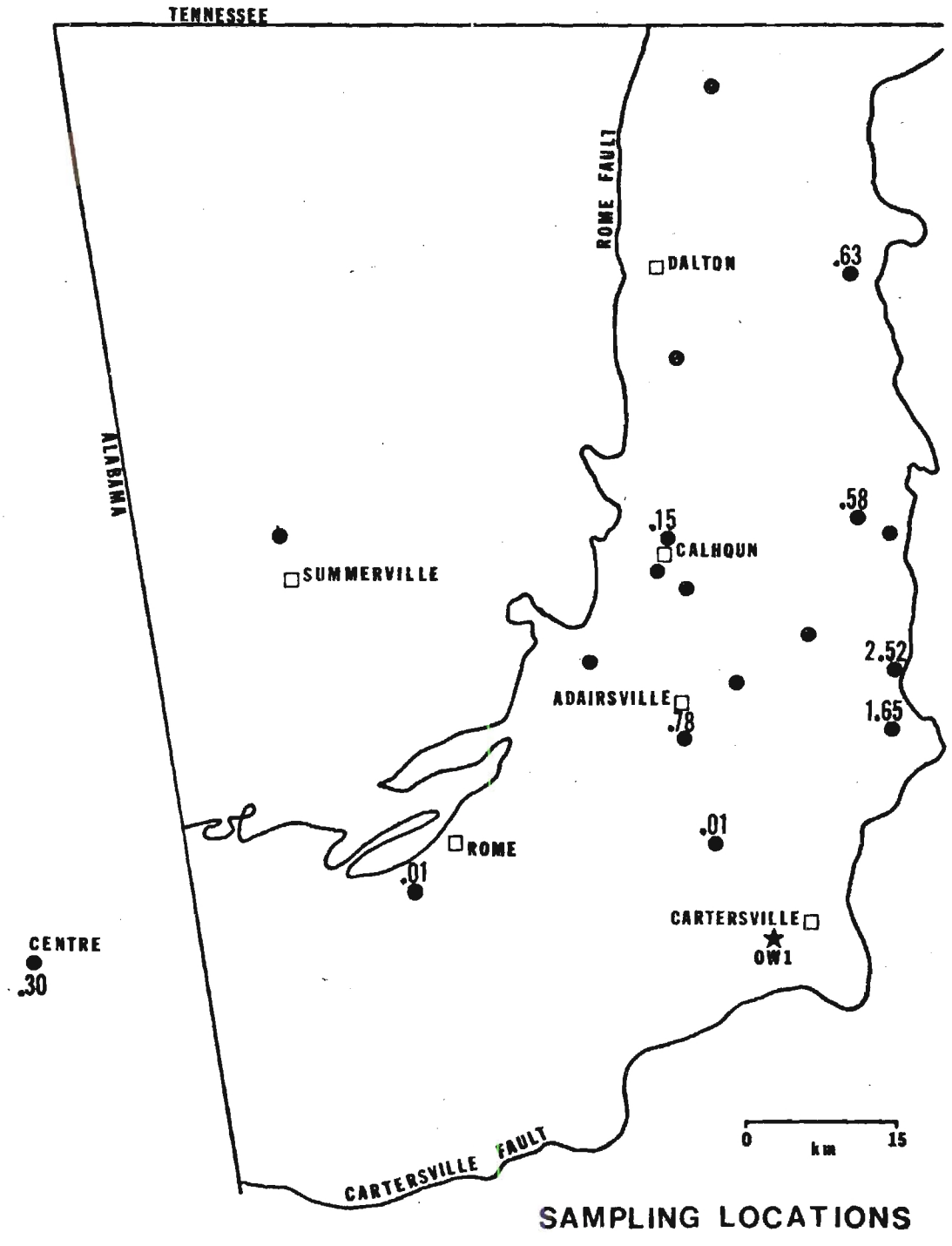

Figure 25. Percent Na_2O for .2-2μm Fraction.

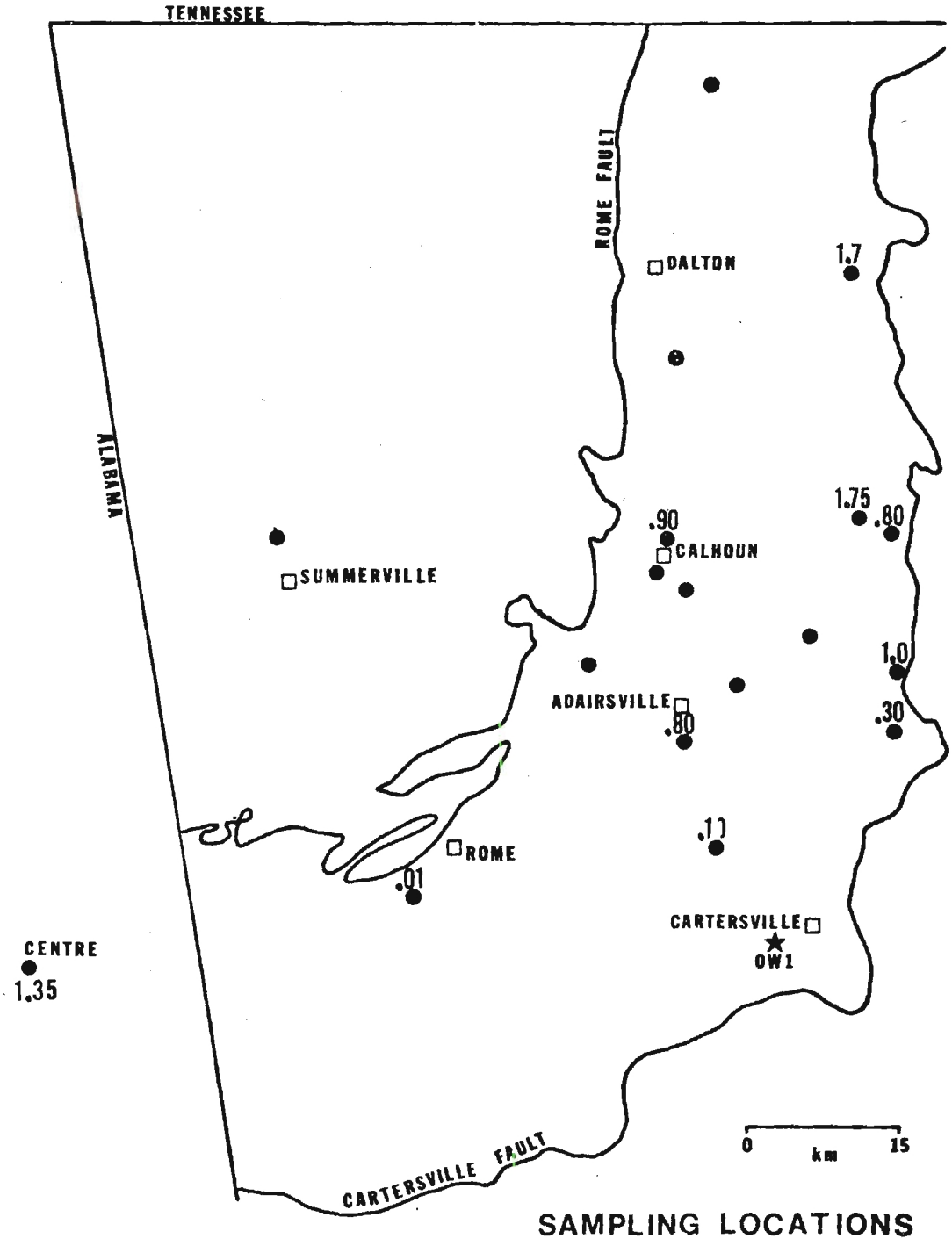

Figure 26. Percent Na_2O for 2-44μm Fraction.

Dioctahedral Mica Polytypes

Yoder and Eugster (1955) and Smith and Yoder (1956) were some of the first to consider dioctahedral mica polymorph structures. Commonly occurring natural polymorphs are 1Md, 1M, and 2M. 3T is a natural form but it is rarely found in nature. The various polymorphs are a result of different stacking of the 2:1 units caused by ordered rotations of structural layers in the a-b crystallographic plane (Smith and Yoder, 1956). Yoder and Eugster found that the 1Md structure is the initial phase and is meta-stable only at relatively low temperatures, while the 2M structure is the stable polymorph at temperatures exceeding 200°C - 350°C. The authors suggest that with increasing temperature and pressure the sequence of transformation is from 1Md to 1M to 2M.

Several authors have written papers on natural occurrences and transformations of illite polymorphs. Velde and Hower (1963) looked at the abundance of illite polymorphs in Paleozoic sediments and discovered that only 1Md and 2M structures are present in appreciable amounts. They found that the 2M is greatly concentrated in course size fractions, and in Paleozoic sediments is less abundant than the 1Md polymorph. Velde and Hower (1963, p. 1253) concluded that

> "illite is a mixture of materials, and assuming any disorded (1Md) material which was derived from the degradation during weathering of a high temperature (2M) progenitor, it would reconvert to 2M by potassium fixation in the marine environment. The 1Md material in the rocks investigated represent structures formed at low temperatures (100°C - 150°). Granting the assumptions made above, it appears that the majority of illitic material is of a low-temperature origin, probably having been formed at some stage of the sediment - lithification process".

Maxwell and Hower (1967) used illite polymorphs to show diagenetic and metamorphic trends across an area with differing stratigraphic depths. The study area is the Precambrian Belt Series in western Montana and Northern Idaho. Rocks in the western portion of the belt have been subjected to high pressures and relatively high temperatures due to extensive thicknesses which reach up to 38,000 feet which those in the east only achieve thicknesses of 4,500 feet. The 1Md polymorph is the dominant one in the eastern parts of the series, while in the thick western portions the 1Md decreases with increasing depths as the 2M polymorph increases and eventually is the only illite structure present.

> "Transformation from 1Md to 2M is attributed to increasing temperature and pressure accompanying deep burial, and perhaps aided by an increases geothermal gradient associated with a batholithic intrusion". (Maxwell and Hower, 1967, p. 855).

Results from this study are similar to both of the previously mentioned papers. The X-ray method of Maxwell and Hower (1967) was used to determine 2M polymorph percentages. Geologic settings from this study strongly resemble those investigated by Maxwell and Hower in that both areas contain sections of differing stratigraphic thicknesses.

In this study area, as in the Precambrian Belt of Montana and Idaho, the abundance of the 2M polytype increases with increasing grain size and stratigraphic depth. Table 15 and Figure 27 show that 2M polytypes are much more abundant in larger grain sizes. Figure 28 shows 2M polymorph percentages plotted on a sample location map of Georgia and Alabama. Percentages decrease from southeast to north and west. Figure 29 shows 2M percentages plotted against distances from reference point

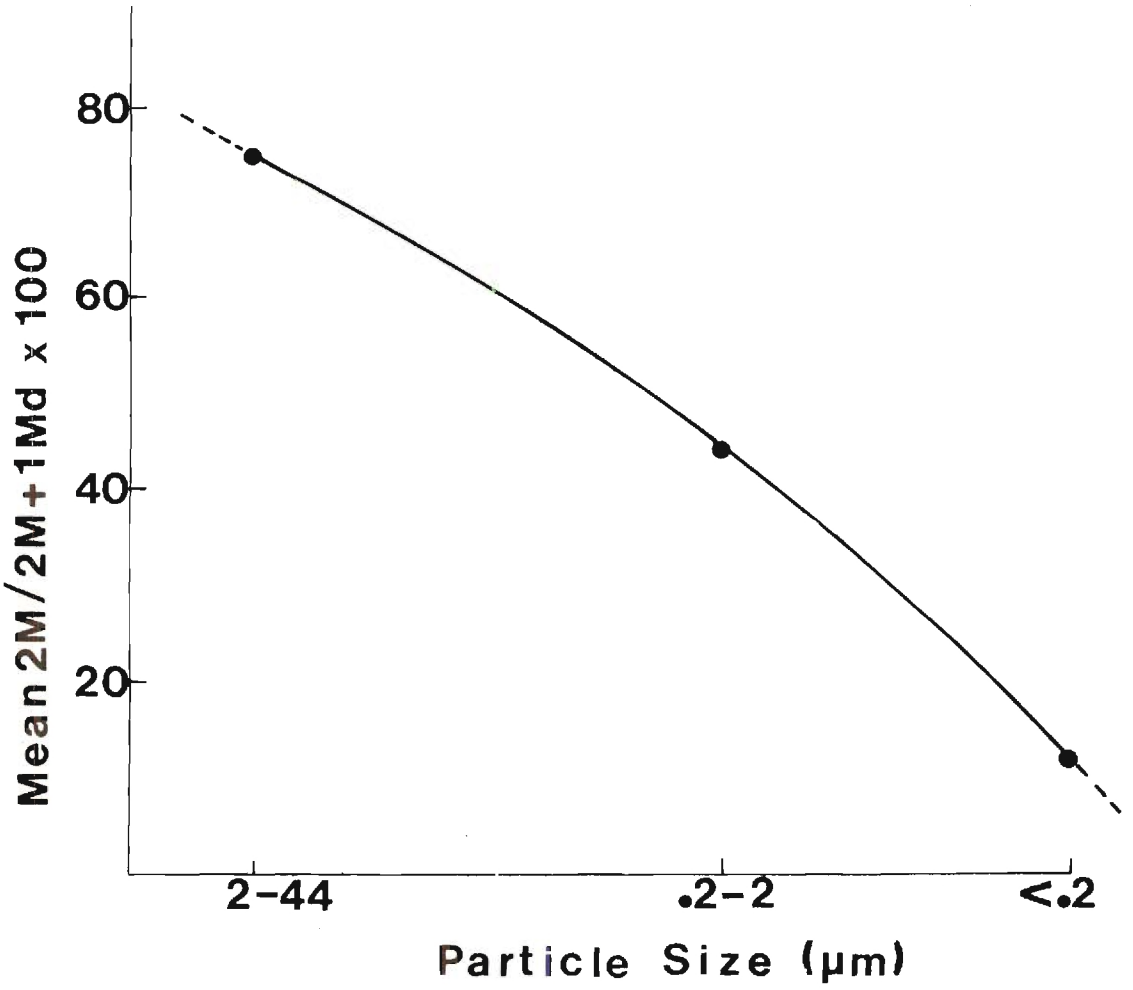

Figure 27. Increase in 2M Polytype with an Increase in Grain Size.

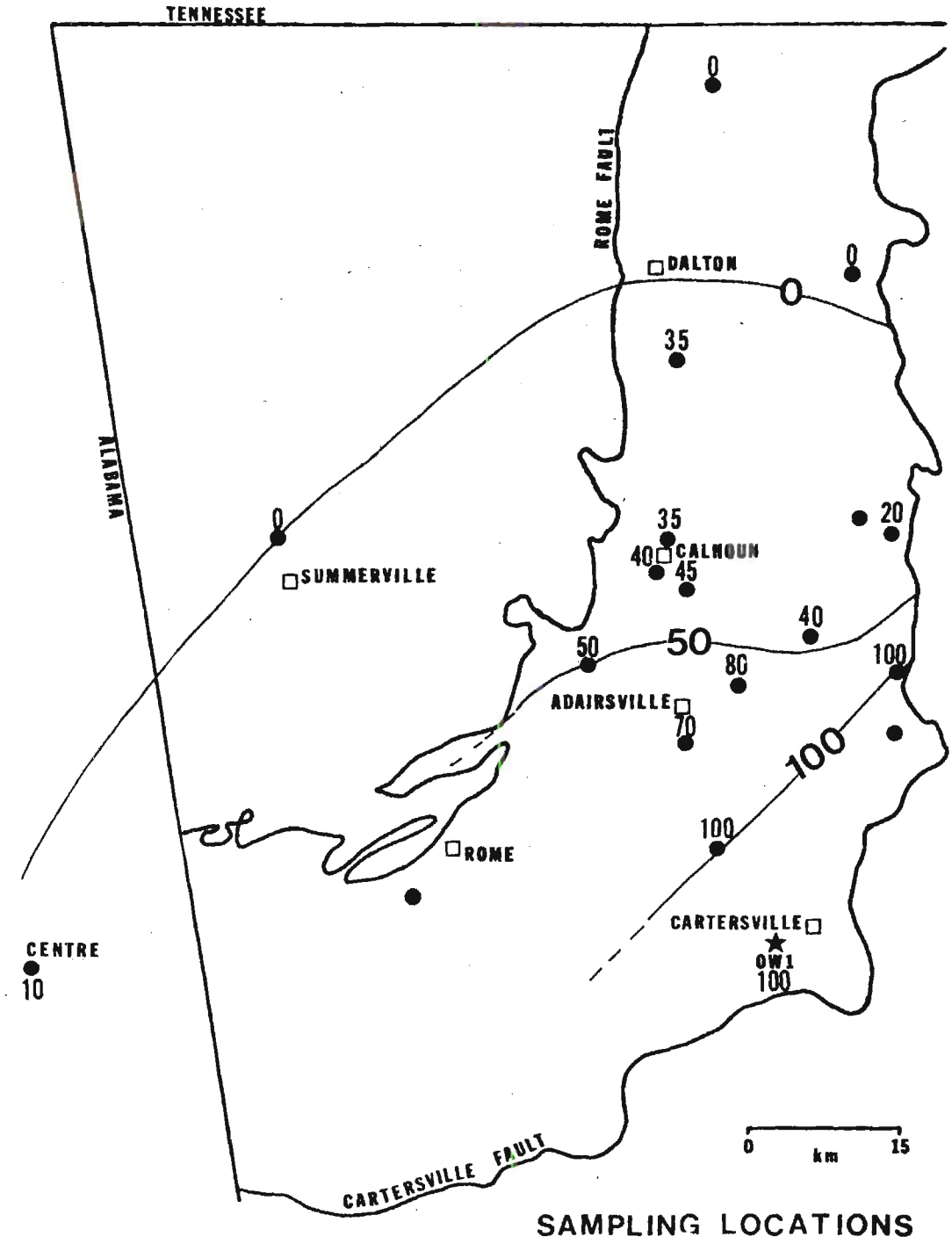

Figure 28. Contoured 2M Polymorph Percentages for the .2-2μm Fraction.

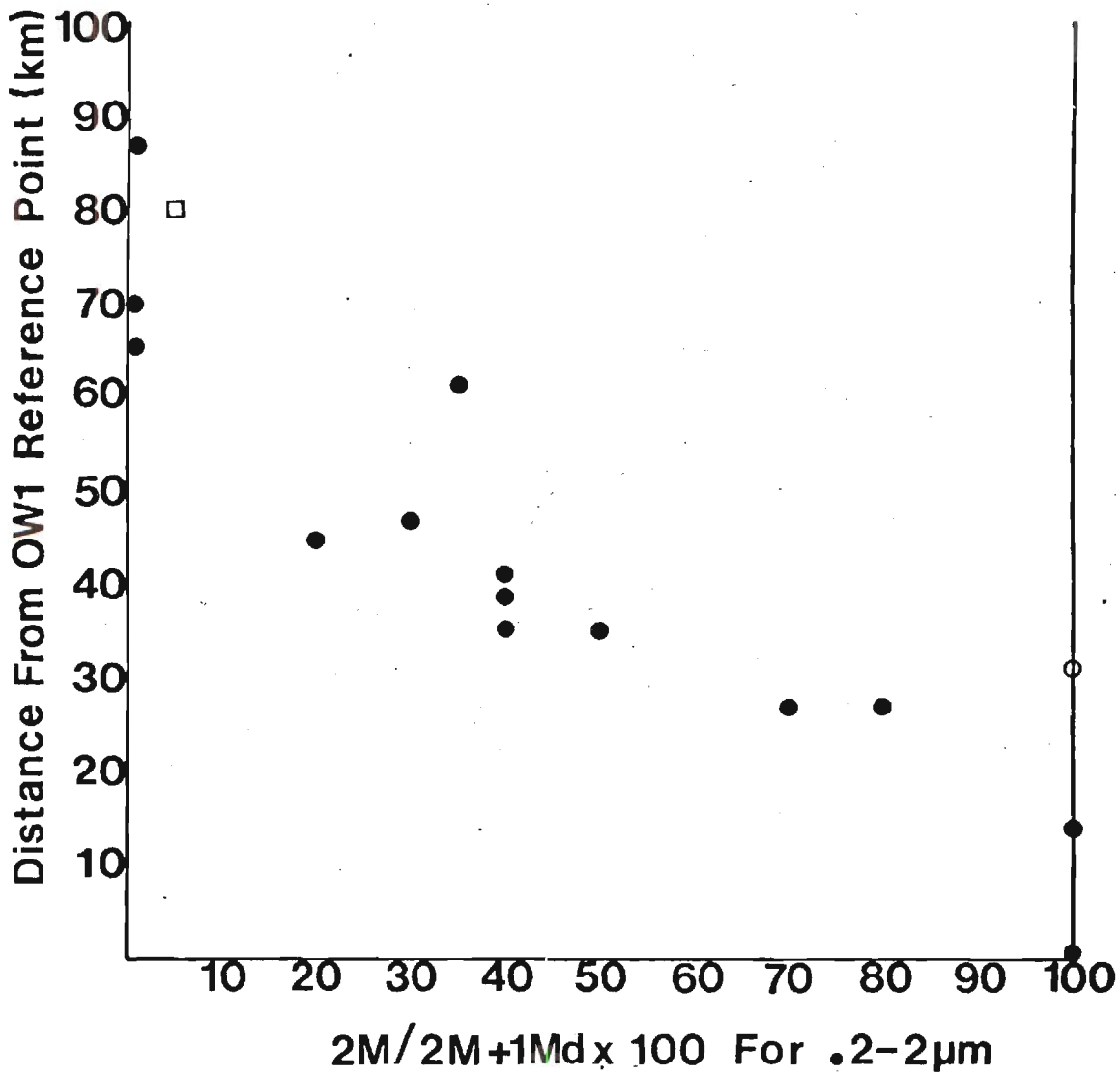

Figure 29. Variation in the 2M Polymorph for the .2-2µm Fraction.

OW1. Points that plot slightly off the trend can be explained by proximity to the Cartersville Fault, and presence of detrital muscovite and biotite. Sample OW3 (having 100% 2M) is close enough to the fault that it might have been slightly affected by frictional temperature and pressure associated with overthrusting. Detrital muscovite and biotite are present in OW23 which has a 2M percentage of 5. This value is really not far enough off the scale to be given special consideration, but the author feels that it should be mentioned because detrital micas, which formed at considerably higher temperatures than mica-like clays, could possibly give erroneous results.

Generally, illites which are not 2M have a 1Md structure. There is one exception (OW24), which has a 1M structure in all size fractions except the <.2μm. Theoretically, transformations are from 1Md to 1M to 2M. The possibility exists that this sample which is at an intermediate position between southeastern, western, and northern locales, is in that rare metastable form which occurs in the transformation of 1Md to 2M.

The <.2μm fractions have considerably less 2M material than larger sizes which stems from the fact that smaller grain sizes have a lower degree of crystallinity, and all of those grains which are small have not been recrystallized by diagenetic activities. This concept will be discussed in greater detail in the section devoted to crystallinity indices.

Figure 30 is a representation of the <.2μm fraction 2M percentage plotted on a sample location map depicting the position of samples in Georgia and Alabama. Only samples in the southeast have 2M polymorphs in this size fraction.

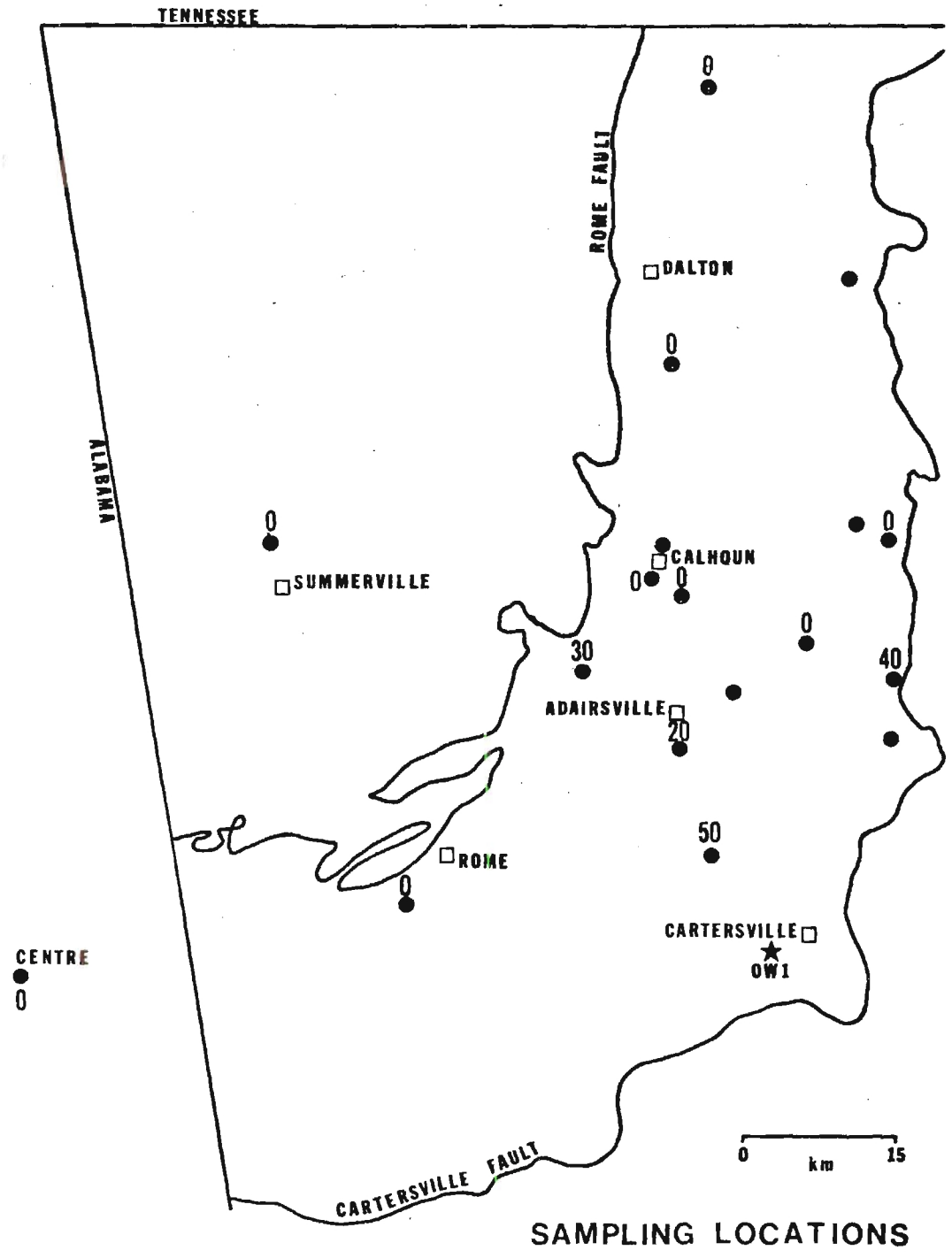

Figure 30. 2m Polymorph Percentages for the <. 2µm Fraction.

Sharpness Ratio

Weaver (1961a) used the sharpness ratio to determine correlations between lithologic, metamorphic, and tectonic divisions of the Ouachita Belt and adjacent foreland in Texas and Oklahoma. Previous to that study, the degree of metamorphism could only be determined by petrographic means, but with the use of the sharpness ratio determined by X-ray diffraction a more precise measurement could be made on clay minerals in particular. The sharpness ratio is a measurement of the 10 Å peak height divided by the height at 10.5 Å (Figure 6). "Since the low angle side is relatively constant measurements for both sides and a kurtosis value are not necessary"(Weaver, 1961a), p. 149). In his study Weaver found that sharpness ratio values range from less than 1 in unmetamorphosed foreland rocks, to more than 12 in metamorphic rocks of the interior Ouachita Belt zone. Table 15 shows the guide that Weaver used to define different grades of metamorphism. Foscolos and Stott (1975) have also proposed a diagenetic scale using sharpness ratios which is seen in Table 17. Foscolos and Stott used sharpness ratios to help determine degrees of diagenesis which have occurred in Lower Cretaceous shales of northeastern British Columbia. Tables 15 and 17 overlap somewhat and are similar except that Weaver has divided his to a greater extent and uses the terms weak and incipient metamorphism instead of different stages of diagenesis. Numbers differ slightly, but scatter, and slight inaccuracies are inherent in sharpness ratio measurements.

Gill, Khalaf, and Massoud (1977), showed a general increase from southeast to northwest in the sharpness ratio following an increase in coal rank and grade of metamorphism in the South Wales Coalfield.

Table 16. Average Sharpness Ratios in Subsurface Rocks of the Ouachita Belt in Texas (Weaver, 1961a).

	Average S.R.
Low-grade metamorphism	12.1
Weak to very weak metamorphism	6.3
Incipient to weak metamorphism	4.5
Incipient metamorphism	2.3
Unmetamorphosed	1.8

Table 17. Diagenetic Stage and Sharpness Ratio Correlation (Foscolas and Stott, 1975).

	Average S.R.
Early diagenesis	1.5
Middle diagenesis	1.9
Late diagenesis	2.3
Metagenesis or Anchizone	2.3 - 12.1

Table 18. General Characteristics of the Diagenetic Zones in the South Wales Coal Field (Gill, et al., 1977).

Zone	Rock Type	Coal Range Type	Fixed Carbon Percent	Illite S.R.	Illite I.R.	I-M Expandable Percent
I Diagenetic Zone	Carbonate	High and Medium Volatile	65	2.1-2.5	-	40-35
	Terrigenous		80	2.1-3.0	.31-.40	-
II Metadiagenetic Zone	Carbonate	Low Volatile	80	2.5-3.2	-	35-20
	Terrigenous	Steam	90	3.0-4.0	.40-.41	-
III Anchimetamorphic Zone	Carbonate			3.2-4.0	-	20-0.0
		Anthracites	>90			
	Terrigenous			4.0-6.0	.111-.53	-

Changes are somewhat controlled by the lithologic character of the sediments. Sharpness ratios increase to a greater extent, and at a faster rate in terrigeneous sediments, than in carbonates (Table 18). Gill et al. (1977) divided the coal field into 3 zones (diagenetic, metadiagenetic, and anchimetamorphic). The anchimetamorphic zone was established by correlating sharpness ratios with coal rank, while the other two were organized by correlating sharpness ratios with the illite 002/001 intensity ratio, and expandibility of illite-montmorillonite mixed-layered material.

Several other authors (van Moort, 1971; Gavish and Reynolds, 1970; and Foscolos and Kodama, 19731) have used Weaver's sharpness ratio and have established results similar to those of the previously discussed papers.

In this study, five size fractionations were examined, and results show that there is a general increase in the sharpness ratio with increasing grain size. Averages of the <.2μm, .2-2μm, ≤2μm, ≤4μm, and 2-44μm fractions for Georgia-Alabama samples are 3.0, 11.9, 7.5, 9.9, and 12.0 respectively. The author believes that when oriented slides are prepared by sedimentation the finest particles of each fraction will be on uppermost portions of the slide, and will be the predominant grains hit by the X-ray beam. This is believed to be the case for discrepancies between the ≤2μm, .2-2μm, and <4μm sizes, and for this reason the ≤2μm and 4μm fractions have been omitted from Figure 31 which is a plot of mean sharpness ratios for Georgia-Alabama samples with respect to particle sizes. Mean values for 2-44 m, and .2-2μm fractions are very close, and then a decrease is seen in <.2μm fractions. Each size fraction

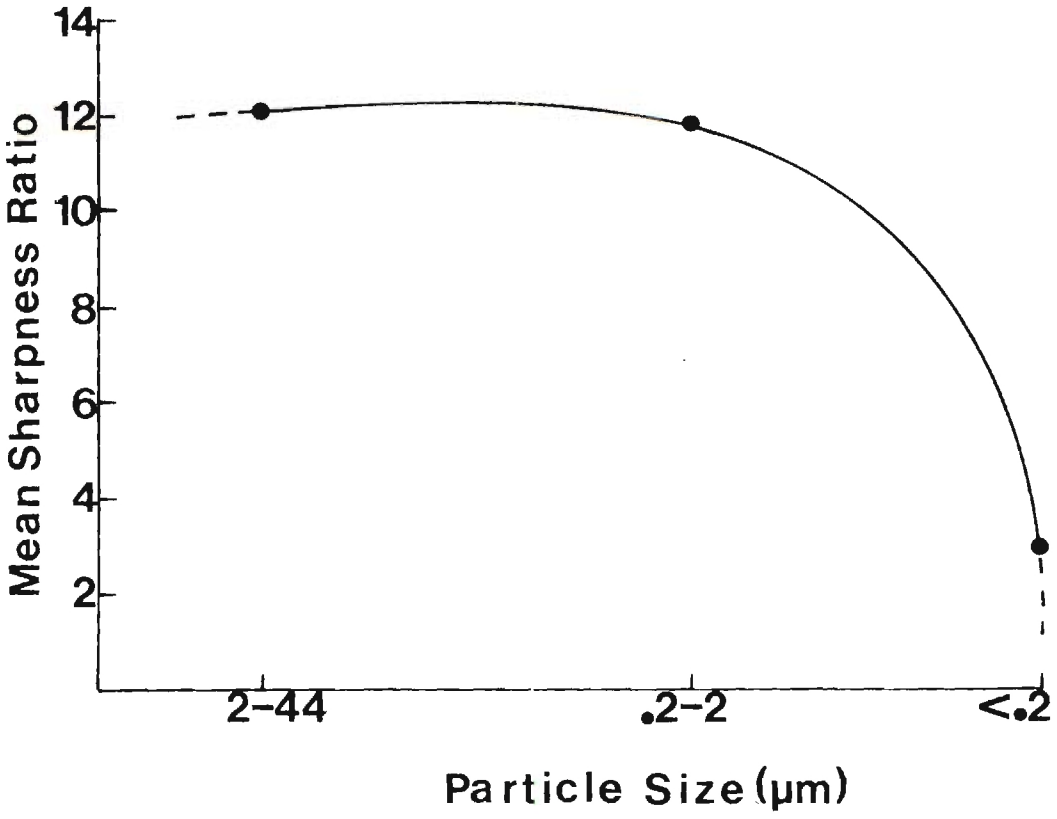

Figure 31. Increase in Mean Sharpness Ratio with an Increase in Particle Size.

displays different values for sharpness ratio measurements, but all show the same general trend which is a decrease in sharpness ratios with increasing distance from reference point OW1 (Figures 32, 33, 34, 35, and 36). Figure 32 shows sharpness ratios plotted for sample locations in Georgia and Alabama. Notice how sharpness ratios decrease from southeast to north and west.

Figures 37, 38 and 39 are diagrams of sharpness ratios from Tennessee samples. All values are rather low, and fall within the unmetamorphosed - early to middle diagenesis range on the scales of Weaver (1961a) and Foscolos and Stott (1975).

Crystallinity Index

The crystallinity index was first proposed by Kubler (1966) as a simple assessment of the crystallinity of 10 Å illite. It is a measurement of the width (in mm) at half height above background level of the 10 Å peak (Figure 5). The crystallinity index is inversely proportional to a minerals crystallinity, in other words, the index value decreases with increasing crystallinity.

Kubler states several advantages and disadvantages of using crystallinity indices: A) The crystallinity index is quick and easy to measure. B) The measurement is independent of peak height. C) Crystallinity indices are independent of statistical fluctuations of the diffractometer. D) Numbers are easily compared.

A disadvantage is that the measurement depends on experimental conditions and instrumental settings. All of the numbers in this study are used as relative values, and instrument settings remainded constant.

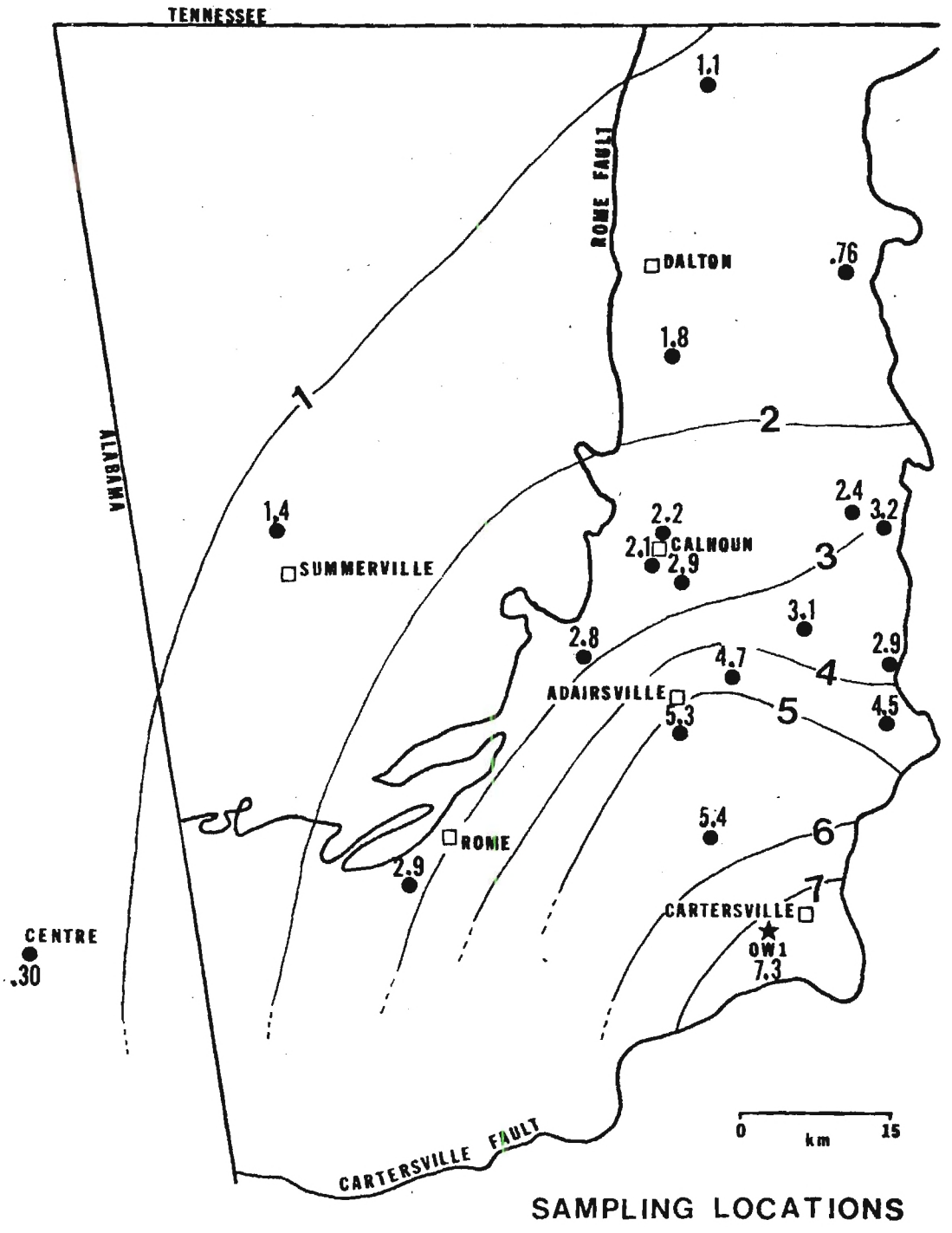

Figure 32. Contoured Sharpness Ratios for <.2μm Fraction.

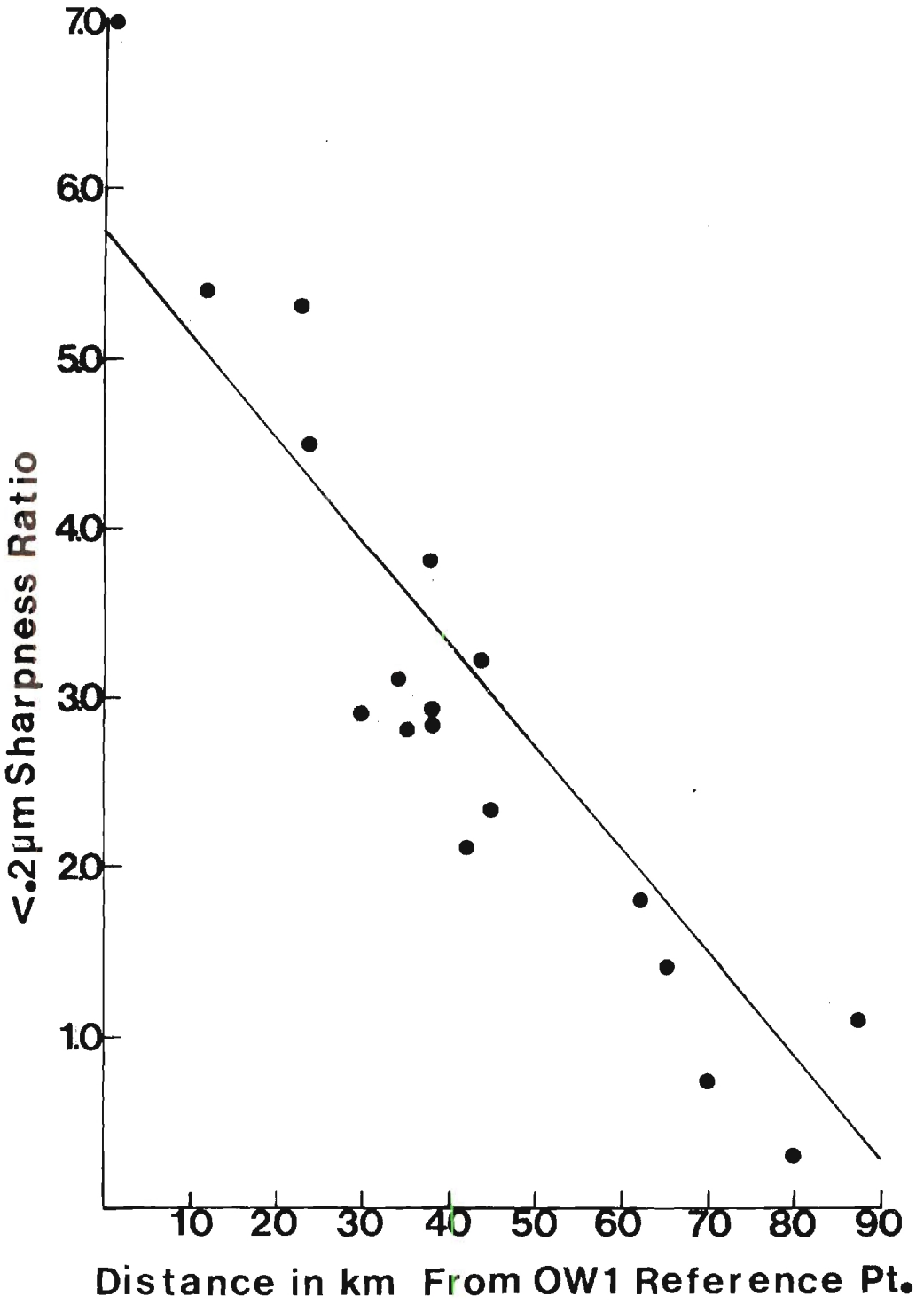

Figure 33. Variation in Sharpness Ratio for the <. 2µm Fraction. (y = -.06x + 5.74, C.C. = -8.36)

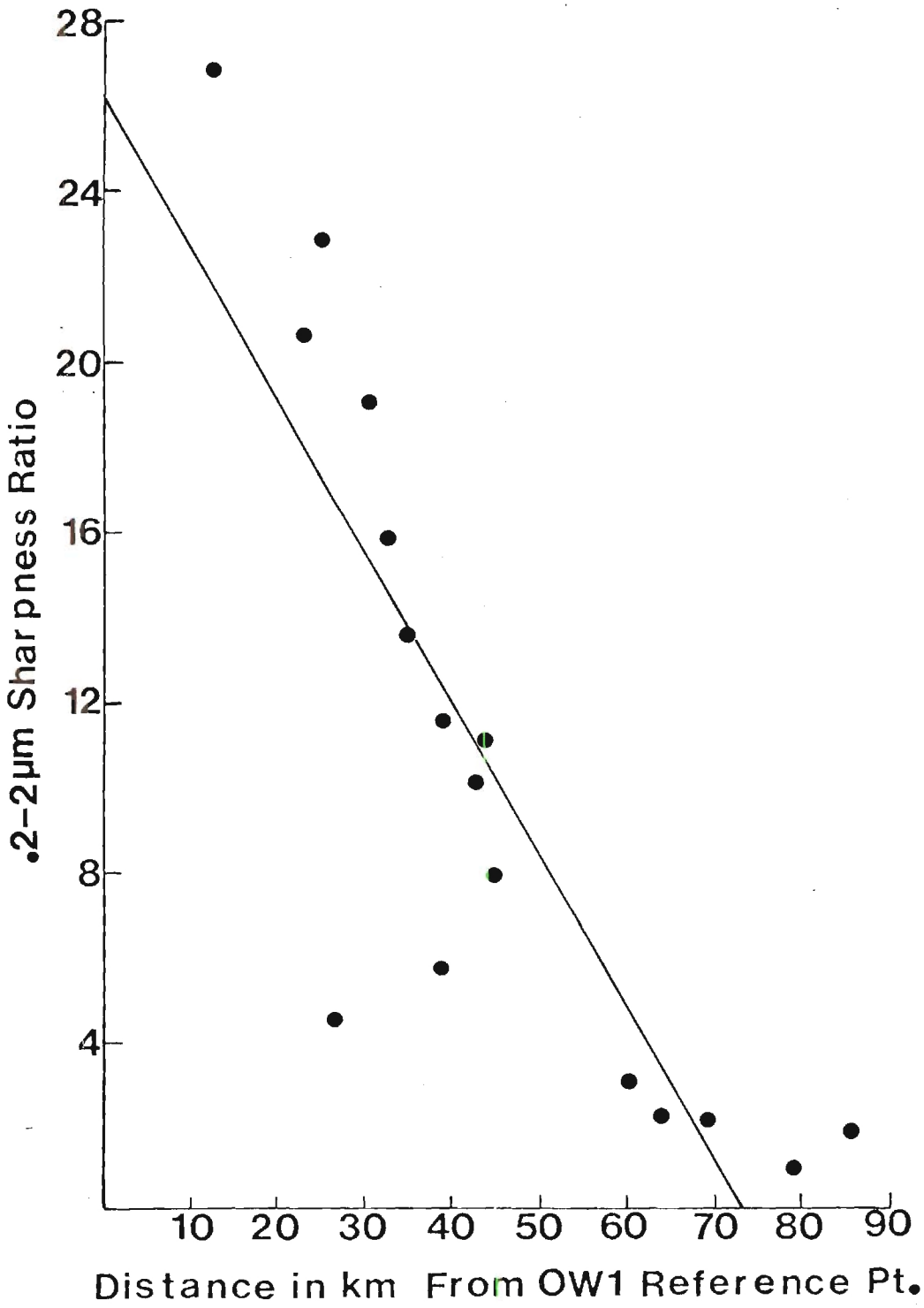

Figure 34. Variation in Sharpness Ratio for the .2-2µm Fraction. ($y = -.35x + 26.02$, C.C. = -.865).

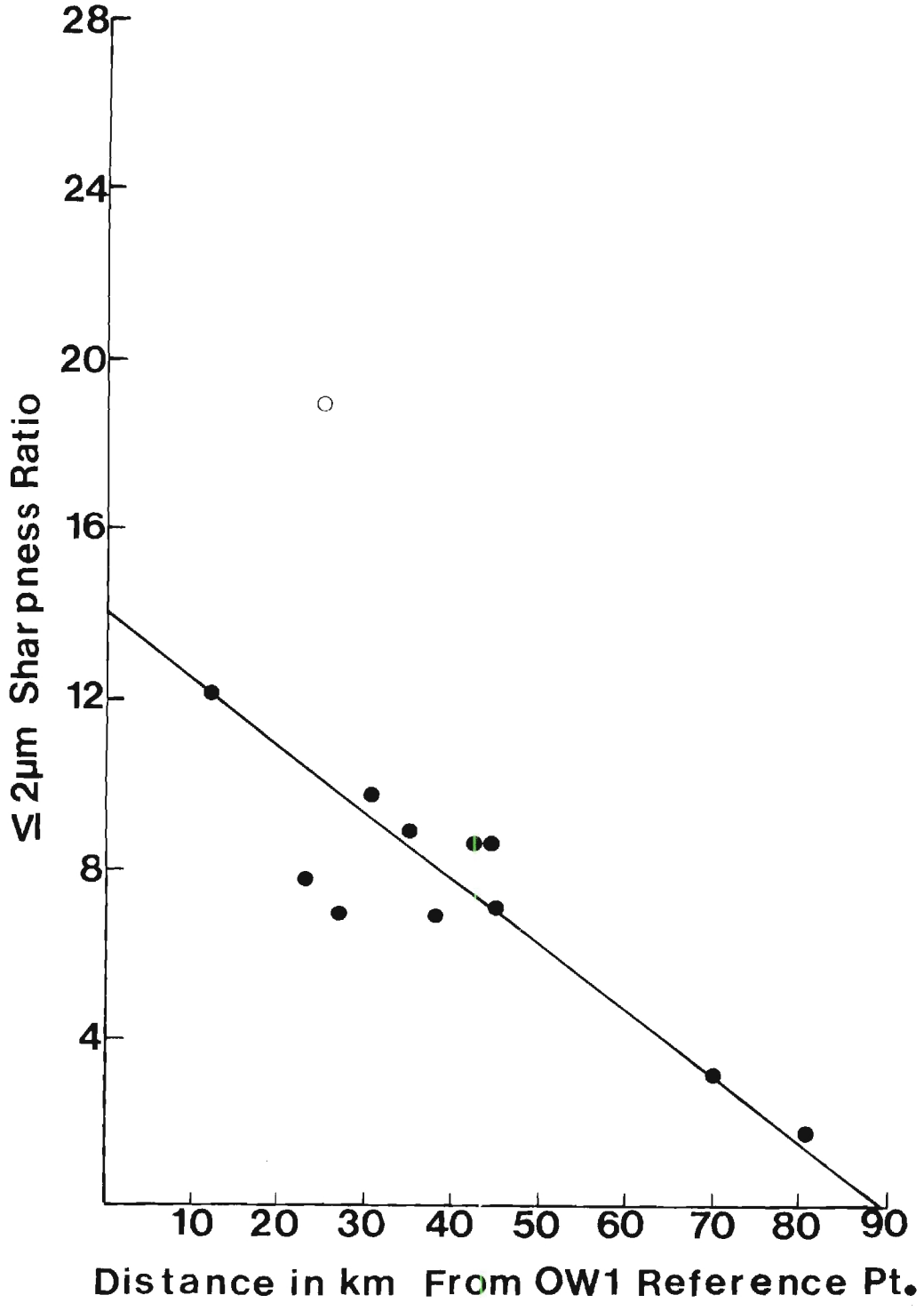

Figure 35. Variation in Sharpness Ratio for the ≤2µm Fraction.

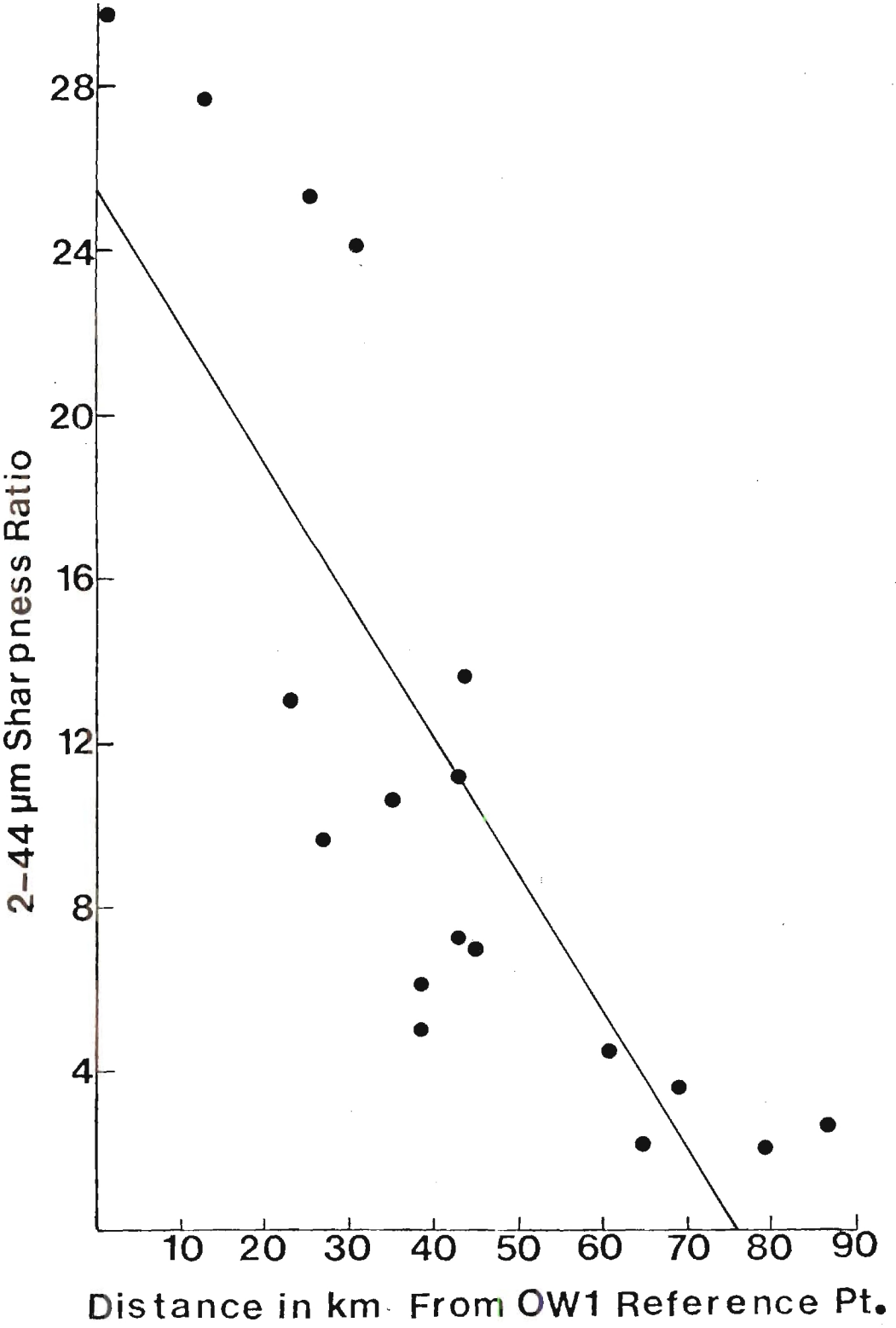

Figure 36. Variation in Sharpness Ratio for the 2-44µm Fraction. (y = -.33x + 25.38, C.C. = -.819)

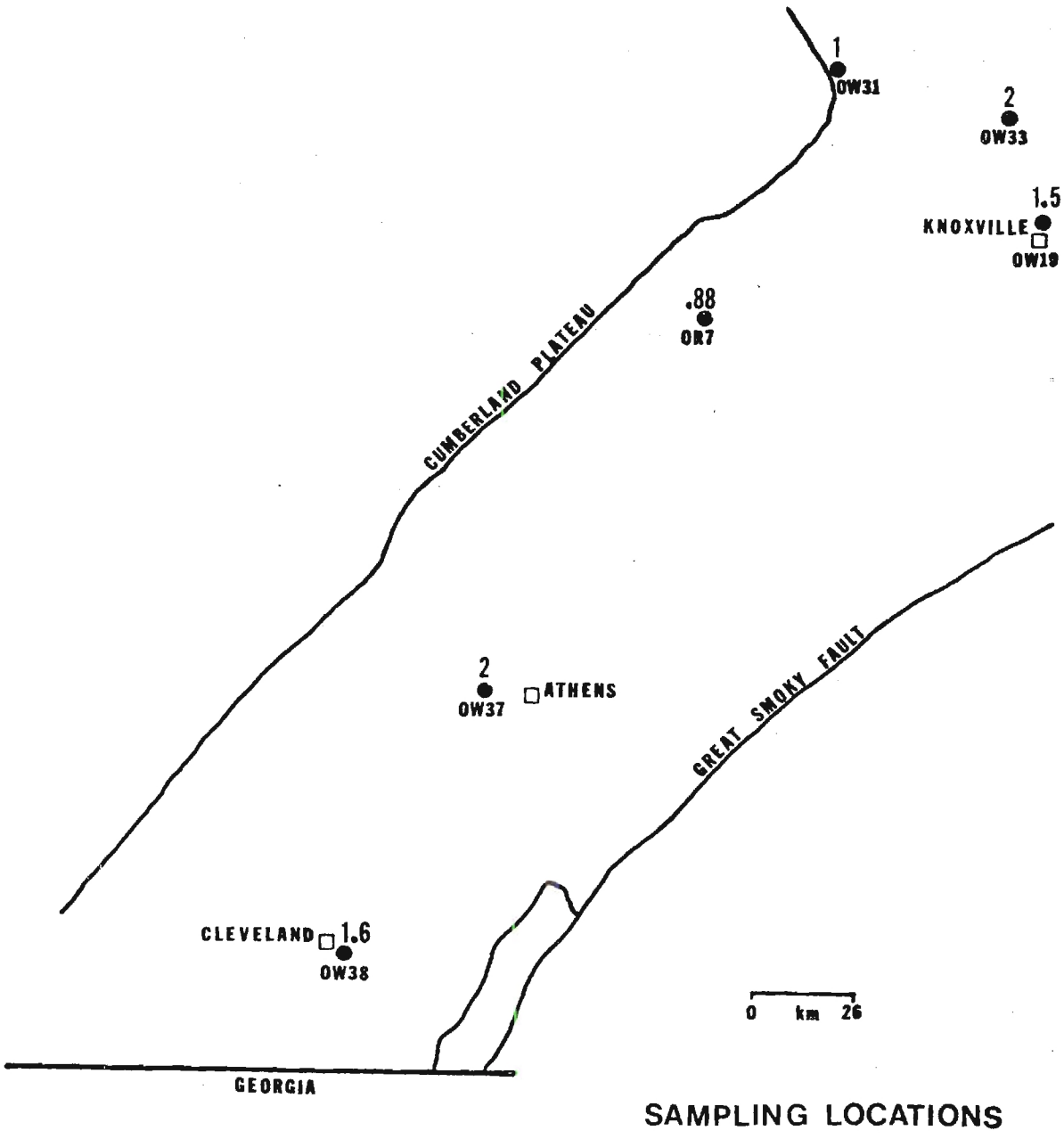

Figure 37. Sharpness Ratio of the <.2μm Fraction for Tennessee Samples.

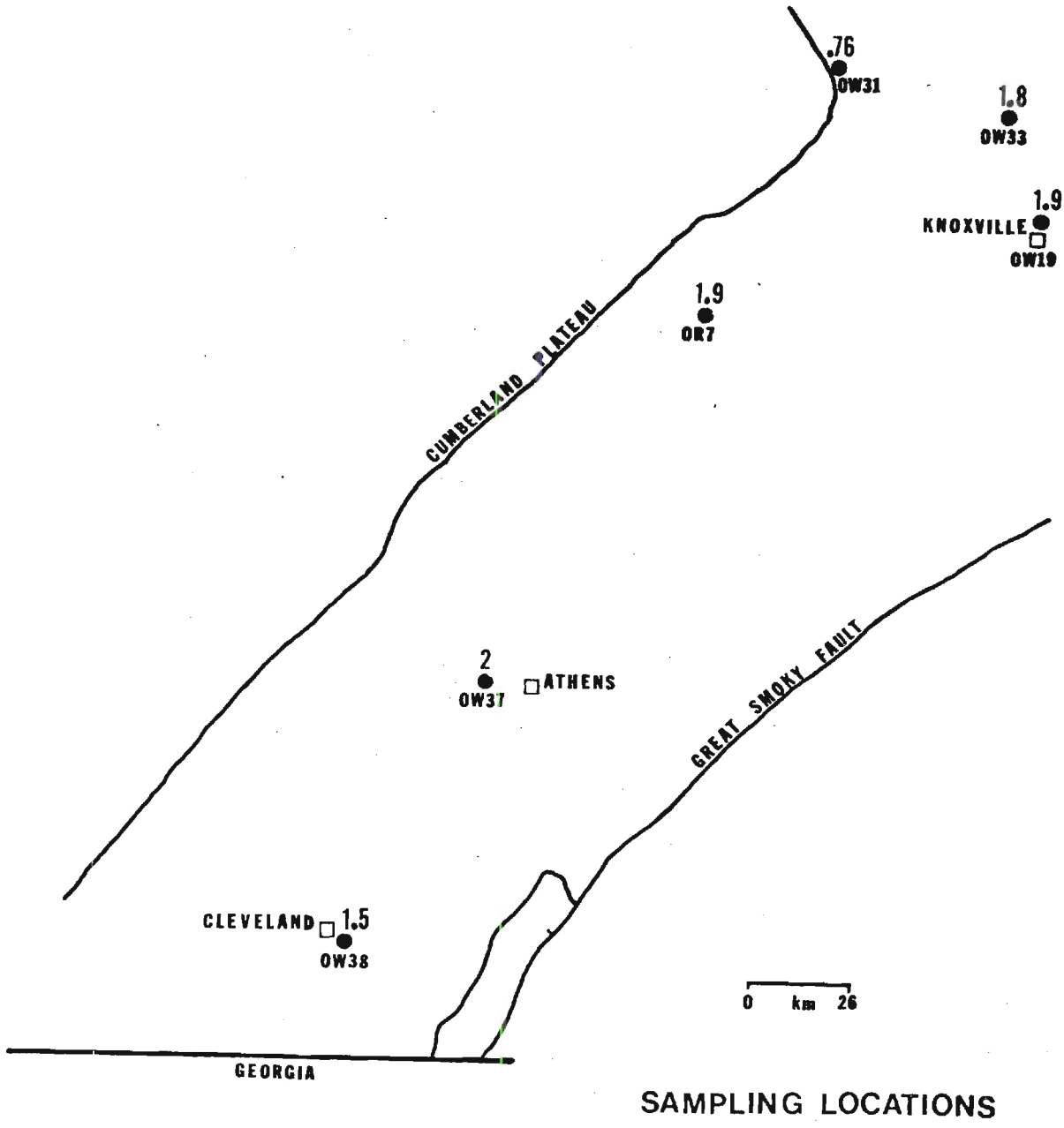

Figure 38. Sharpness Ratio of the .2-2μm Fraction for Tennessee Samples.

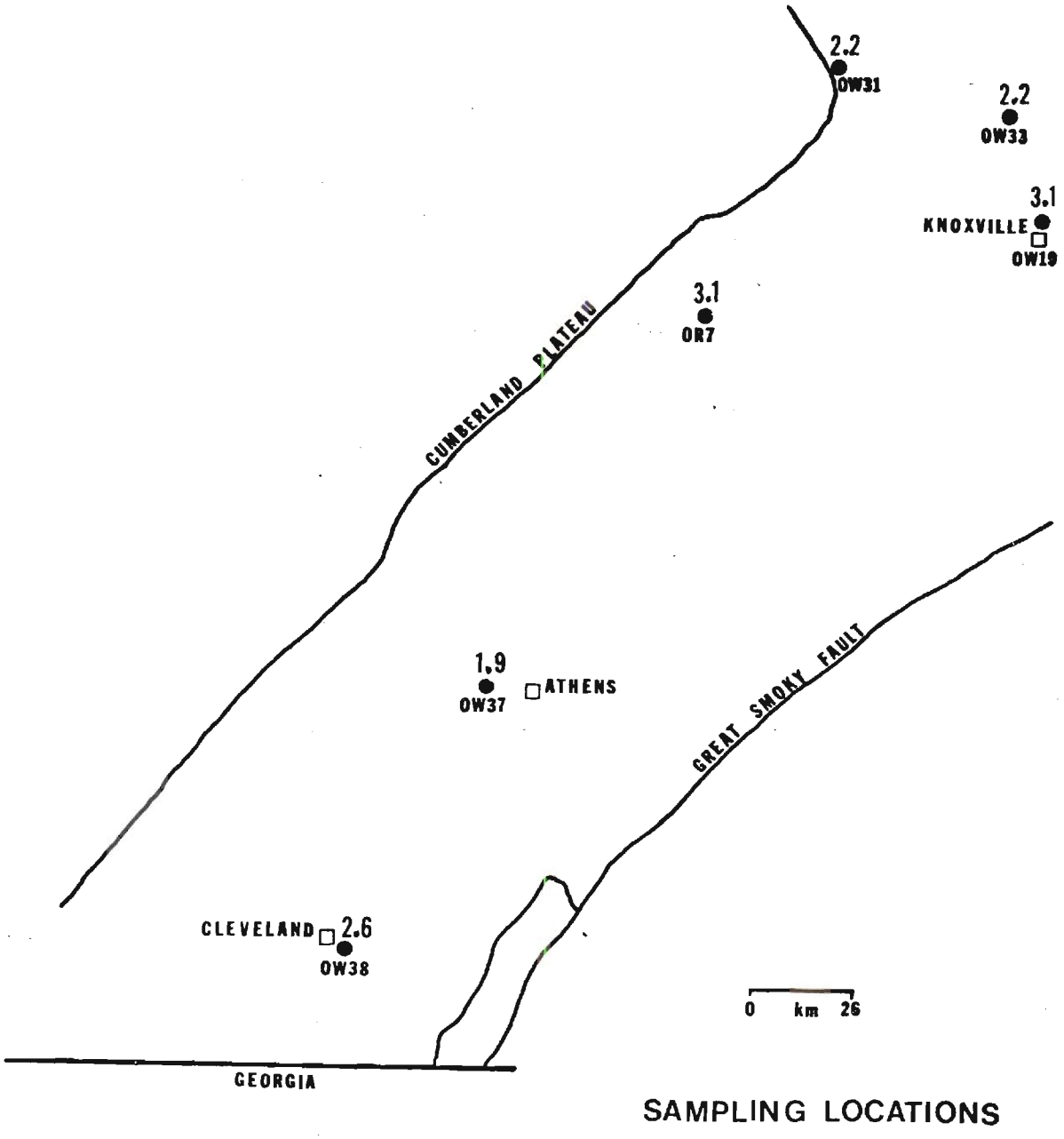

Figure 39. Sharpness Ratio of the 2.44μm Fraction for Tennessee Samples.

The crystallinity index is a working relative value which can be used to approximate degrees of diagenesis or metamorphism which a sediment has reached. It has been used by many authors, but most notibly (Dunoyer de Segonzac and Abbas, 1976; Weber, 1972; and Foscolos and Kodama, 1973). The crystallinity index values of the illites examined in this study decrease with increasing size fraction indicating that mineral crystallinities increase with increasing size fraction. The mean value for <.2μm, .2-2μm, and 2-44μm fractions is 3.4, 2.2, and 1.3 respectively for all Georgia-Alabama samples. There are several possibilities why such a trend is apparent in this and other studies. A crystallinity measurement on an illite (001) reflection can be thought of as largely a measure of structural regularity of an illite crystallite in the c-axis direction. Structural regularity can be diminished by the presence of interlayered montmorillonite or other units or by crystal defects. Also, for very small particle sizes (less than 0.02 microns; Jackson, 1956, p. 208), peak broadening begins to occur. Smaller grain sizes have greater temperature sensitivity and therefore will be altered first by diagenetic processes. During heating accompanying burial metamorphism the trends to be expected would be a decrease in montmorillonite layers in illite/montmorillonite and recrystallization of smaller crystallites into larger crystallites. Both of these factors would result in increased crystallinity and thus smaller crystallinity index values. Another factor to consider in the data interpretation is that the degree the burial the higher the degree of lithification; this could have the result of having a crystallite that is less than 0.2 micron in size before burial moved into the 0.2 to 2.0 micron size fraction after

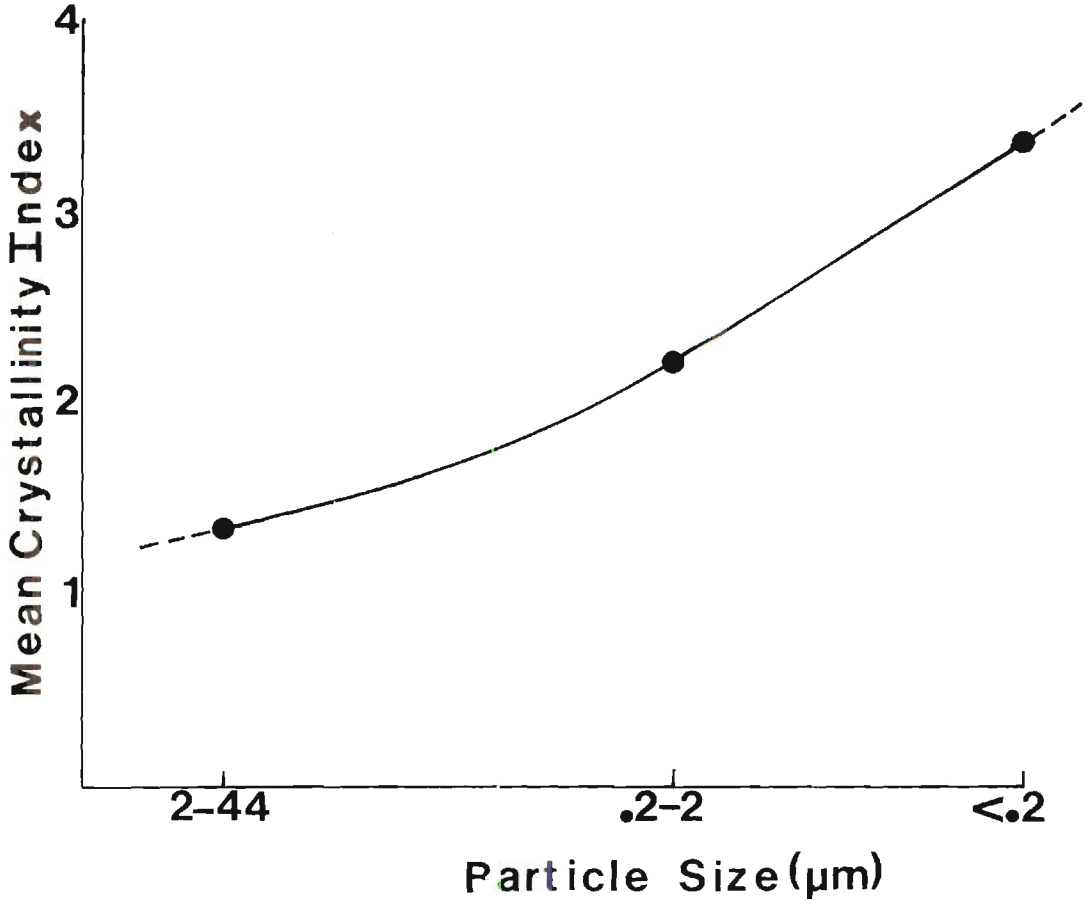

Figure 40. Increase in Mean Crystallinity Index with a Decrease in Particle Size.

burial due to cementation with other crystallites even though its real crystal size has not increased. Data from this study can be interpreted using the above model.

Figure 41 shows fraction percentages for the <.2μm fraction plotted on a sample location map for Georgia and Alabama. Fraction percentages are low in the southeast and increase to the north and west. Figure 42 shows the percent abundance of the <.2μm fraction vs. distance from OW1. The .2-2μm and 2-44μm fraction are similarly represented in Figure 43. The results are not as astounding as the <.2μm, but it is apparent that higher percentages of larger grain sizes are found in the southeast. The .2-2μm fraction shows the same directional slope as the <.2μm fraction and the 2-44μm fraction exhibits an opposite tendency. It is possible that finer grain sizes are a product of mechanical breakdown from larger grains which occur during grinding procedures. If this were the case then some of the softer accessory minerals (feldspars) would be expected to be found in the finest fraction. Feldspars are only present in the .2-2μm, and 2-44μm fractions, and therefore mechanical breakup of particles is probably not sufficient enough to alter size fraction percentages. This author tends to believe the first case concerning small grain sensitivity.

In all size fractions the trend is a decrease in crystallinity (increase in crystallinity index) from southeast to west, and north (Figures 44, 45, 46 and 47). Sample OW1 has the lowest crystallinity index, while samples OW8 (northern most in Georgia), OW12 (northwestern most in Georgia), and OW23 (western most) have the highest crystallinity indices. Remaining samples fall somewhere in between. Relationships

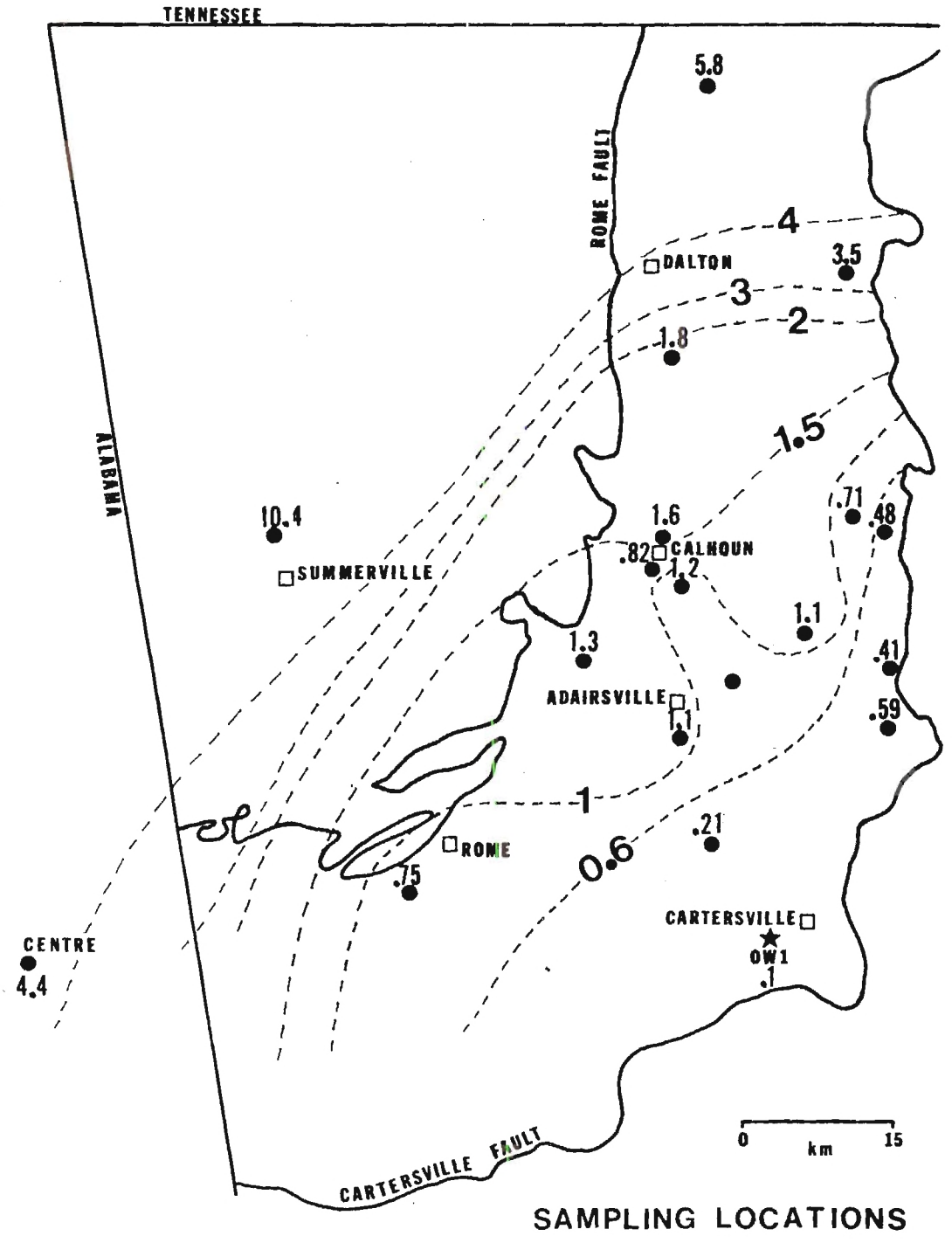

Figure 41. Contoured <.2µm Fraction Percentage.

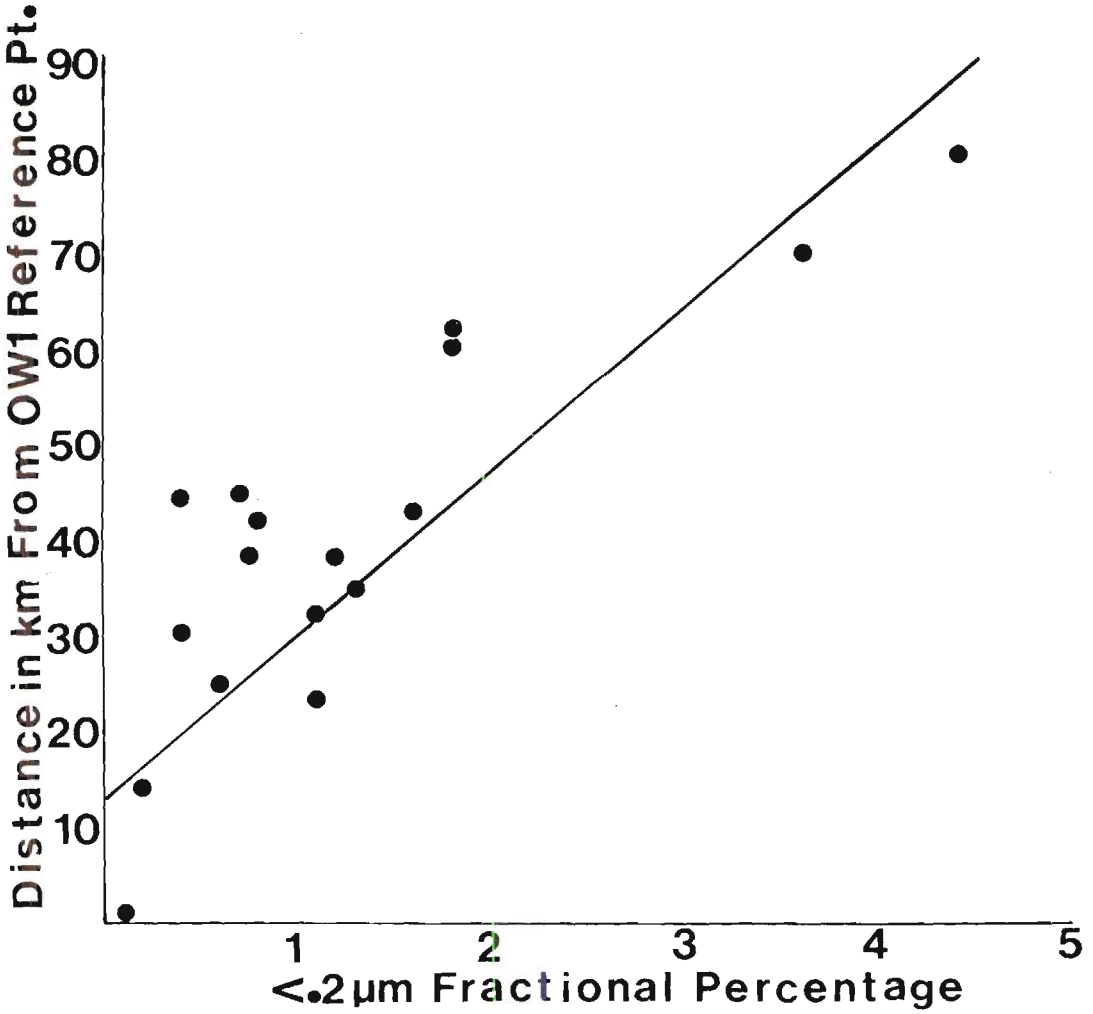

Figure 42. Variation in <.2µm Fraction Percentage.
(y = 16.66x + 13.5, C.C. = .877)

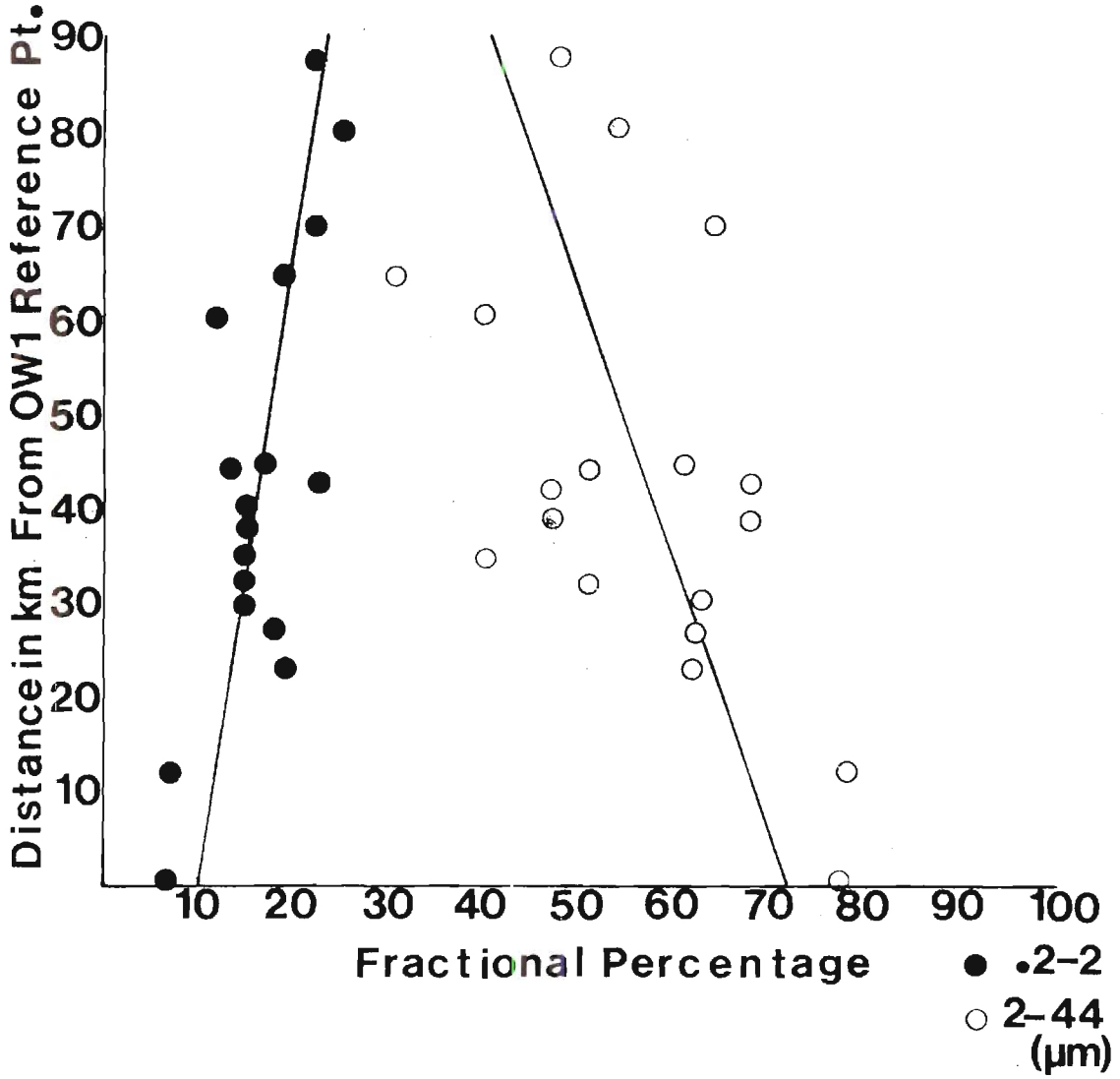

Figure 43. Variation in .2-2μm and 2.44 Fraction Percentages.
(y = 6.66x + -66.86, C.C. = .704)
(y = -2.94x + 210, C.C. = -.574)

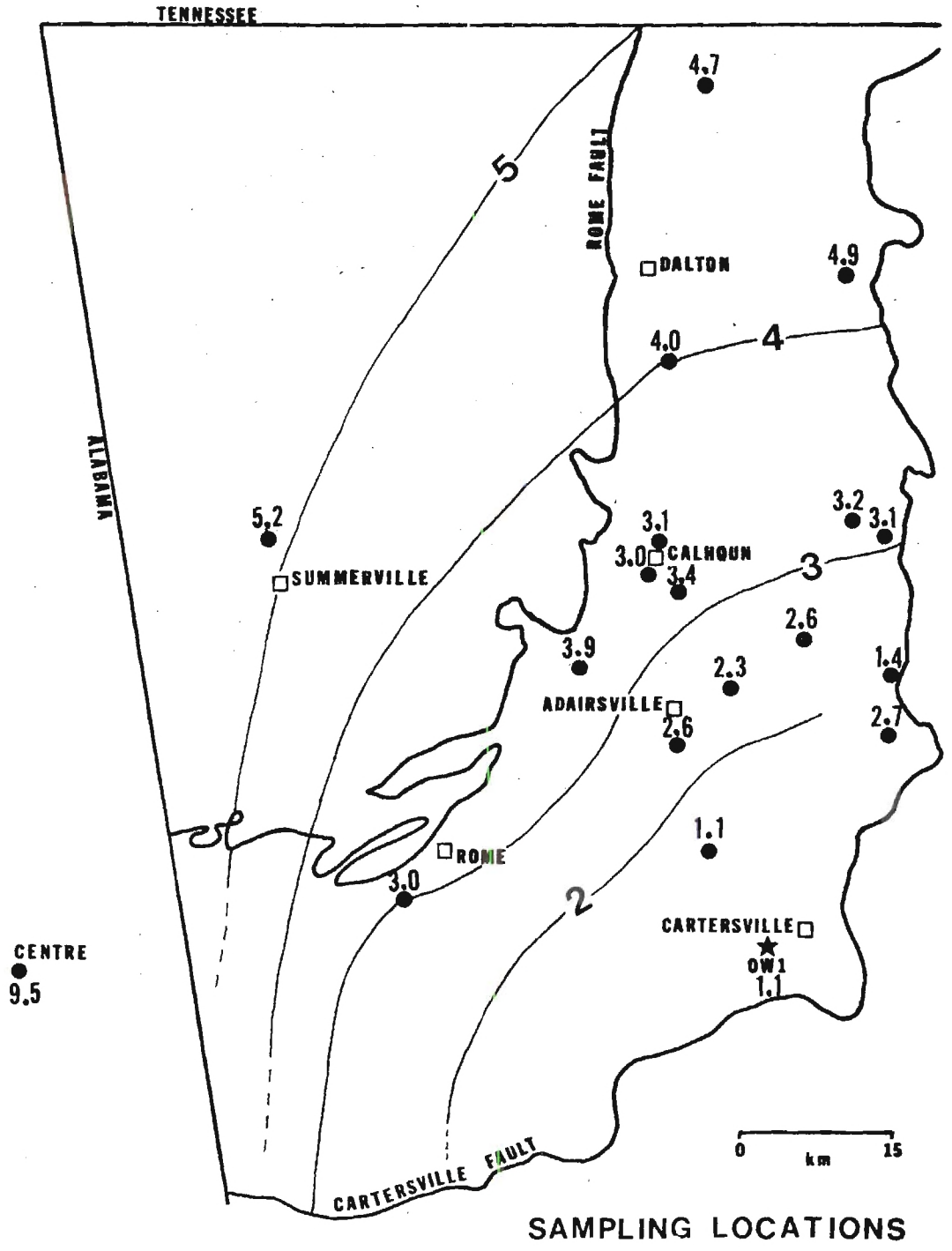

Figure 44. Contoured Crystallinity Indices for <.2μm Fraction.

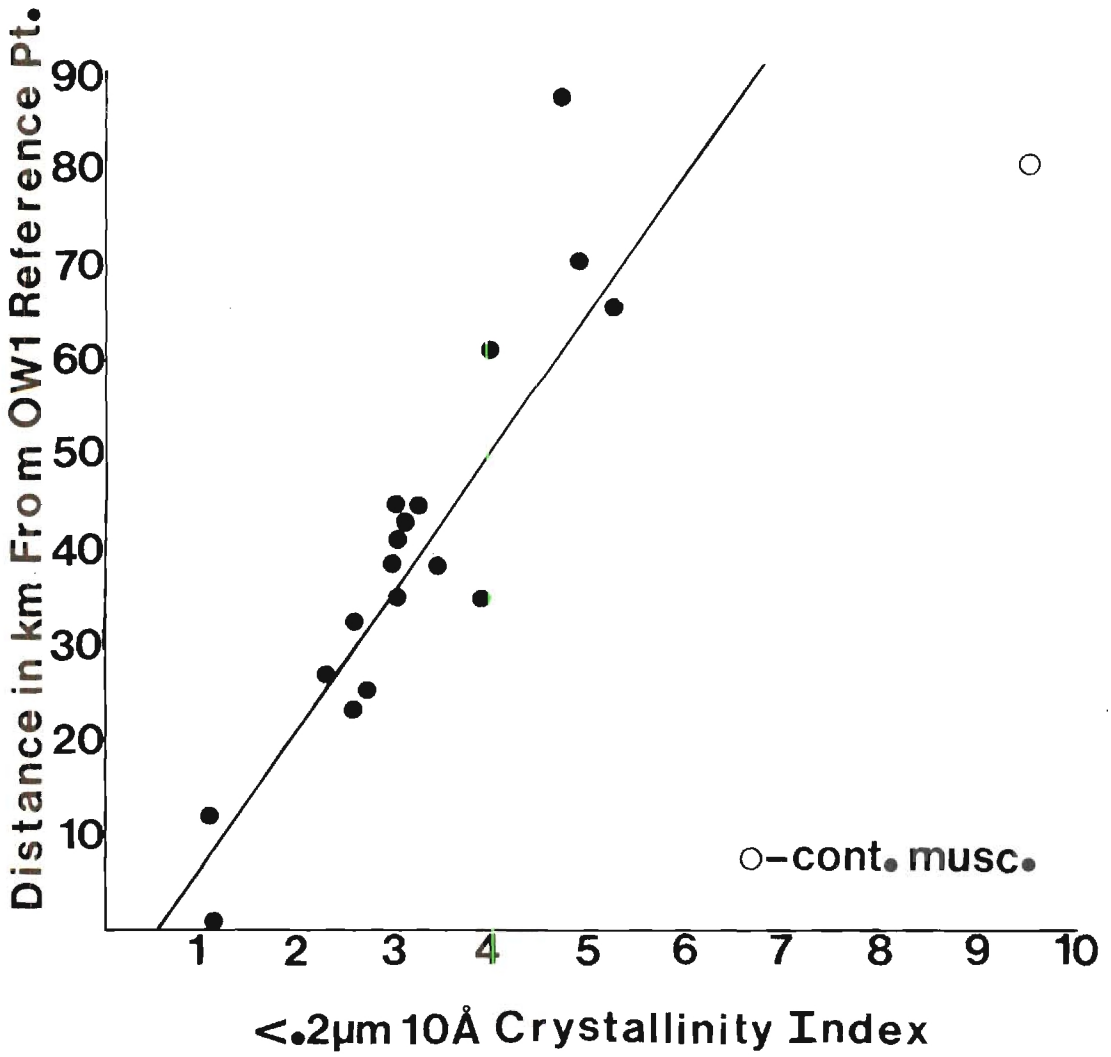

Figure 45. Variation in <.2µm Crystallinity Index.
(y = 14.28x + 7.14, C.C. = .825).

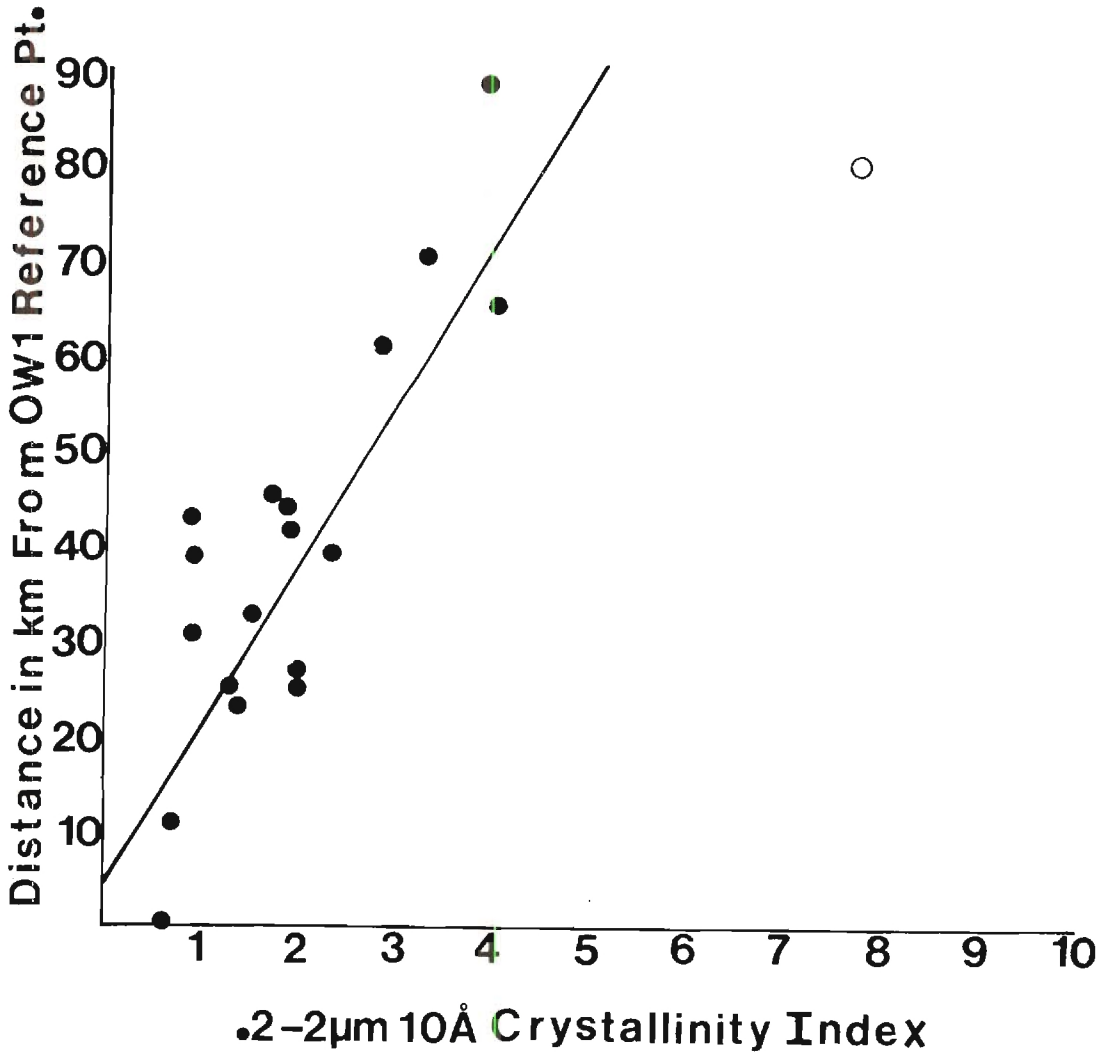

Figure 46. Variation in Crystallinity Index.
(y = 16.66x + 4.83, C.C. = .796).

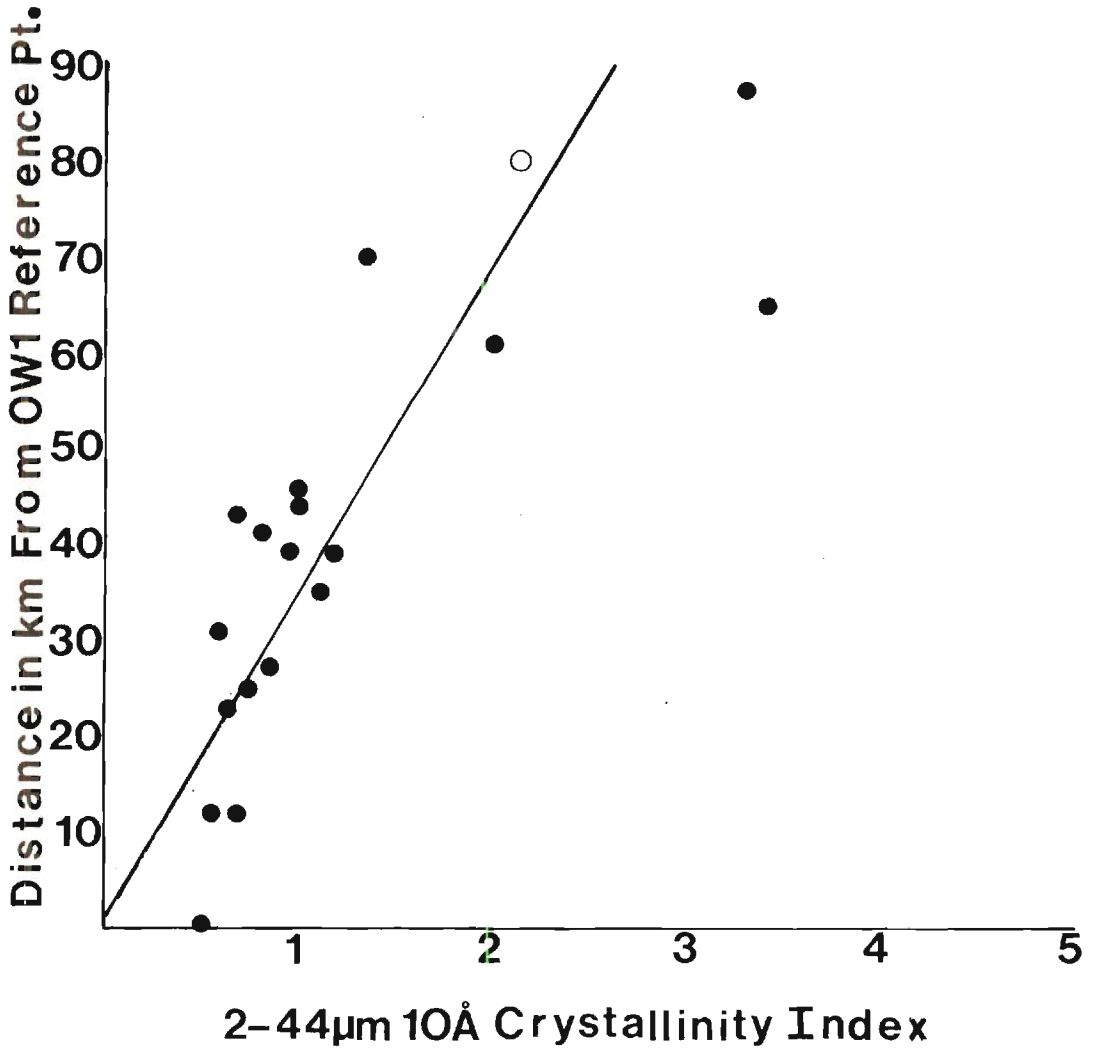

Figure 47. Variation in 2-44µm Crystallinity Index.
(y = 3.33x + 1.33, C.C. =.816)

show that samples in the southeastern area have undergone greater diagenetic changes than those in the north, northwest, and west. Sample OW23 falls slightly off the trend, and this is probably due to some contamination from detrital muscovite.

Tennessee samples do not show a discernible geographic trend, although all numbers are quite high (Figures 48, 49 and 50). Sample OW31, which is the northern most sample has the highest value. Detrital muscovite and biotite may contribute to the variation seen in these samples.

Figure 51 shows a plot of the difference in crystallanity indices between the <.2μm and 2-44μm fractions. Figure 52 shows the same relation versus distance from reference point OW1. The increase in crystallinity difference with an increase in distance to the west and north suggests that some of the coarse illite is detrital, or that fine fraction material in the west and north has been affected less by diagenetic activity than those in the southeast. At higher temperatures and pressures where more fines have been influenced by diagenesis, those sizes (<.2μm, and 2-44μm) have been effected homogeneously, and show less of a difference in crystallinity indices.

Intensity Ratio 002/001 Illite Basal Reflections

The degree of crystallinity of illite is dependent on its chemical composition. Esquevin (1969) proposed that the intensity ratio of illite 5 $\mathring{A}$/10 $\mathring{A}$ peaks (002/001) which gives an estimate of the relative amounts of Aℓ in the octahedral layers, plays an important role in the recrystallization of illite. Weaver (1965) presented data to indicate the 002/001 ratio was a measure of the amount of K in illite. Both K + Aℓ

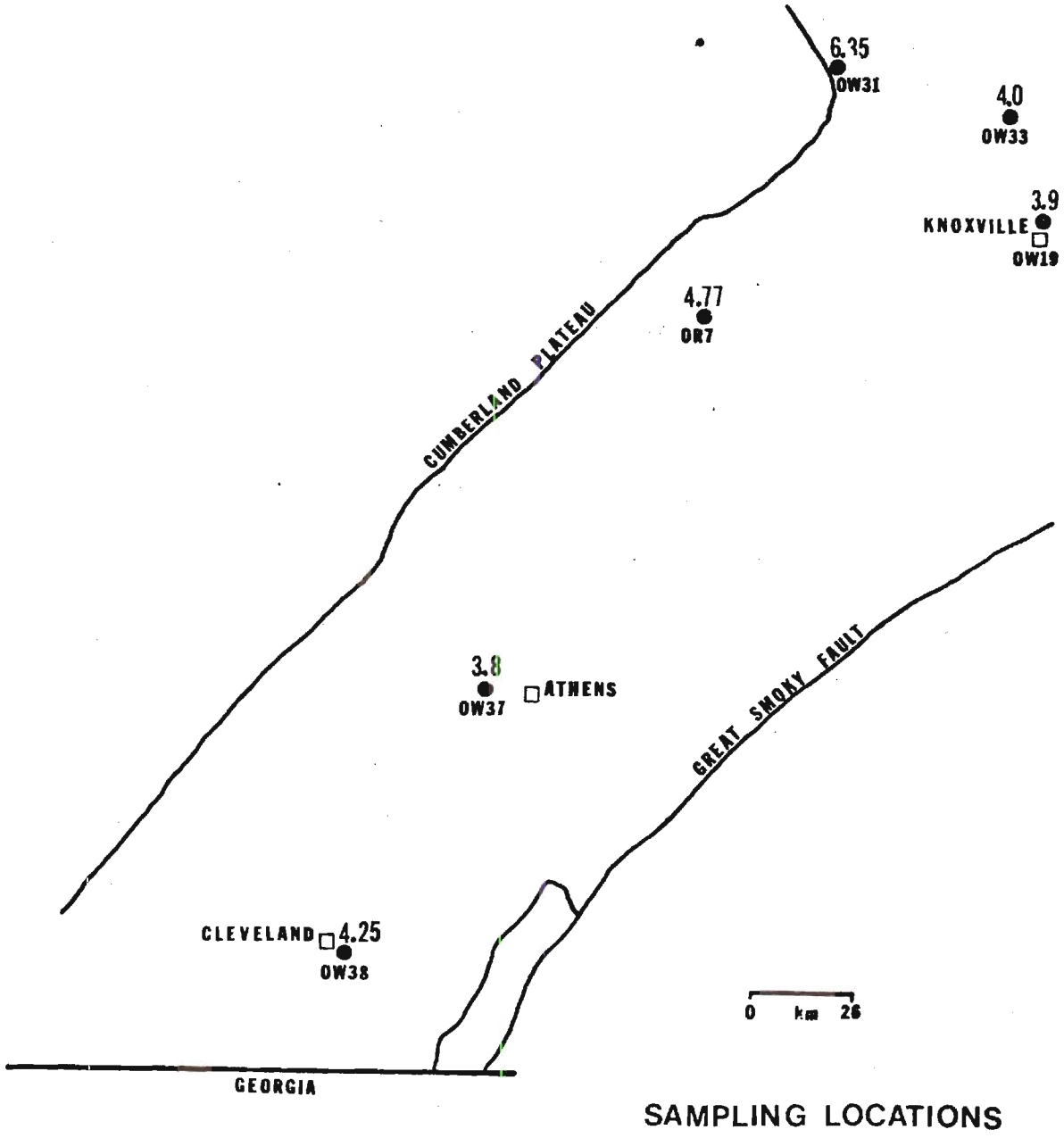

Figure 48. Crystallinity Index of the <.2μm Fraction For Tennessee Samples.

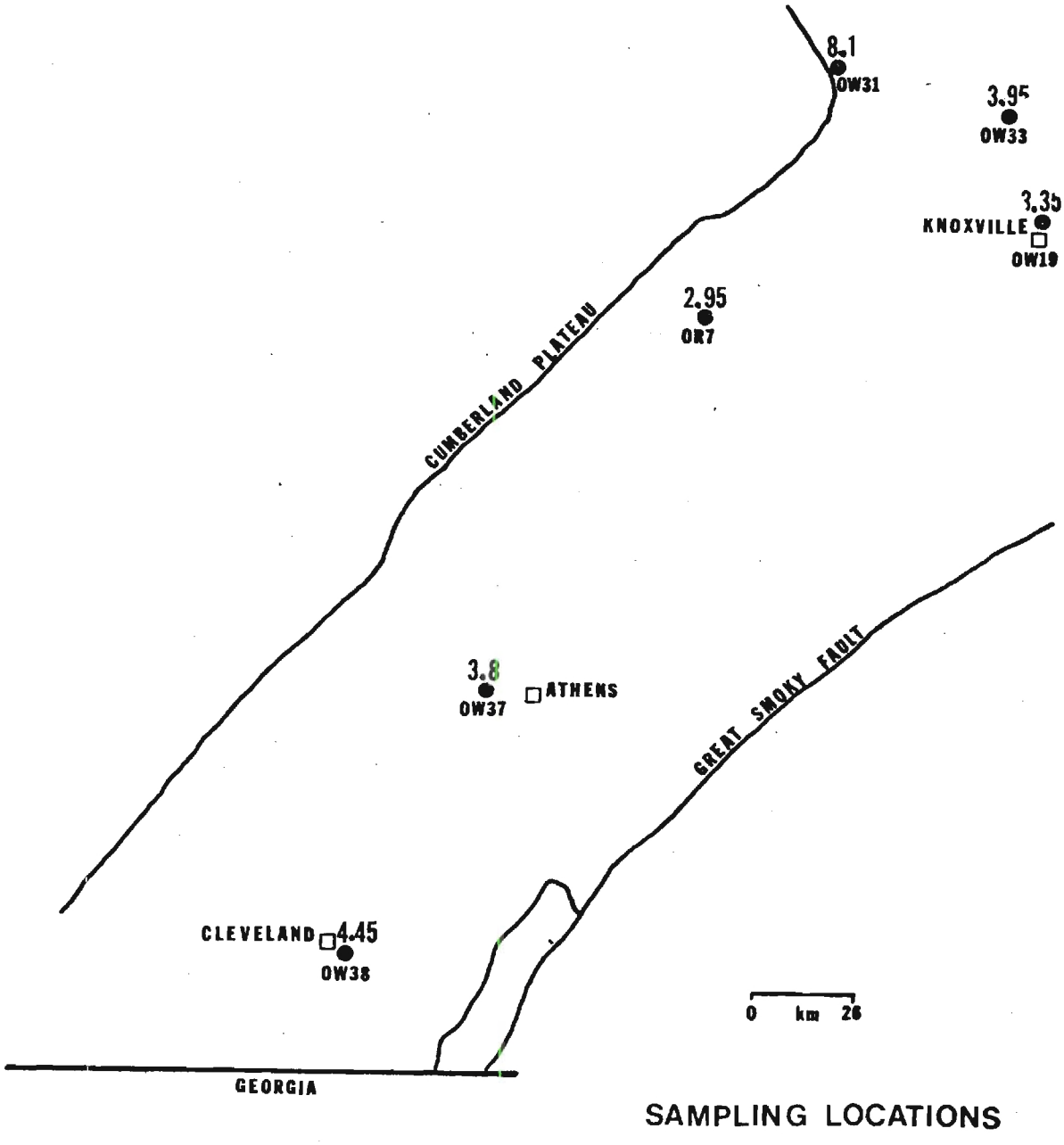

Figure 49. Crystallinity Index of the .2-2μm Fraction for Tennessee Samples.

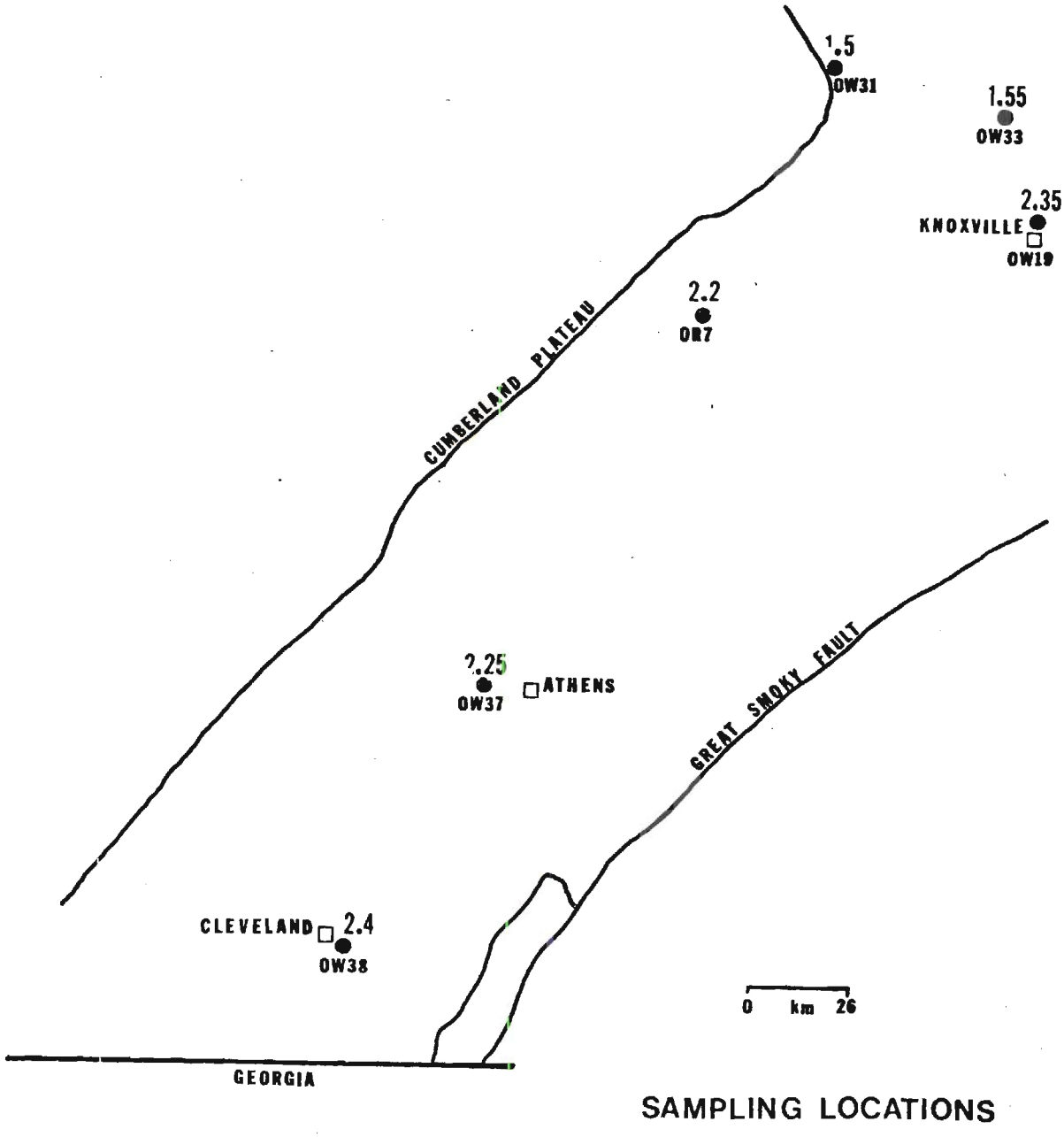

Figure 50. Crystallinity Index of the 2-44μm Fraction for Tennessee Samples.

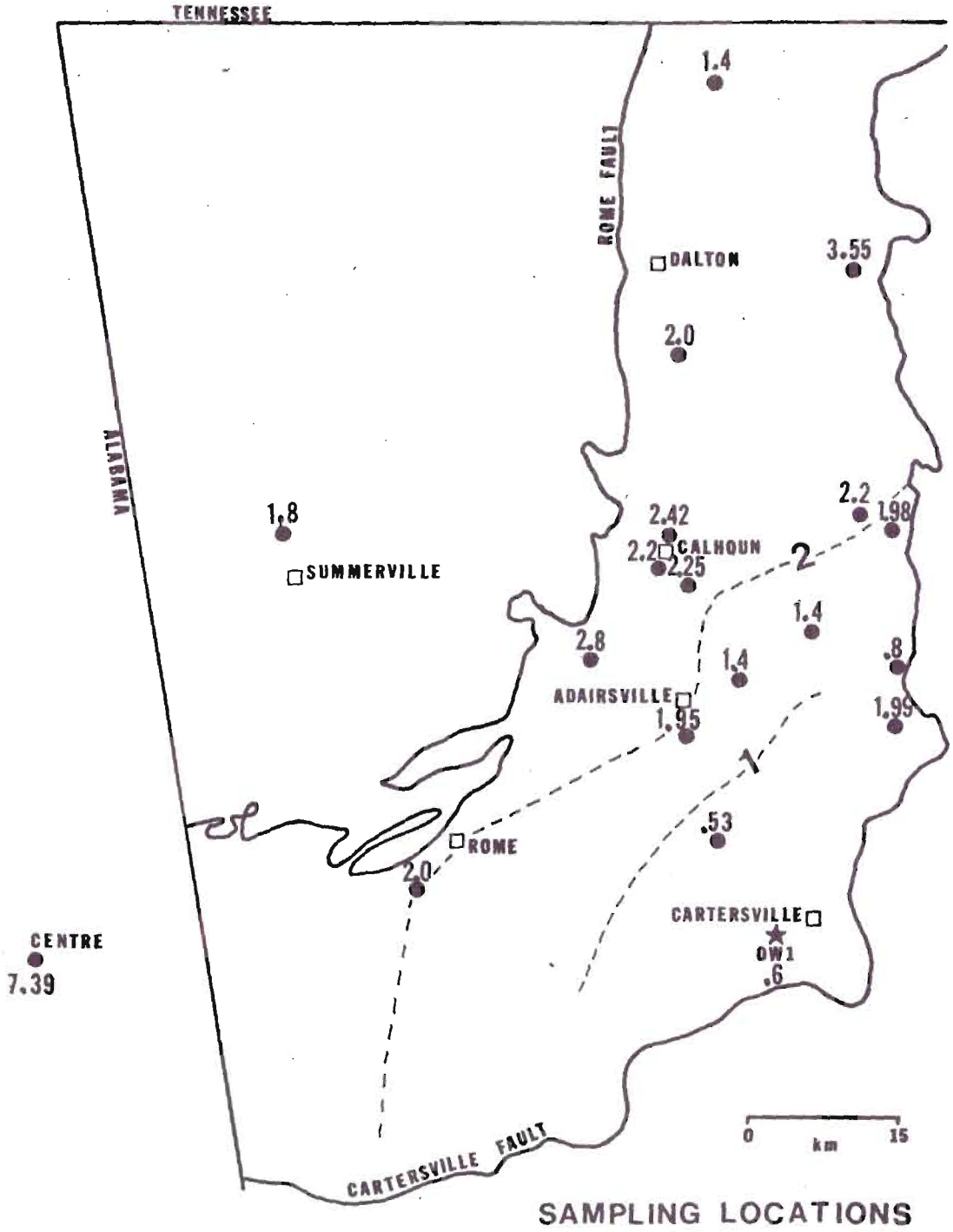

Figure 51. Contoured Difference in Crystallinity Indices from <.2μm to 2-44μm.

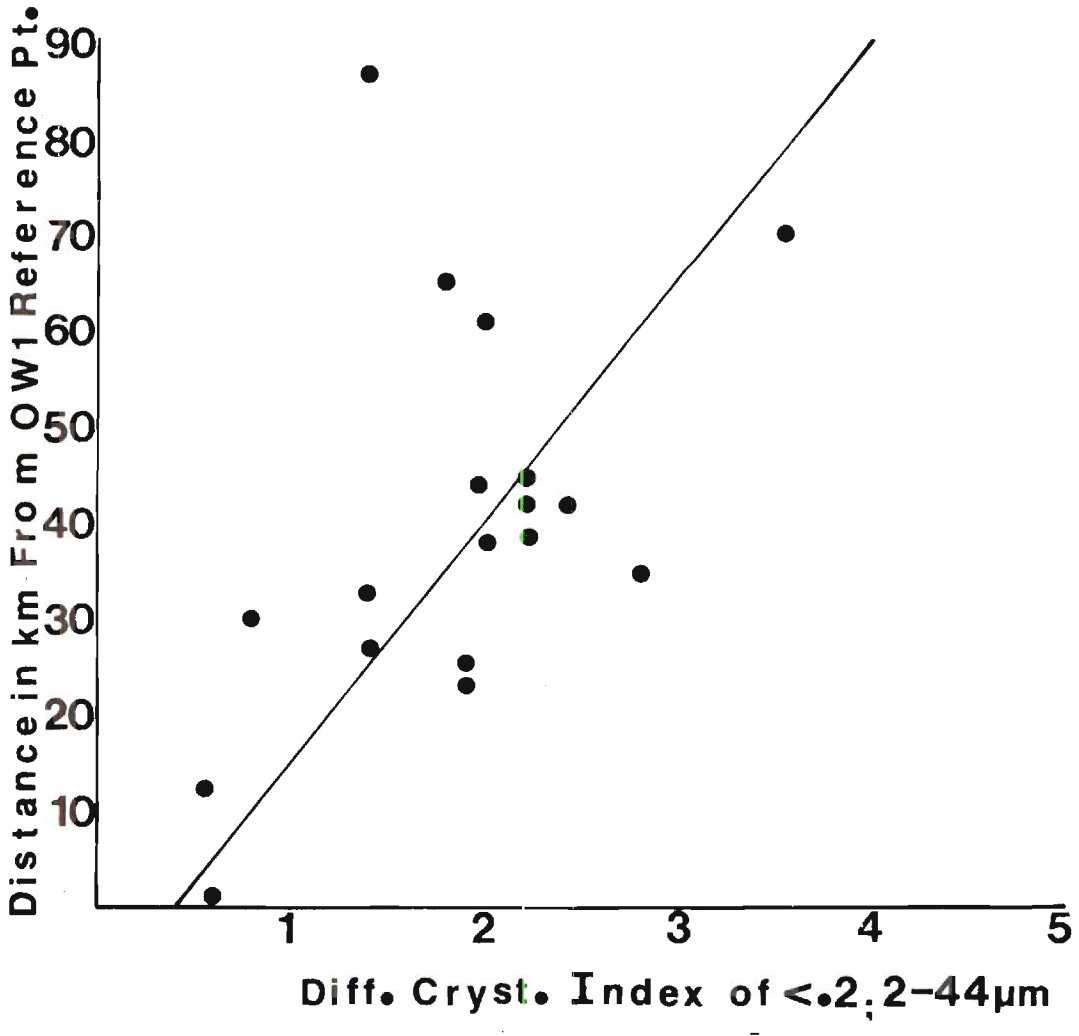

Figure 52. Variation in the Difference of Crystallinity Indices from <.2µm to 2-44µm. (y = 25x + -9.5, C.C. = .608).

effects the 002/001 ratio. Dunoyer de Segonzac (1970) used this technique, and concluded that an increase in the 002/001 is produced by an increase in metamorphism. He plotted the 002/001 against crystallinity indices, and found an expected inverse correlation. An increase in the 002/001 reflects a decrease in crystallinity index. The same plot was made for this study, and similar results were obtained (Figure 53). All size fractions show the same general trend. The <.2μm fraction had the least amount of scatter, and therefore was chosen for graphic displayal.

Figures 54, 55, 56, and 57 exhibit 002/001 plotted against distance from reference point OW1. Increasing distance from OW1 corresponds to a decreasing value of 002/001, suggesting that greater amounts of Aℓ or K have been incorporated into (or Mg and Fe are being removed from) octahedral layers of illite in southeastern samples, than in western and northern samples. Increased Aℓ is related to increased diagenetic activity. The slopes of the best fit equation of least squares line (Figures 53, 55 and 56) change considerably. Slopes increase from the fine to coarse fractions indicating that there is a greater chemical change occurring in the fine fraction than in the coarse fraction. In the <.2μm fraction ratios range from .23 to .53, and these numbers vary with differing overburden thicknesses. The 2-44μm fraction ratios are clustered between .3 and .4 indicating very little change between samples in the southeast, west, and north. This indicates that chemical reactions are already complete suggesting the 2-44μm fraction is primarily detrital. The 002/001 is one more example demonstrating that rocks in southeastern areas have been subjected to greater diagenetic changes

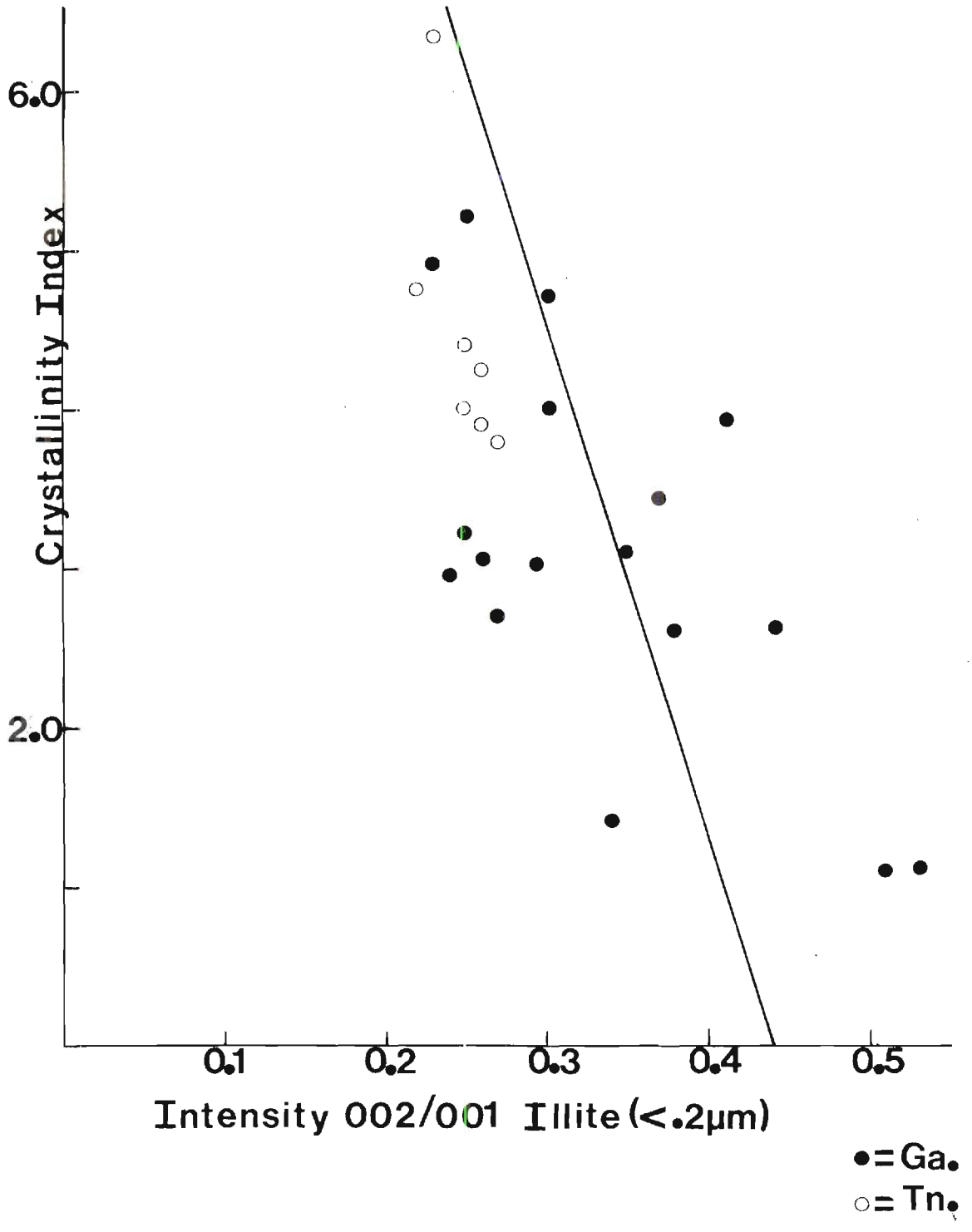

Figure 53. Variation in <.2µm Fraction Illite 002/001 Intensity Ratio with Crystallinity Index. (y = -33.33x + 14.66, C.C. = -.587)

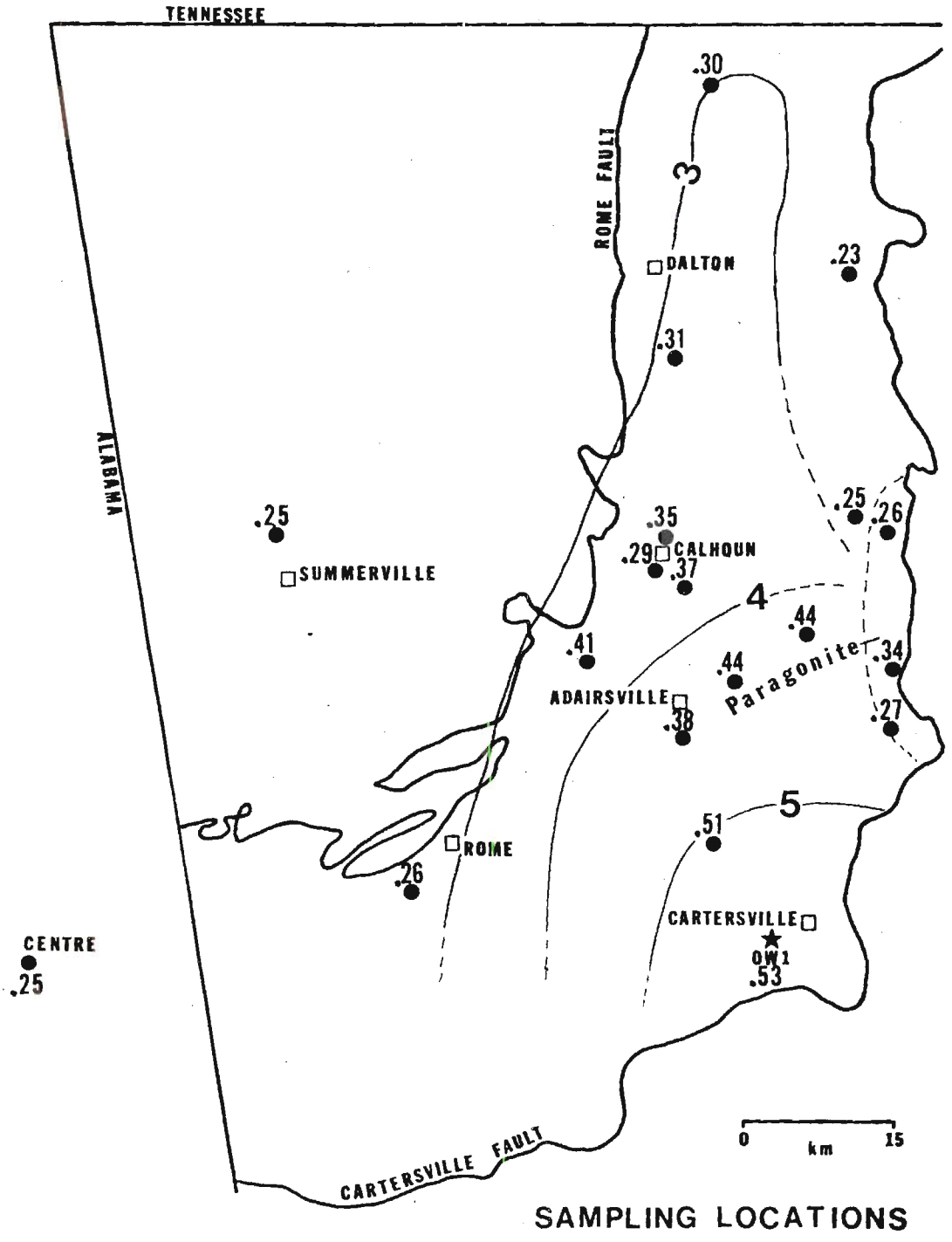

Figure 54. Contoured Illite 002/001 Intensity Ratio for the <.2μm Fraction.

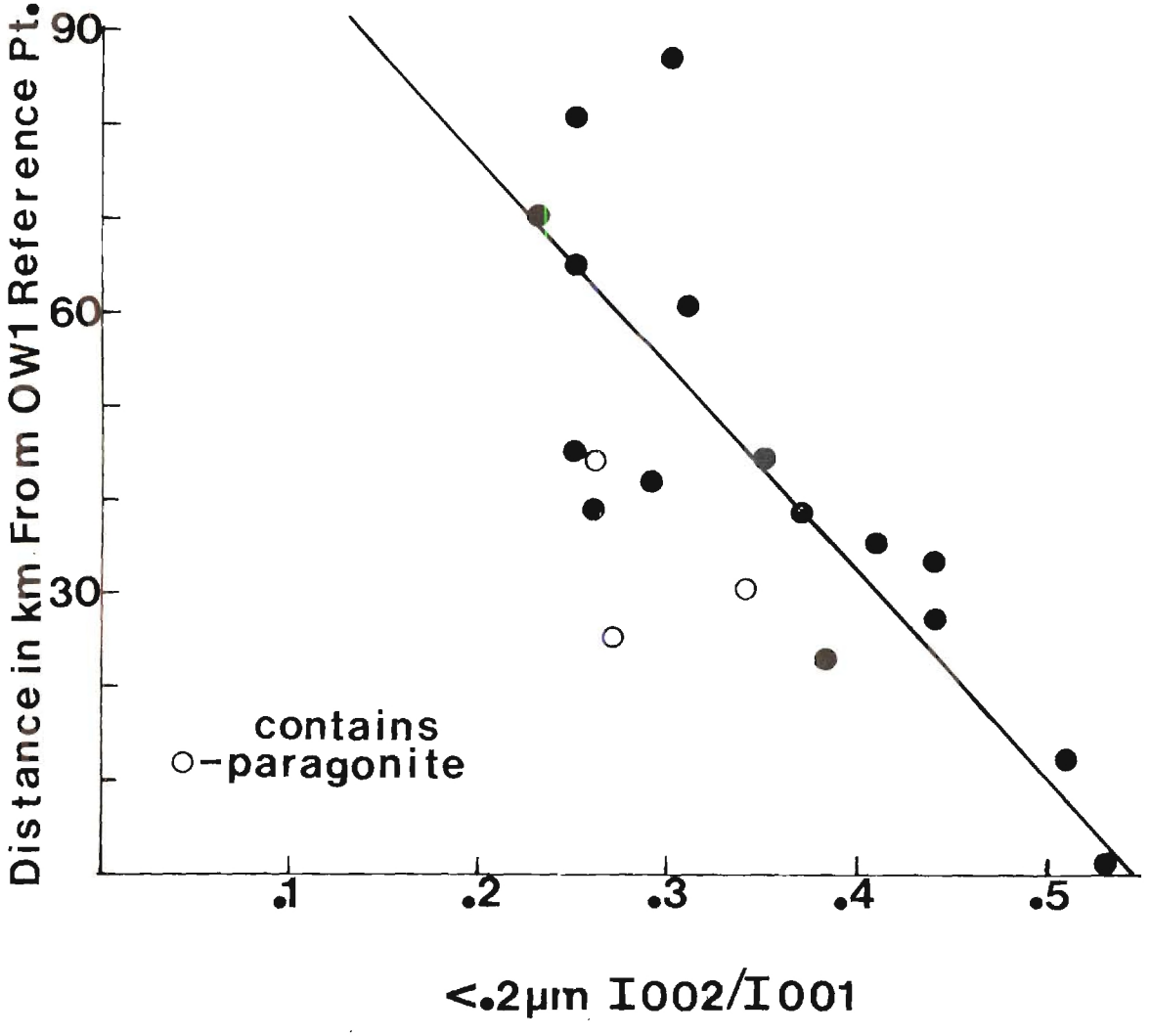

Figure 55. Variation in <.2µm Illite 002/001 Intensity Ratio. (y = -1.11x + 120, C.C. = -.721).

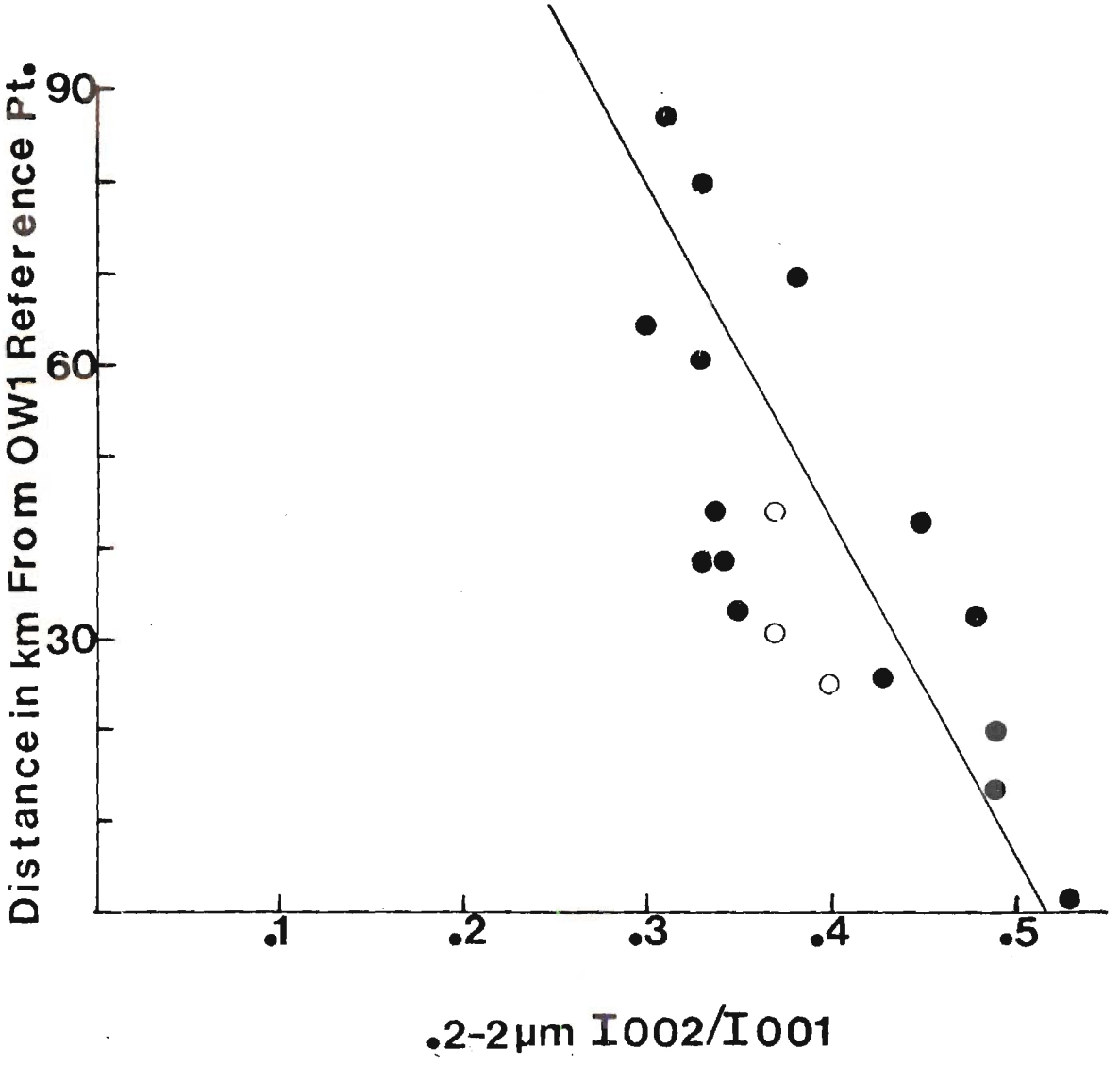

Figure 56. Variation in .2-2µm Illite 002/001 Intensity Ratio. (y = -1.97 + 190, C.C. = -.760).

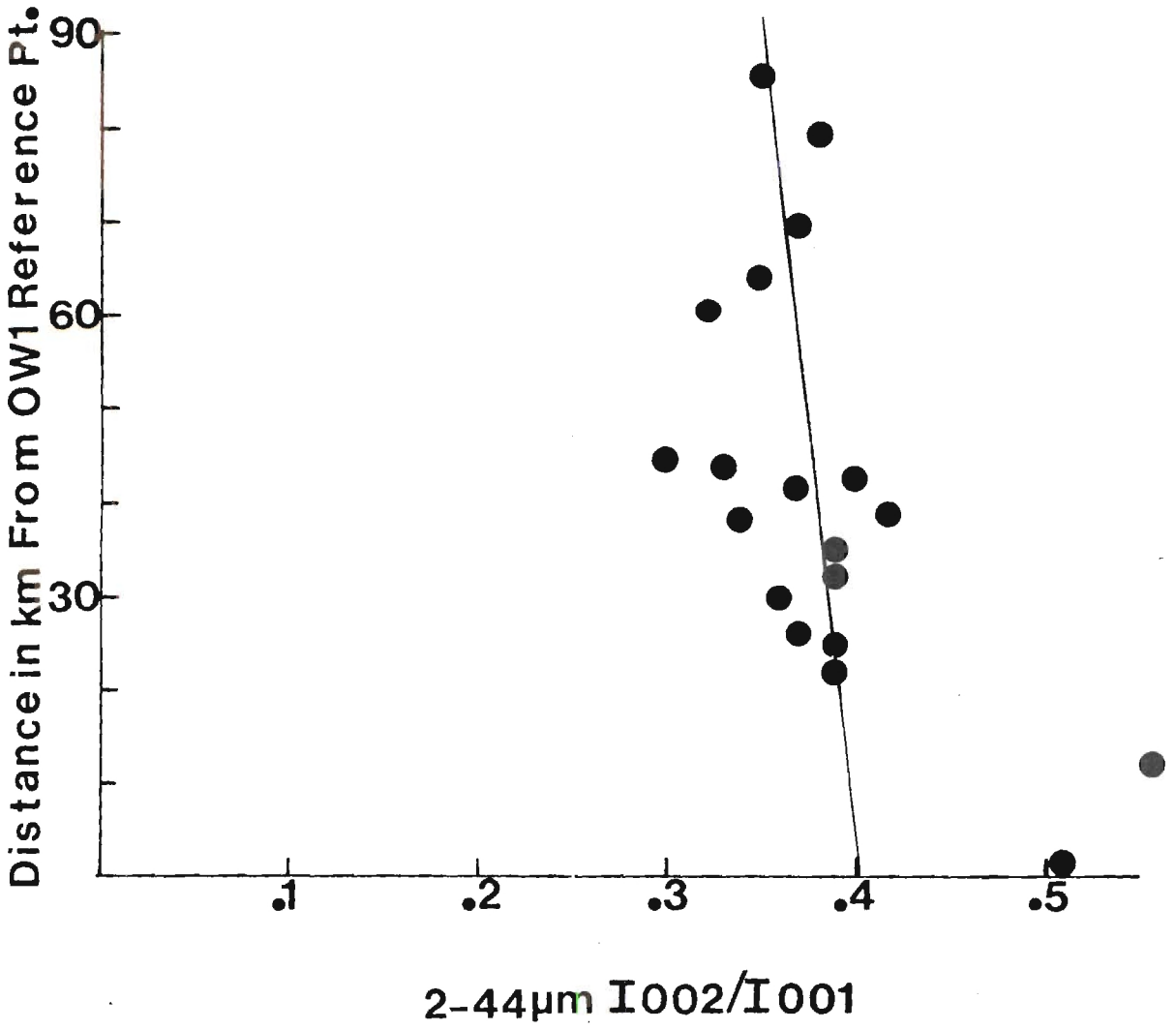

Figure 57. Variation in 2-44µm Illite 002/001 Intensity Ratio. (y = -1000x + 450, C.C. = -.590).

than their counterparts in the west and north.

Values for Tennessee samples are erratic (Figures 58, 59 and 60), which is probably caused by differing concentrations of detrital muscovite contaminations. As expected, numbers are considerably lower than those in Georgia. Mean 002/001 are .25, .27, .34 for $<2\mu m$, .2-2μm, and 2-44μm respectively.

Petrography

Several petrographic slides were prepared from selected samples to obtain knowledge of any textural changes which might have occurred in Conasauga Shale samples due to increased temperatures and pressures from varying overburden thicknesses, and adjacent thrust faults in the area. Descriptions of 7 perpendicularly oriented samples follow: see Figure 2 for sample locations.

OW3: Contains primarily illite and chlorite which are laminated parallel to foliation and bedding planes. The chlorite is contained in large chlorite prophyroblasts which are very common and elongated parallel to foliation bands. Porphyroblasts consist of several to many euhedral chlorite flakes not necessarily oriented towards foliation planes. Several porphyroblasts are folded and disrupt foliation lineation. Darker bands composed of large numbers of illite flakes usually surround porphyroblasts, (Figure 61). Such textural features are usually caused by dynamothermal metamorphism resulting from large scale folding and faulting (Bayley, 1968). Small secondary calcite veinlets cut across foliation planes, but show no preferred orientation.

OW5: Some iron oxide is present in the form of hematite, or possibly limonite suggesting some weathering has taken place. Illite,

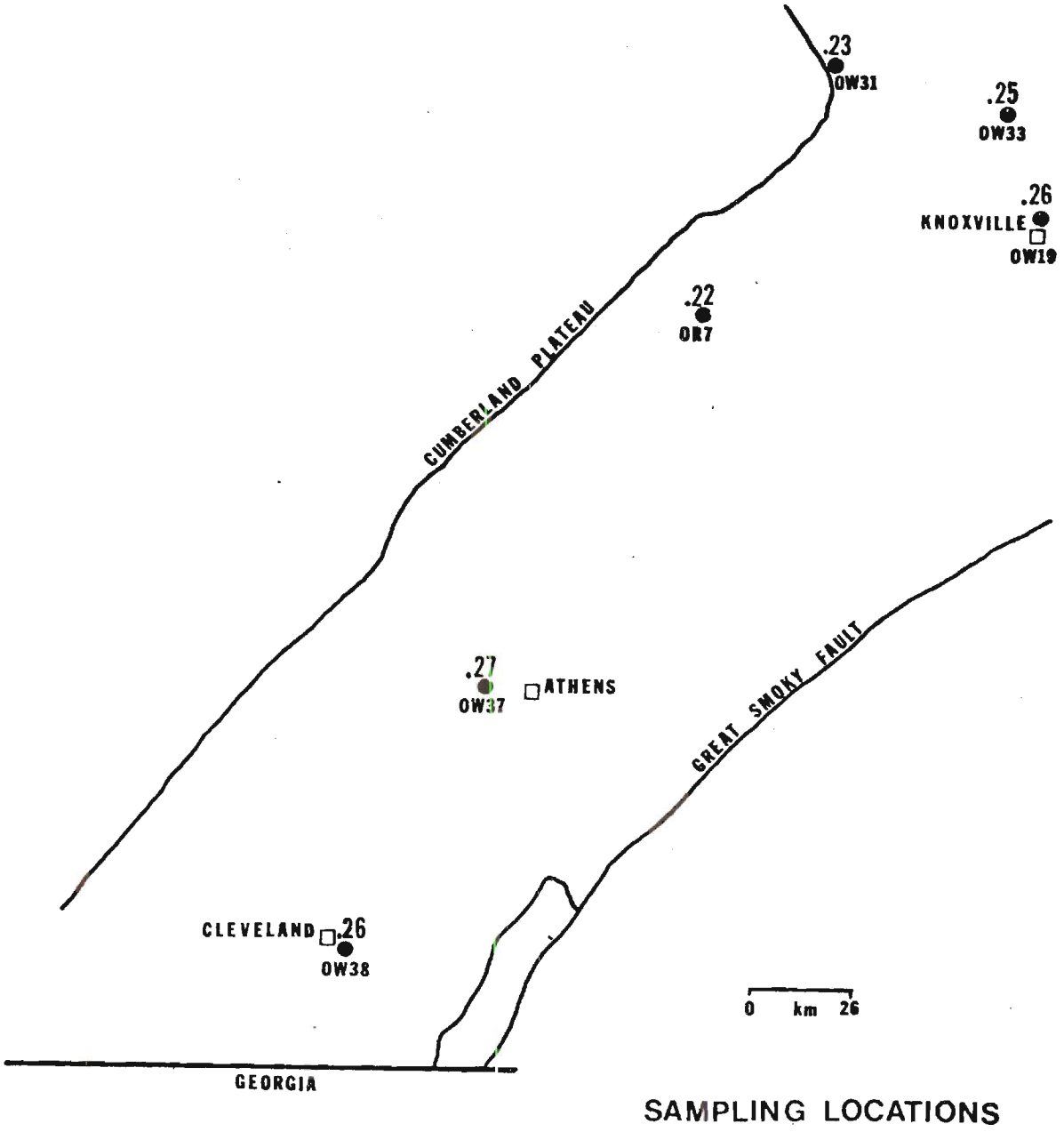

Figure 58. Illite (002)/(001) Intensity Ratio of the <.2μm Fraction for Tennessee Samples.

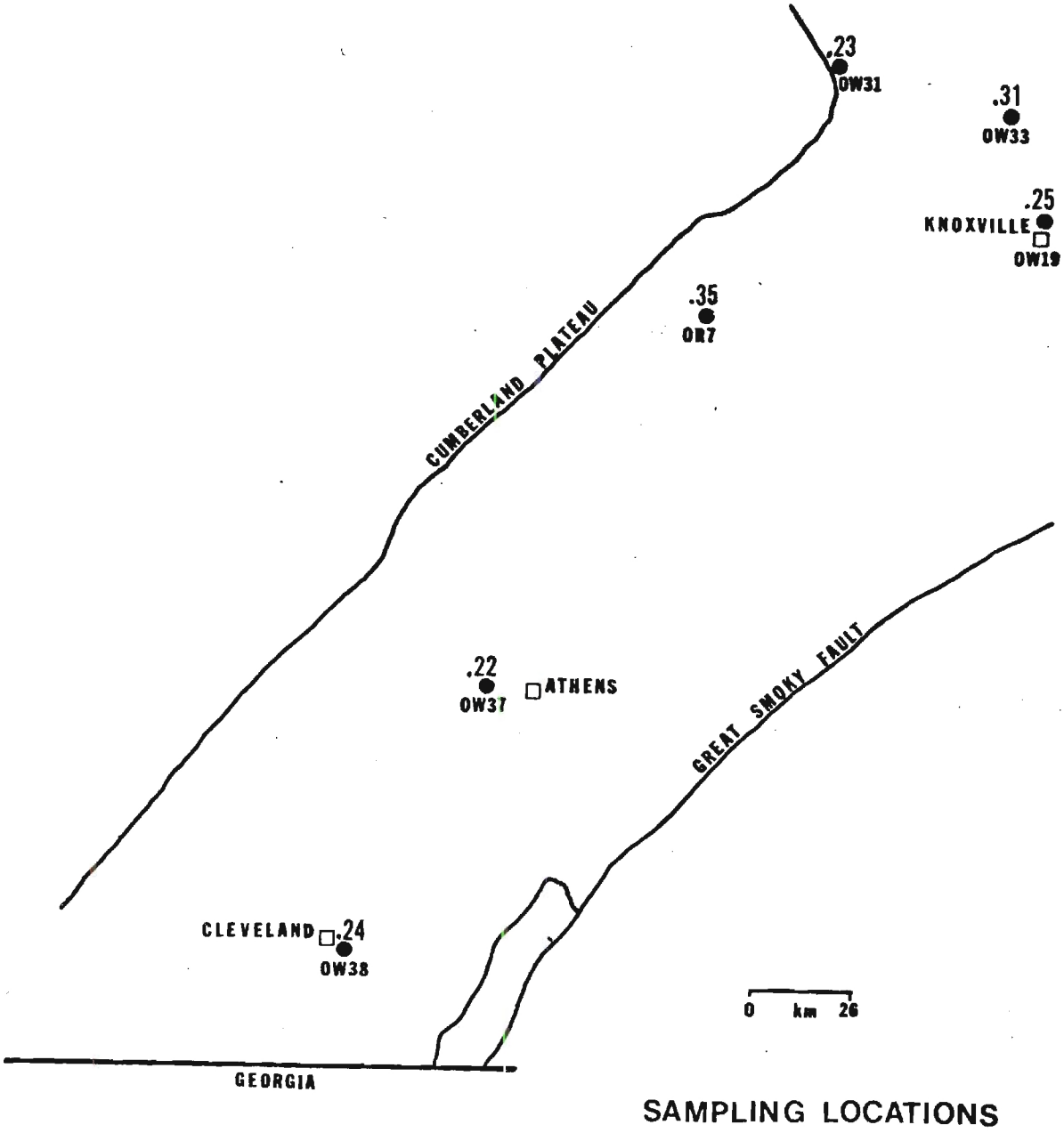

Figure 59. Illite (002)/(001) Intensity Ratio of the .2-2μm Fraction for Tennessee Samples.

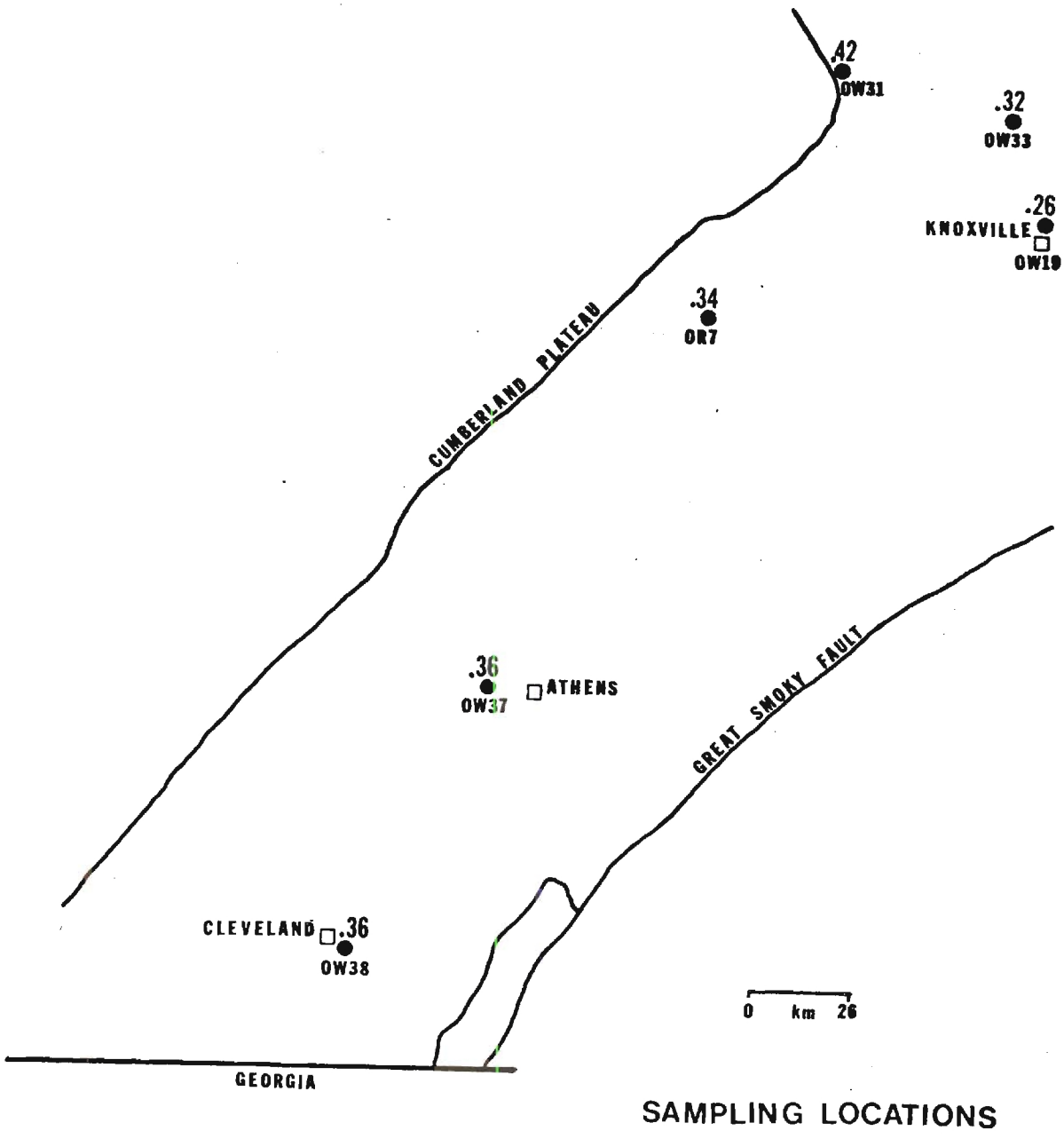

Figure 60. Illite (002)/(001) Intensity Ratio of the 2-44μm Fraction for Tennessee Samples.

quartz, feldspars, and thin parallel lenses of chlorite and chert show preferred orientation in foliation direction (Figure 62).

OW7: No preferred orientation is visible in platy minerals, calcite, or accessory minerals (Figure 63). Sample OW7 is from the same formation as OW3. Chlorite porphyroblasts are present, but are much smaller, and show no preferred orientation. Fossilized trilobites are abundant. They are relatively well preserved, and do not seem to have been altered to any great extent (Figure 64).

OR7: Platy minerals show a preferred orientation but not to the same extent as those found in the southern Valley and Ridge in Georgia (Figure 65). Detrital grains are larger, possibly suggesting a different environment of deposition. Also, discrete muscovite and biotite are present which are not found in Georgia samples. OR7 has graded bedding in a coarser to finer sequence. Chamosite oolithes are present and are associated with larger quartz grains in isolated pockets suggesting deposition in a shallow marine environment (Figure 66).

OW9: This slide was made from a limey sequence in the shale, and very few clays or accessory minerals are present. Calcite crystals are quite large and some overlap each other. Anhedral calcite crystals show rhombohedral cleavage, and some are exhibited as isolated splotches (porphyroblasts), which are possible remnants of recrystallized fossil fragments. Dark opaque organic material fills in fissures and cracks. Small euhedral-pryrite crystals are present, and are generally associated with organic streaks. Pyrite probably formed during diagenesis possibly resulting from the release of Fe from the mixed-layer clays.

OW11: Fine grained calcareous argillite with very well defined

Figure 61. Chlorite Porphyroblasts in OW3.

Figure 62. Perferred Orientation in OW5.

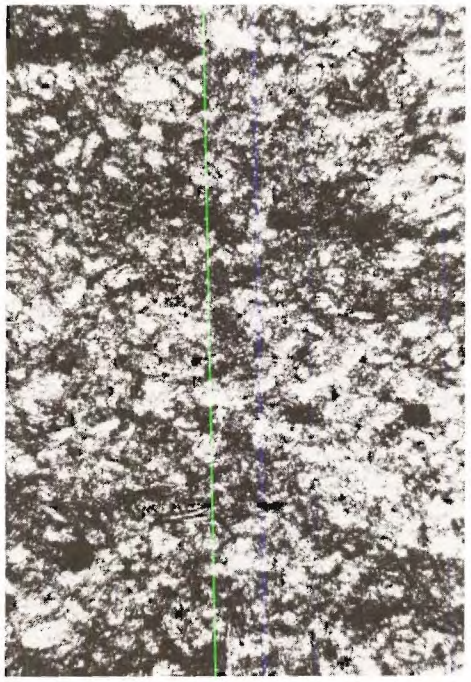

Figure 63. Randomly Oriented Grains with No Preperred Orientation in OW7.

Figure 64. Replaced But Unaltered Trilobite in OW7.

Figure 65. Some preferred Grain Orientation in OR7.

Figure 66. Unaltered Chamasite Oolithes in OR7.

foliation bands made up of platy minerals (primarily illite) (Figure 67). Bands are generally separated by euhedral calcite crystals. Abundant pyrite splotches are present, and are generally associated with organic material similar to that found in OW9. Secondary calcite fills cracks and fissures. Many of the calcite crystals are elongated, stretched, and folded, showing somewhat the same orientation as foliated bands (Figure 68).

OW17: There are some traces of preferred orientation in platy minerals, but not to the extent of those samples further to the southeast (Figure 69). The shale is composed mostly of illite, chlorite, and quartz. A light brown iron oxide stain covers all grains suggesting some weathering or oxidation has occurred, but mineral grains show no signs of deterioration.

The Petrographic data suggests that samples in the southeastern area have been exposed to a greater amount of temperature and pressure than those in northern and western areas. Evidence supporting this proposal is: A) Well defined foliation bands in southern samples. B) Recrystallized elongated calcite veinlets present in southern samples. C) Well defined chlorite porphyroblasts aligned parallel to foliation plains present in OW3. D) Accessory mineral grains showing some preferred orientation in southern samples. E) Randomly oriented grains with no preferred orientation in northern samples (OW7 especially). F) Well preserved fossil trilobite parts in OW7 which show little signs of deformation, and G) Round chamosite oolithes in OR7 showing no elongation or preferred orientation.

Figure 67. Very Well Defined Foliation Bands Made-Up of Platy Minerals in OW11.

Figure 68. Elongated, Stretched, and Folded Calcite Crystals in OW11.

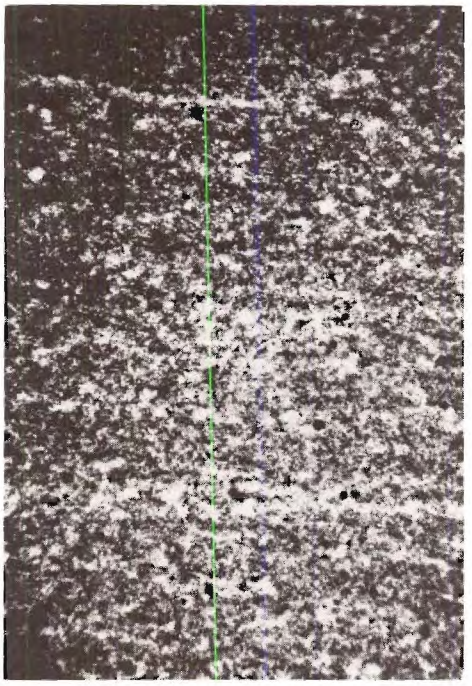

Figure 69. Traces of Preferred Grain Orientation in OW11.

All samples collected by the author were well lithified, but some better than others. Hand specimens in the south appeared to be harder than those in the north. Towe (1962) suggested that clay mineral diagenesis is a possible source of silica cement in sedimentary rocks. In the transformation of montmorillonite and mixed-layered clays to illite there is a substitution of Aℓ for Si in the tetrahedral layer which will cause an increase in layer charge enabling the fixation of K in the interlayer position (Weaver, 1958). Si may be released into the system and precipitated as quartz cement aiding the lithification process. As depth of burial and temperature increase, more Si should be released as montmorillonite is transformed to illite. Quantitative analyses of Si were not made on Conasauga samples, but it seems logical that because of increased overburden thicknesses in southeastern areas, more Si should have been released, therefore explaining hardness variations between the shales collected. However, it would be desirable to prove this.

CHAPTER V

CONCLUSIONS

Conasauga shales to the southeast, which have been exposed to greater temperatures and pressures because of increased overburden thicknesses, have undergone greater diagenetic changes than their counterparts to the north and west. Parameters which show the best correlation coefficients related to relative depths are sharpness ratios, crystallinity indices, 2m polymorph percentages, and size fraction percentages. Samples in the southeastern portion of the Valley and Ridge fit into the category of low-grade metamorphism proposed by Weaver (1961a), or metagenesis or anchizone proposed by Foscolas and Stott (1975). Samples in Tennessee, Alabama, and extreme northwestern Georgia fall into categories of early, middle, and late diagenesis.

Kaolinite and K-feldspar are relatively abundant in the areas which have been subjected to minimum diagenesis. They are absent or occur in minor amounts in shales subjected to the more advanced stages of diagenesis.

High stress adjacent to the Cartersville Fault appears to have been the cause of the formation of paragonite. The Na was apparently derived from Na feldspar.

AI'PENDIX

SAMPLE LOCATIONS AND DESCRIPTIONS

Colors described are in accordance with the Rock Color Chart distributed by The Geologic Society of America.

OW1: Located approximately 1.6 Km (1 mile) south of Cartersville, Georgia. OW1 is moderate orange pink (5 yr 8/4), and fairly weathered. It has been mapped as upper Conasauga Shale.

OW3: Located a few hundred meters east of U.S. Highway 411 approximately 27 Km (17 miles) north of cartersville, Ga., in a mine owned by the G.A.F. Co., formerly known as the Flexatile mine. The shale, which is almost phyllitic, was mined for aggregate and roofing tile. Sample OW3 is dark greenish gray (5G 4/1) and possesses a slight sheen. It is extremely hard and has fissility, but not to the extreme of a slate or phyllite. Sample OW3 has been mapped as the lower Conasauga Shale unit which is a possible equivalent of the Pumpkin Valley Shale mapped in Tennessee.

OW5: Located at the junction of Georgia Highway 156 and U.S. Route 41 within the city limits of Calhoun, Ga., found in an open excavation pit which appeared to be the foundation for a new large building. Sample OW5 is light olive gray (5Y 5/2), hard, and fissile. It has been mapped as the upper Conasauga unit, which possibly is equivalent to the Nolichucky Shale of Tennessee. Sample OW5 is very close to a branch of the Rome Thrust Fault.

OW7: Located a few hundred meters each of Chatsworth, Ga. city limits, and directly east of Holly Creek on U.S. Route 76. It was found in a quarry owned by Dillard Hays. He uses the shale for cement aggregate. Sample OW7 is medium bluish gray (5B 5/1), hard, and has slight fissility. It has been mapped as the lower Conasauga unit.

OR7: Located approximately 8 Km (5 miles) southwest of Oak Ridge, Tennessee. Taken from a core drilled to a depth of 27 meters (89 feet). Sample OR7 is grayish red (5R 4/2), moderately hard, and has visible mica flakes. It has been mapped as Pumpkin Valley Shale.

OW8: Located 16.9 Km (10.5 miles) northeast of Dalton, Ga., and 3.6 Km (2.25 miles) east of Georgia Highway 81 at a semi-fresh road cut. OW8 is light olive gray (5Y 5/2), thinly laminated, breaks along bedding planes easily, and is not very hard. It has been mapped as the upper Conasauga Shale Unit.

OW9: Located 12.9 Km (8 miles) northwest of Cartersville, Ga., 4.8 Km (3 miles) west of Cassville, Ga., off Georgia Highway 20 in a quarry owned by Florida Rock Co. The rock of the quarry is primarily limestone, but there are some shaley interlayers from which OW9 was extracted. OW9 is dark gray (N3), calcareous, carbonaceous, has a sheen, and is very hard. It has been mapped as the middle limestone unit.

OW10: Located 14.1 Km (8.75 miles) south of Dalton, and approximately 2 miles east of Interstate Route 75 in a sanitary landfill cut bank. OW10 is dusky yellow (5Y 6/4) and is one of the more weathered

samples collected. It is fairly hard, but shows signs of iron oxide stains. OW10 has been mapped as the lower Conasauga Shale unit.

OW11: Located 4 Km (2.5 miles) south of Adairsville, Ga., off Halls Road at the Martin Marietta Cement Quarry. Most of the rock is limestone, but some shaley layers are present. OW11 is dark gray (N3) with sparry calcite veins cutting through fissures in the shale. The shale itself is calcareous, carbonaceous, and very hard. It has been mapped as the middle limestone unit.

OW12: Located 2 Km (1.25 miles) north of Summerville, Ga., just off U.S. Route 27 in a cut bank in back of a Winn Dixie super market. OW12 is dusky yellow (5Y 6/4), contains silty layers, shows iron oxide stain, and is moderately hard. It has been mapped as the middle Conasauga Shale unit, which is a possible equivalent to the Rogersville Shale in Tennessee.

OW13: Located at the intersection of Georgia Highway 140, and U.S. Route 411, 1.6 Km (1 mile) north of Rydal, Georgia. The road cut has experienced a recent slide and has exposed fresh rock. OW13 is grayish green (5G 5/2), very hard, fissile, and has a slight sheen. It has been mapped as the lower shale unit.

OW17: Located 1.6 Km (1 mile) east of Plainsville, Ga., in a shale pit once used for raw material to manufacture bricks. OW17 is dusky yellow (5Y 6/4), contains silty layers, and is moderately hard. It has been mapped as the middle Conasauga Shale unit.

OW18: Located 1.6 Km (1 mile) southeast of Calhoun, Georgia in an old shale pit just off Georgia Route 53. OW18 is light olive gray (5Y 5/2), and moderately hard. It has been mapped as the upper shale unit.

OW19: Located in Shalite Co. Quarry approximately 5.6 Km (3.5 miles) north of Knoxville, Tennessee. OW19 is grayish red (5R 4/2), and has visible mica flakes. It has fissility along bedding planes, contains silty layers, and is moderately hard. OW19 has been mapped as Rogersville Shale.

OW23: Located approximately 1.8 Km (1 mile) south of Centre, Alabama on Alabama Highway 9. Comprised of well cuttings taken from a water well drilled one week earlier. OW23 is medium dark gray (N3), calcareous, soft relative to other samples, and contains abundant mica flakes. It has been mapped as upper Conasauga Shale unit.

OW24: Located 7.2 Km (4.5 miles) southwest of Rome, Georgia, on U.S. Route 411. It was extracted from the foundation of a new Coca Cola Plant. OW24 is medium gray (N5), and calcareous. It has been mapped as lower Conasauga Shale Unit.

OW25: Located 4.8 Km (3 miles) southeast of Calhoun, Georgia, off Georgia Highway 53 in a Highway Department maintenance pit. There is primarily limestone present, but some shaley layers are interbedded with limestone. OW25 is medium dark gray (N4), calcareous, with limestone modules contained in the shale, and is moderately hard. It has been mapped as middle Conasauga Limestone unit.

OW27: Located 5.6 Km (3.5 miles) west of the U.S. Route 411 and Georgia Route 156 exchange on Highway 156. The road cut is fresh, and no apparent weathering has taken place. OW27 is greenish gray (5G 6/1), fissile, and moderately hard. It has been mapped as lower Conasauga Shale.

OW28: Located approximately .8 Km (.5 miles) south of Sonoraville, Georgia in a driveway road cite. OW28 is yellowish gray (5Y 8/2) slightly weathered, and moderately hard. It has been mapped as the upper shale unit.

OW29: Located 3.7 Km (2.3 miles) east of the Interstate Route 75 and Georgia Route 140 interchange on Highway 140, and 5.6 Km (3.5 miles) east of Folsom, Georgia. Comprised of well cuttings from a water well drilled two weeks earlier. OW29 is medium gray (N5), and moderately hard. It has been mapped as upper Conasauga Shale unit.

OW33: Located 16.1 Km (10 miles) north of Knoxville, Tennessee, on State Route 33, 1.6 Km (1 mile) north of the Union and Knox County boundary. It was found in a quarry used for production of cement aggregate, which is comprised primarily of limestone with some shaley layers. OW33 is medium dark gray (N4), calcareous, with visible mica flakes, and is hard. It has been mapped as undifferentiated Conasauga.

OW37: Located a few hundred meters east of Interstate Route 75 at the junction with Tennessee Highway 30, in a quarry operated by Dalton Rock Products. OW37 is medium dark gray (N4), calcareous, hard, and contains mica flakes. It has been mapped as Nolichucky Shale.

OW38: Located approximately 1.6 Km (1 mile) south of Cleveland, Tennessee, just off Route 64 in a quarry operated by Dalton Rocks Products. OW38 is dark gray (N3), calcareous, and hard. It has been mapped as Nolichucky Shale.

Table 2. Clay Mineral Percentages and Presence of Accessory Minerals in the <.2μm Fraction for Georgia and Alabama Samples.

Sample #	Illite	10Å I/S	Chlorite	Kaolinite	Quartz	NA Plag.	K Feld.	Paragonite	Cal. or Dol.
OW1	ND	-	ND	ND	-	-	-	-	-
OW3	69	-	31	-	-	-	-	x	-
OW5	90	-	10	-	-	-	-	-	-
OW7	61	35	4	-	-	-	-	-	-
OW8	ND	25	ND	ND	-	-	-	-	-
OW9	88	-	12	-	-	-	-	-	*
OW10	ND	41	ND	ND	-	-	-	-	-
OW11	89	-	11	-	-	-	-	-	-
OW12	ND	41	ND	ND	-	-	-	-	-
OW13	89	-	11	-	-	-	-	x	-
OW17	ND	33	ND	ND	-	-	-	-	-
OW18	ND	24	ND	ND	-	-	-	-	-
OW23	28	63	9	-	-	-	-	-	-
OW24	100	-	-	-	-	-	-	-	-
OW25	79	12	9	-	-	-	-	-	-
OW26	69	24	7	-	-	-	-	x	-
OW27	80	18	2	-	-	-	-	-	x
OW28	ND	18	ND	ND	-	-	-	-	-
OW29	ND	10	ND	-	-	-	-		-
OW30	32	58	10	-	-	-	-		-

TR = Trace

x = present

xx = present in abundance

- = not present

ND = no data

10Å I/S = mixed-layer clays

Table 3. Clay Mineral Percentages and Presence of Accessory Minerals in the .2-2μm Fraction Georgia and Alabama Samples.

Sample II	Illite	10A I/S	Chlorite	Kaolinite	Quartz	Na Plag.	K Felds.	Paragonite	Cal. or Dol.
OW1	ND	-	ND	ND	TR	-	TR	-	-
OW5	71	-	29	-	x	-	-	xx	-
OW7	44	40	27	-	x	x	-	-	x
OW8	ND	66	ND	ND	x	TR	TR	-	-
OW9	82	-	18	-	x	x	TR	-	xx
OW10	ND	33	ND	ND	x	TR	TR	-	-
OW11	75	-	25	-	x	x	TR	-	xx
OW12	ND	34	ND	ND	x	-	-	-	-
OW13	89	-	11	-	x	-	TR	xx	x
OW17	ND	19	ND	ND	x	TR	-	-	-
OW18	ND	17	ND	ND	x	TR	-	-	-
OW23	9	48	43	-	x	x	TR	-	x
OW24	82	15	3	-	x	x	-	-	x
OW25	56	12	32	-	x	x	TR	-	xx
OW26	86	-	14	-	x	TR	-	x	-
OW27	86	-	14	-	x	x	-	-	-
OW28	ND	0	ND	ND	x	x	x	-	-
OW29	63	14	23	-	x	x	TR	-	x
OW30	4	59	37	-	x	x	TR	-	x

Table 4. Clay Mineral Percentages and Presence of Accessory Minerals in the 2-44μm Fraction for Georgia and Alabama Samples.

Sample #	Illite	10A I/S	Chlorite	Kaolinite	Quartz	Na Plag.	K Felds.	Paragonite	Cal. or Dol.
OW3	52	-	48	-	xx	x	-	x	-
OW5	68	-	32	-	xx	x	-	-	-
OW7	28	20	52	-	xx	x	-	-	x
OW8	ND	12	ND	ND	xx	x	x	-	-
OW9	76	-	24	-	xx	x	TR	-	xx
OW10	ND	-	ND	ND	xx	x	x	-	-
OW11	61	-	39	-	xx	x	TR	-	xx
OW12	ND	-	ND	ND	xx	TR	TR	-	-
OW13	67	-	33	-	xx	TR	TR	x	x
OW17	ND	0	ND	ND	xx	TR	-	-	-
OW18	ND	0	ND	ND	xx	x	-	-	-
OW23	33	9	58	-	xx	x	TR	-	x
OW24	79	11	10	-	xx	x	-	-	xx
OW25	41	10	49	-	xx	xx	TR	-	xx
OW26	57	-	43	-	xx	TR	-	x	-
OW27	51	-	49	-	xx	x	TR	-	-
OW28	ND	-	ND	ND	xx	x	x	-	-
OW29	63	-	37	-	xx	x	TR	-	x
OW30	14	33	53	-	xx	x	TR	-	x

Table 5. Clay Mineral Percentages and Presence of Accessory Minerals in the <.2μm Fraction for Tennessee Samples.

Sample #	Illite	10Å I/S	Chlorite	Kaolinite	Quartz	Na Plag.	K Felds	Cal. or Dol.
OR7	54	35	-	11	-	-	-	-
OW19	64	36	-	-	-	-	-	-
OW31	38	38	12	12	-	TR	TR	-
OW33	60	32	4	4	-	-	-	-
OW37	71	25	4	-	-	-	TR	-
OW38	79	14	7	-	-	-	-	-

Table 6. Clay Mineral Percentages and Presence of Accessory Minerals in the .2-2μm Fraction for Tennessee Samples.

Sample #	Illite	10Å I/S	Chlorite	Kaolinite	Quartz	Na Plag.	K Felds	Cal. or Dol.
OR7	21	29	17	33	x	TR	TR	x
OW19	55	36	36	-	x	-	x	x
OW31	4	40	22	34	x	x	TR	xx
OW33	45	33	11	11	x	-	x	x
OW37	65	22	13	-	x	TR	TR	x
OW38	37	51	12	-	x	x	x	x

Table 7. Clay Mineral Percentages and Presence of Accessory Minerals in 2-44μm Fraction of Tennessee Samples.

Sample #	Illite	10Å I/S	Chlorite	Kaolinite	Quartz	Na Plag.	K Felds	Cal. or Dol.
OR7	36	14	17	33	xx	xx	TR	x
OW19	49	38	13	-	xx	xx	x	x
OW31	22	22	24	32	xx	xx	x	xx
OW33	19	22	23	36	xx	xx	x	x
OW37	48	32	20	-	xx	TR	x	x
OW38	54	23	23	-	xx	x	x	x

Table 8. Intensity Ratio (10Å/7Å) for Georgia-Alabama Samples.

Sample #	<.2μm	.2-2μm	≤2μm	≤4μm	2-44μm
OW1	ND	ND	ND	ND	ND
OW3	.91	1.0	1.4	1.8	.43
OW5	3.5	1.4	1.5	1.0	.80
OW7	10.2	1.1	2.7	1.8	.40
OW8	ND	ND	ND	ND	ND
OW9	2.9	1.8	ND	2.3	1.3
OW10	ND	ND	ND	ND	ND
OW11	3.4	1.2	1.5	1.1	.60
OW12	ND	ND	ND	ND	ND
OW13	3.2	3.3	4.0	1.5	.80
OW17	ND	ND	ND	ND	ND
OW18	ND	ND	ND	ND	ND
OW23	1.7	.5	.7	.7	.30
OW24	ND	ND	ND	ND	ND
OW25	4.0	.9	.7	.7	.40
OW26	5.0	2.4	ND	2.6	.50
OW27	7.8	2.5	3.2	2.0	.40
OW28	ND	ND	ND	ND	ND
OW29	ND	1.3	1.0	1.0	.70

Table 9. Percent K_2O for Georgia-Alabama and Tennessee Samples.

Sample #	<.2μm	.2-2μm
OW3	ND	4.9
OW5	5.27	5.2
OW7	5.26	6.0
OW9	4.61	6.68
OW11	5.65	6.68
OW13	4.65	4.60
OW23	4.85	5.75
OW24	ND	7.28
OW27	ND	6.92
OR7	5.49	7.78
OW19	7.29	7.95
OW31	5.34	6.84
OW33	7.66	8.42
OW37	7.89	8.19
OW38	7.25	9.78

Table 10. X-ray Diffraction Measurement (Å) of Illite 001 Peak of the <.2μm For Georgia Samples.

Sample #	% Mixed Layered Material	Untreated	Glycolated	Heated at 300°C
OW1	0	10.0	10.0	10.0
OW3	0	10.0	10.0	10.0
OW5	0	10.0	10.0	10.0
OW7	35	10.51	10.51	10.0
OW8	25	10.27	10.27	10.0
OW9	0	10.0	10.0	10.0
OW10	41	10.27	10.27	10.0
OW11	0	10.0	10.0	10.0
OW12	41	10.27	10.27	10.0
OW13	0	10.0	10.0	10.0
OW17	33	10.15	10.15	10.0
OW18	24	10.27	10.27	10.0
OW23	63	11.0	11.0	10.15
OW24	0	10.27	10.27	10.0
OW25	12	10.15	10.15	10.0
OW26	24	10.27	10.27	10.0
OW27	18	10.27	10.27	10.0
OW28	18	10.0	10.0	10.0
OW29	10	10.0	10.0	10.0

Table 11. X-Ray Diffraction Measurement (Å) of Illite 001 Peak of the .2-2μm For Georgia Samples.

Sample #	% Mixed Layered Material	Untreated	Glycolated	Heated
OW1	0	10.0	10.0	10.0
OW3	0	10.0	10.0	10.0
OW5	0	10.0	10.0	10.0
OW7	40	10.15	10.15	10.0
OW8	66	10.27	10.27	10.0
OW9	0	10.0	10.0	10.0
OW10	33	10.0	10.0	10.0
OW11	0	10.0	10.0	10.0
OW12	34	10.27	10.27	10.0
OW13	0	10.0	10.0	10.0
OW17	19	10.0	10.0	10.0
OW18	17	10.15	10.15	10.0
OW23	48	10.54	10.0 + 12.61 Peak	10.0
OW24	15	10.0	10.0	10.0
OW25	12	10.15	10.15	10.0
OW26	13	10.0	10.0	10.0
OW27	10	10.0	10.0	10.0
OW28	0	10.0	10.0	10.0
OW29	14	10.15	10.15	10.0

Table 12. X-Ray Diffraction Measurement (A) of Illite 001 Peak of the 2-44μm Georgia Samples.

Sample #	% Mixed Layered Material	Untreated	Glycolated	Heated
OW1	0	10.0	10.0	10.0
OW3	0	10.0	10.0	10.0
OW5	0	10.0	10.0	10.0
OW7	20	10.0	10.0	10.0
OW8	12	10.15	10.15	10.0
OW9	0	10.0	10.0	10.0
OW10	0	10.0	10.0	10.0
OW11	0	10.0	10.0	10.0
OW12	0	10.0	10.0	10.0
OW13	0	10.0	10.0	10.0
OW17	0	10.0	10.0	10.0
OW18	0	10.0	10.0	10.0
OW23	9	10.51	10.0 + 12.61	10.0
OW24	11	10.0	10.0	
OW25	10	10.0	10.0	10.0
OW26	0	10.0	10.0	10.0
OW27	0	10.0	10.0	10.0
OW28	0	10.0	10.0	10.0
OW28	0	10.0	10.0	10.0

Table 13. A,B,C, X-Ray Diffraction Measurement (Å) of Illite 001 Peak Tennessee Samples.

Sample #	% Heated Layered Material	Untreated	Glycolated	Heated
A. <.2μm				
OR7	35	10.39	10.39	10.27
OW19	36	10.27	10.27	10.15
OW31	38	10.39	10.39	10.0
OW33	32	10.15	10.15	10.05
OW37	25	10.27	10.27	10.0
OW38	14	10.15	10.15	10.15
B. .2-2μm				
OR7	29	10.15	10.15	10.0
OW19	36	10.27	10.27	10.0
OW31	40	10.64	10.27+shoulder	10.15
OW33	33	10.27	10.39	10.0
OW37	22	10.27	10.27	10.0
OW38	51	10.39	10.39	10.15
C. 2-44μm				
OR7	14	10.0	10.0	10.0
OW19	38	10.15	10.27	10.15
OW31	22	10.51	10.0 + 11.93 Peak	10.15
OW33	22	10.27	10.0 + 11.93 Peak	10.15
OW37	32	10.27	10.27	10.0
OW38	23	10.0	10.0+shoulder	10.0

Table 14. Percent Na_2O for Georgia-Alabama and Tennessee Samples.

Sample #	<.2μm	.2-2μm	2-44μm
*OW3	1.05	2.52	1.0
OW5	.08	.15	.9
OW7	.48	.63	1.7
OW9	ND	.01	.1
OW11	.60	.78	.8
*OW13	ND	1.65	.3
OW23	.18	.30	1.35
OW24	.01	.01	.01
OW26	ND	ND	.8
OW27	.35	.58	1.75
OR7	.01	.09	ND
OW19	.01	.10	ND

* = contains paragonite

Table 15. 2m Polytype Percentages for Georgia-Alabama Samples.

Sample #	<.2μm	.2-2μm	≤2μm	≤4μm	2-44μm
OW1	ND	100	ND	100	100
OW3	40	100	100	ND	ND
OW5	ND	35	ND	ND	ND
OW7	0	0	ND	ND	ND
OW8	0	0	ND	ND	ND
OW9	50	100	100	100	100
OW10	0	35	ND	ND	ND
OW11	20	70	ND	ND	ND
OW12	0	0	ND	ND	ND
OW17	30	50	ND	ND	ND
OW18	0	40	ND	ND	ND
OW23	0	5	10	15	25
OW24	0	1m	1m	1m	ND
OW25	0	45	ND	ND	ND
OW26	0	20	ND	ND	ND
OW28	0	40	ND	ND	ND
OW29	ND	80	ND	ND	ND

ND = no data

1m = 1m Polymorph

Table 19. Sharpness Ratio for Georgia - Alabama Samples.

Sample #	<.2μm	.2-2μm	≤2μm	≤4μm	2-44μm
OW1	7.3	30	ND	ND	39
OW3	2.9	19.5	9.5	26.1	24.2
OW5	2.2	10.1	8.5	9.4	7.2
OW7	.76	2.0	3.0	2.1	3.5
OW8	1.1	1.8	ND	ND	2.5
OW9	5.4	26.9	12.0	21.6	27.7
OW10	1.8	2.8	ND	ND	4.3
OW11	5.3	20.3	7.5	7.0	12.9
OW12	1.4	2.0	ND	ND	2.1
OW13	4.5	22.8	16.9	25.2	25.4
OW17	2.8	13.7	8.4	4.3	10.5
OW18	2.1	8.2	ND	ND	11.1
OW23	3.0	.9	.86	.66	2.0
OW24	2.9	11.5	5.9	2.8	5.9
OW25	2.9	5.8	2.8	3.6	4.8
OW26	3.2	11.1	8.5	13.2	13.5
OW27	2.4	7.9	7.0	4.6	6.9
OW28	3.1	15.7	ND	ND	16.4
OW29	4.7	4.2	6.9	7.9	9.5

Table 20. Sharpness Ratio for Tennessee Samples.

Sample #	<.2μm	<.2-2μm	≤2μm	≤4μm	2-44μm
OW7	.88	1.9	1.3	1.2	3.1
OW19	1.5	1.9	2.5	3.5	3.1
OW31	1.0	.76	1.5	.52	2.2
OW33	2.0	1.8	2.3	2.5	2.2
OW37	2.0	2.0	2.6	1.8	1.9
OW38	1.6	1.5	1.9	1.7	2.6

Table 21. Crystallinity Index for Georgia-Alabama Samples.

Sample #	<.2μm	<2-2μm	≤2μm	≤4μm	2-44μm
OW1	1.1	.7	ND	ND	.5
OW3	1.4	.95	1.4	.7	.6
OW5	3.1	.88	1.3	1.3	.68
OW7	4.9	3.3	3.4	3.9	1.35
OW8	4.7	3.9	ND	ND	3.3
OW9	1.1	.77	1.0	.7	.57
OW10	4.0	2.8	ND	ND	2.0
OW11	2.6	1.4	1.6	1.3	.65
OW12	5.2	4.0	ND	ND	3.4
OW13	2.7	1.3	1.1	.9	.75
OW17	3.9	2.0	1.5	1.7	1.1
OW18	3.0	1.9	ND	ND	.8
OW23	9.5	7.7	6.7	8.6	2.2
OW24	3.0	.9	1.0	2.2	.95
OW25	3.5	2.4	1.5	2.2	1.2
OW26	3.1	1.9	1.5	1.1	1.1
OW27	3.2	1.7	1.5	2.1	1.0
OW28	2.6	1.5	ND	ND	1.2
OW29	2.3	1.95	1.5	1.1	.87

Table 22. Crystallinity Index for Tennessee Samples.

Sample #	<.2μm	.2-2μm	≤2μm	≤4μm	2-44μm
OR7	4.77	2.95	4.8	6.1	2.2
OW19	3.9	3.35	2.85	2.7	2.35
OW31	6.35	8.1	3.9	7.4	1.5
OW33	4.0	3.95	3.1	3.0	1.55
OW37	3.8	3.8	3.3	3.1	2.25
OW38	4.25	4.45	3.6	4.5	2.4

Table 23. Sample Fraction Percentages for Georgia-Alabama Samples.

Sample #	<.2μm	.2-2μm	≤2μm	≤4μm	2-44μm	>44μm
OW1	.1	7.2	ND	ND	76.9	15.8
OW3	.41	15.2	ND	ND	62.7	21.7
OW5	1.6	23.6	ND	ND	68.2	6.6
OW7	3.5	22.3	ND	ND	63.9	10.3
OW8	5.8	21.4	ND	ND	48.8	24.0
OW9	.21	7.7	ND	ND	78.1	13.9
OW10	1.8	11.9	ND	ND	38.9	47.4
OW11	1.1	19.8	ND	ND	62.6	16.5
OW12	10.4	19.5	ND	ND	30.9	39.2
OW13	.59	13.6	ND	ND	73.4	12.4
OW17	1.3	15.4			40.5	42.8
OW18	.82	14.3	ND	ND	47.6	37.3
OW23	4.4	25.7	ND	ND	54.2	15.7
OW24	.75	15.7	ND	ND	47.7	35.8
OW25	1.2	15.6	ND	ND	68.6	14.6
OW26	.48	13.7	ND	ND	51.5	34.3
OW27	.71	17.3	ND	ND	60.8	21.2
OW28	1.1	15.1	ND	ND	50.8	33.0
OW29	ND	18.1	ND	ND	62.3	19.6

Table 24. Sample Fraction Percentages for Tennessee Samples.

Sample #	<.2μm	.2-2μm	≤2μm	≤4μm	2-44μm	>44μm
OR7	9.4	19.8	ND	ND	50.4	20.4
OW19	2.7	7.9	ND	ND	37.5	51.9
OW31	.3	7.6	ND	ND	49.4	42.7
OW33	ND	ND	ND	ND	ND	ND
OW37	1.7	13.7	ND	ND	54.7	29.9
OW38	1.8	11.2	ND	ND	56.9	30.1

Table 25. Difference in Crystallinity Index from <.2μm to 2-44μm.

Sample #	Difference
OW1	.6
OW3	.8
OW5	2.42
OW7	3.55
OW8	1.4
OW9	.53
OW10	2.0
OW11	1.95
OW12	1.8
OW13	2.0
OW17	2.8
OW18	2.2
OW23	7.39
OW24	2.0
OW25	2.25
OW26	2.0
OW27	2.2
OW28	1.4
OW29	1.4

Table 26. Illite 002/001 Intensity Ratio for Georgia-Alabama Samples.

Sample #	<.2μm	.2-2μm	≤2μm	≤4μm	2-44μm
OW1	.53	.53	ND	ND	.5
OW3	.34	.37	.33	.34	.36
OW5	.35	.45	.53	.45	.40
OW7	.23	.38	.34	.38	.37
OW8	.30	.31	ND	ND	.35
OW9	.51	.49	.68	.50	.56
OW10	.31	.33	ND	ND	.32
OW11	.38	.49	.42	ND	.39
OW12	.25	.30	ND	ND	.35
OW13	.27	.40	.38	.42	.39
OW17	.41	.35	.41	.32	.39
OW18	.29	.34	ND	ND	.37
OW23	.25	.33	.27	.27	.38
OW24	.26	.33	.43	.33	.34
OW25	.37	.34	ND	.41	.42
OW26	.26	.37	.35	.28	.33
OW27	.25	.34	.36	.35	.30
OW28	.44	.48	ND	ND	.39
OW29	.44	.43	.48	.39	.37

Table 27. Illite 002/001 Intensity Ratio for Tennessee Samples.

Sample #	<.2μm	.2-2μm	≤2μm	≤4μm	2-44μm
OR7	.22	.35	.25	.26	.34
OW19	.26	.25	.29	.30	.26
OW31	.23	.23	ND	.33	.42
OW33	.25	.31	.23	.27	.32
OW37	.27	.22	ND	ND	.36
OW38	.26	.24	ND	.20	.36

Table 28. List of Equations of Least Squares Line (y on x) and Correlation Coefficients, v For All Relationships Having |C.C.| >0.7 <0.7. (First Variable Listed is y in Each Case.)

	COMPONENT	E.L.S.L.	C.C.
	2-44 micron fraction		
1.	Distance vs. Crystallinity Index	y = 33.33x + 1.33	.816
2.	Distance vs. Sharpness Ratio	y = -.33x + 25.38	-.819
3.	Percent Na_2O Distance	y = .02x + -.00	.877
4.	Percent Chlorite vs. Distance	y = .71x + 4.81	.861
5.	Percent Na_2O vs. Distance	y = .72x + .04	.782
6.	Percent Chlorite vs. Crystallinity Index	y = 29.18 + 4.99	.847
7.	$\frac{10\text{Å}}{7\text{Å}}$ vs. Sharpness Ratio	y = .02x + .10	.832
8.	Percent Illite vs. Sharpness Ratio	y = 2.27x + 18.97	.722
9.	001/002 Chlorite vs. Sharpness Ratio	y = .01x + .07	.749
10.	002/001 Illite vs. $\frac{10\text{Å}}{7\text{Å}}$	y = .47x + .05	.912
11.	Difference in <.2 to 2-44 vs. $\frac{10\text{Å}}{7\text{Å}}$	y = 17.86x + .48	.806
12.	Fraction Percentage vs. $\frac{10\text{Å}}{7\text{Å}}$	y = 73.83x + 9.33	.891
13.	Percent Illite vs. $\frac{10\text{Å}}{7\text{Å}}$	y = 70.13x + 6.48	.913
14.	001/002 Chlorite vs. $\frac{10\text{Å}}{7\text{Å}}$	y = .36x + .03	.945
15.	Percent Illite vs. 002/001	y = 146.45x + .10	.939
16.	Percent Chlorite vs. 002/001	y = 84.57x + 1.87	.802

Table 28 (Continued)

	COMPONENT	E.L.S.L.	C.C.
17.	002/001 Illite vs. 001/002 Chlorite	y = .73x + -.00	.988
18.	Difference of <.2 to 2-44 for Crystal Index vs. Percent Na_2O	y = 2.67x + .30	.764
19.	Percent Chlorite vs. Percent Na_2O	y = 34.46x + 5.98	.917
20.	Shift in 10Å vs. Difference in <.2 to 2-44 Cryst. Index	y = .06x + -.08	.773
21.	Percent Chlorite vs. Difference in <.2 to 2-44 Crystallinity Index	y = 8.44x + 8.70	.783
22.	001/002 Chlorite vs. Difference in <.2 to 2-44 Sharpness Ratio	y = .01x + .07	.739
23.	Percent Illite vs. Fraction Percentage	y = .89x + 2.96	.889
24.	Percent Chlorite vs. Fraction Percentage	y = .55x + 1.03	.832
25.	001/002 Chlorite vs. Fraction Percentage	y = .00x + -.00	.978
26.	001/002 Chlorite vs. Percent Illite	y = .00x + .01	.950
27.	001/002 Chlorite vs. Percent Chlorite	y = .01x + .04	.777
	.2-2 Micron Fraction		
1.	Distance vs. Crystallinity Index	y = 16.66x + 4.83	.796
2.	Sharpness Ratio vs. Distance	y = -.35x + 26.02	-.865
3.	Distance vs. 002/001 Illite	y = 1.97x + 190	-.760

Table 28 (Continued)

	COMPONENT	E.L.S.L.	C.C.
4.	Percent K_2O vs. Distance	y = .08x + 1.42	.735
5.	Distance vs. Fraction Percentage	y = 6.66x + -66.86	.704
6.	Distance vs. Percent Mixed-Layered Material	y = 1.30x + 20.16	.902
7.	Percent Chlorite vs. Distance	y = .42x + 2.06	.799
8.	Shift of 10Å vs. Crystallinity Index	y = .09x + -.09	.825
9.	Percent Mixed-Layered Material vs. Crystallinity Index	y = 9.25x + -3.50	.805
10.	Percent Chlorite vs. Chrystallinity Index	y = 5.71x + 4.84	.822
11.	Half Width Glycolated - Half Width Heated vs. Crystallinity Index	y = 1.19x + -1.85	.846
12.	Percent 2m Polymorph vs. Sharpness Ratio	y = 3.48x + 3.54	.922
13.	10Å/7Å vs. Sharpness Ratio	y = .08x + .18	.821
14.	002/001 Illite vs. Sharpness Ratio	y = .01x + .32	.789
15.	Percent Mixed-Layered Material vs. Sharpness Ratio	y = -1.62x + 35.43	-.761
16.	Percent Illite vs. Sharpness Ratio	y = 3.47x + 10.26	.881
17.	001/002 Chlorite vs. Sharpnexx Ratio	y = .01x + .06	.821
18.	10Å/7Å vs. 2m Polymorph Percentage	y = .01x + .21	.789
19.	Percent Illite vs. 2m Polymorph Percentage	y = .79x + 9.06	.843

Table 28 (Continued)

	COMPONENT	E.L.S.L.	C.C.
20.	001/002 Chlorite vs. 2m Polymorph Percentage	y = .00x + .05	.802
21.	002/001 Illite vs. 10Å/7Å	y = .18x + .09	.771
22.	Percent K_2O vs. 10Å/7Å	y = 2.14x + 1.37	.707
23.	Percent Illite vs. 10Å/7Å	y = 35.08x + 7.36	.879
24.	001/002 Chlorite vs. 10Å/7Å	y = .12x + .06	.753
25.	Percent K_2O vs. 002/001 Illite	y = 13.32x + .19	.944
26.	Percent Illite vs. 002/001 Illite	y = 164.09x + -.65	.901
27.	Percent Chlorite vs. 002/001 Illite	y = 47.37x + .55	.724
28.	001/002 Chlorite vs. 002/001 Illite	y = .66x + -.00	.969
29.	Fraction Percentage vs. Percent K_2O	y = 2.85x + .68	.865
30.	Percent Illite vs. Percent K_2O	y = 10.85x + 1.99	.840
31.	001/002 Chlorite vs. Percent K_2O	y = .05x + .00	.953
32.	Percent Chlorite vs. Fraction Percentage	y = 1.13x + .23	.805
33.	001/002 Chlorite vs. Fraction Percentage	y = .01x + .04	.769
34.	Half Width Glycolated-Half Width Heated vs. Shift in 10Å	y = 9.54x + -.30	.767
35.	001/002 Chlorite vs. Percent Illite	y = .00x + .03	.899
36.	001/002 Chlorite vs. Percent Chlorite	y = .01x + .05	.714

Table 28 (Continued)

	COMPONENT	E.L.S.L.	C.C.
<.2 micron fraction			
1.	Distance vs. Crystallinity Index	y = 14.28x + 7.14	.825
2.	Sharpness Ratio vs. Distance	y = .06x + 5.74	-.836
3.	Distance vs. 002/001 Illite	y = -1.11x + 120	-.721
4.	Percent K_2O vs. Distance	y = .07x + .91	.781
5.	Distance vs. Fraction Percentage	y = 16.68x + 13.5	.877
6.	Distance vs. Percent Mixed-Layered Material	y = 1.59x + 13.65	.771
7.	001/002 Chlorite vs. Distance	y = .01x + .08	.749
8.	Crystallinity Index vs. Percent K_2O	y = 1.47x + -1.59	-.728
9.	Fraction Percentage vs. Crystallinity Index	y = .60x + -.48	.776
10.	Percent Mixed-Layered Material vs. Crystallinity Index	y = 8.48x + -10.48	.863
11.	Half Width Glycolated-Half With Heated vs. Crystallinity Index	y = 1.22x + -2.75	.926
12.	002/001 Illite vs. Sharpness Ratio	y = .04x + .21	.723
13.	Percent K_2O vs. Sharpness Ratio	y = .98x + .75	.819
14.	Percent Na_2O vs. Sharpness Ratio	y = .15x + .05	.738
15.	Percent Illite vs. Sharpness Ratio	y = 17.31x + 10.53	.842
16.	001/002 Chlorite vs. Sharpness Ratio	y = .07x + .07	.716
17.	Percent Na_2O vs. 2m Polymorph Percentage	y = .03x + .06	.916

Table 28 (Continued)

	COMPONENT	E.L.S.L.	C.C.
18.	Percent Illite vs. 2m Polymorph Percentage	y = 1.75x + 9.50	.812
19.	Percent Chlorite vs. 2m Polymorph Percentage	y = .44x + .82	.834
20.	001/002 Chlorite vs. 2m Polymorph Percentage	y = .01x + .04	.839
21.	Percent K_2O vs. $10\text{Å}/7\text{Å}$	y = .69x + 1.02	.759
22.	Shift 10A vs. $10\text{Å}/7\text{Å}$	y = .04x + -.04	.851
23.	Percent K_2O vs. 002/001 Illite	y = 13.11x + .32	.421
24.	Percent Na_2O vs. 002/001 Illite	y = 1.64x + .01	.784
25.	Percent Illite vs. 002/001 Illite	y = 217.31x + 3.65	.908
26.	001/002 Chlorite vs. 002/001 Illite	y = 1.01x + .02	.872
27.	Percent Na_2O vs. Percent K_2O	y = .07x + -.00	.843
28.	Percent Illite vs. Percent K_2O	y = 14.62x + .16	.921
29.	001/002 Chlorite vs. Percent K_2O	y = .08x + .00	.912
30.	Percent Illite vs. Percent Na_2O	y = 81.58x + 10.73	.721
31.	Percent Chlorite vs. Percent Na_2O	y = 24.42x + .17	.907
32.	Half Width Glycolated-Half Width Heated vs. Mixed Layered	y = .11x + -.51	.793
33.	001/002 Chlorite vs. Percent Illite	y = .00x + .04	.813

BIBLIOGRAPHY

Bayley, B., 1968, Introduction to Petrology, Prentice-Hall, Inc., New York, 371 p.

Berry, R. and Jorgensen, P., 1969, Separation of Illite and Chlorite by Electromagnetic Techniques, Clay Minerals, V. 8, 201-212.

Berner, R. A., 1971, Principles of Chemical Sedimentology, McGraw-Hill, New York, 240 p.

Bodine, M. W., Jr., and Standaer, R. R., 1976, Chlorite and Illite Compositions from Upper Silurian Rock Salts Retsof, New York, Clays and Clay Minerals, V. 25, 57-71.

Bradley, W. F., 1953, Analysis of Mixed-Layer Clay Mineral Structures, Anal. Chem. V. 25, 727-730.

Brown, G., Ed., 1961, The X-ray Identification and Crystal Structures of Clay Minerals, Mineral Soc. London, 544 p.

Brown, B. E., and Bailey, S. W., 1962, Chlorite Polytypism:1, Regular and Semi-Random One Layer Structures, Am. Min. V. 47, 819-850.

Brown, B. E., and Bailey, S. W., 1963, Chlorite Polytypism: 2, Crystal Structure of a One-Layer Cr-chlorite. Am. Min. V. 48, 42-61.

Burst, J. F., 1959, Postdiagenetic Clay-Mineral Environmental Relationships in the Gulf Coast Eocene, Proc. 6th Nat'l. Conf. Clays and Clay Minerals, Nat. Res. Council Publ. 327-341.

Burst, J. F., 1969, Diagenesis of Gulf Coast Clayey Sediments and Its Possible Relationships to Petroleum Migration, Bull. Am. Assoc. Petro. Geol. V 53, 73-93.

Butts, C., and Gildersleeve, B., 1948, Geology and Mineral Resources of the Paleozoic in Northwest Georgia, Georgia Geological Survey Bull. N. 54.

Chowns, T. M., 1977, Stratigraphy and Economic Geology of Cambrian and Ordovician Rocks in Bartow and Polk Counties, Georgia. Georgia Geological Survey 12th Annual Meeting and Field Trip.

Colton, G. W., 1970, The Appalachian Basin-its Depositional Sequences and their Geologic Relationships, in Studies of Appalachian Geology pp. 5-48, Fisher et al., ed, 1970. Interscience Publishers, New York.

Cressler, C. W., 1963, Geology and Ground Water Resources of Catoosa County, Georgia, Georgia Geol. Surv. Inf. Cir. N. 28.

Cressler, C. W., 1964, Geology and Ground Water Resources of the Paleozoic Rock Area, Chattooga County, Georgia, Ga. Geol. Surv. Inf. Cir. N. 27.

Cressler, C. W., 1964, Geology and Ground Water Resources of Walker County, Georgia. Ga. Geol. Surv. Inf. Cir. N. 29.

Cressler, C. W., 1970, Geology and Ground Water Resources of Floyd and Polk Counties, Georgia. Ga. Geol. Surv. Inf. Cir. N. 39.

Cressler, C. W., 1974, Geology and Ground Water Resources of Gorden, Whitefield, and Murry Counties, Georgia. State of Georgia Dept. of Nat'l. Res. Inf. Cir., N27, Prepared in cooperation with the U.S. Geol. Surv.

Croft, M. G., 1953, Geology and Ground Water Resources of Bartow County, Georgia. Geol. Surv. Water Supply Paper 1619-FF.

Dunoyer de Segonzac, G., 1970, The Transformation of Clay Mimerals During Diagenesis and Low Grade Metamorphism-A Review, Elesevier Publishing Co., Amsterdam.

Dunoyer de Segonzac, G., and Abbas, M., 1976, Metamophisme des Argiles dan le Rhe'Tien des Alpes sud-occidentales. Sci. Geol. Bull. V. 29, 3-20.

Drever, J. I., 1971, Early Diagenesis of Clay Minerals, Rio Ameca Basin, Mexico. J. Sed. Pet. V. 41 982-994.

Eggleton, R. A., and Bailey S. W., 1967, Structural Aspects of Dioctahedral Chlorites. Am. Min. V. 52 673-689.

Epstein, Anita G., Epstein, J. B., and Harris L. D., 1976, Conodont Color Alteration-An Index to Organic Metamorphism. Geol. Surv. Prof. Paper 995, U.S. Gov. Print. Office, Washington.

Esquevin, J. 1969, Influence de la Composition Chimique des Illites Sur Leur Cristallinite. Bull. Centre Rech. Pav. 3, 147-154.

Fisher, G. W., Pettijohn, F. J., Reed, J. C., Jr., and Weaver, K. N., Ed., 1970, Studies of Appalachian Geology: Central and Southern. John Wiley and Sons, Inc. 460 p.

Folk, R. L., 1974, Petrology of Sedimentary Rocks; Hemphill Publishing Company, Austin, Texas, 182 pages.

Foscolos, A. E., and Kodama, H., 1973, Diagenesis of Clay Minerals from Lower, Cretaceous Shales of Northeastern British Columbia, Clays and Clay Minerals, V. 22, 319-335.

Foscolos, A. E., and Stott, D. F., 1975, Degree of Diagenesis, Stratigraphic Correlation and Potential Sediment Sources of Lower Cretaceous Shales of Northeastern British Columbia, Geol. Surv. of Canada, Bull. 250.

Foster, M. D., 1962, Interpretation of the Composition and Classification of the Chlorites, U.S. Geol. Surv. Prof. Paper 414-A, A 1-33.

Frey, M. 1969, A Mixed-Layer Paragonite/Phengite of Low Grade Metamorphic Origin, Contrib. Min. Petr. V. 24, 63-65.

Frey, M. 1970, The Step from Diagenesis to Metamorphism in Pelitic Rocks During Alpine Orogenesis. Sedimentology-Elsevier Publishing Co. Amsterdam.

Freund, J. E., 1970, Statistics a First Course; Prentice-Hall, Inc. Englewood Cliffs, New Jersey, 340 p.

Gavish, E., and Reynolds, R. C., 1970, Structural Changes and Isomorphic Substitution in Illites from Limestones of Variable Degree of Metamorphism, Israel J. of Chem. V. 8, 477-485.

Gieskes,J. M., and Kastner, M., 1975, Evidence for Extensive Diagenesis, Madagascar Basin, deep sea drilling site, 245. Geochimica Cosmochim Acta. V. 39, 1385-1393.

Gill, W. D., Khalaf, F. I., and Massoud, M. S., 1977, Clay Minerals and an Index of the Degree of Metamorphism of the Carbonate and Terrigenous Rocks in the South Wales Coalfield. Sedimentology, V. 24, 675-691.

Goddard, E. N., Trask, P. D., Deford, R. K., Rove, O. N., Stingewald, J. T. Jr. and Overbeck, R. M., 1963, Rock Color Chart. The Geological Society of Am. New York. Published by Huyskes-Enschede.

Grim, R. E., 1953, Clay Mineralogy, McGraw-Hill Book Co., New York, 596 p.

Grim, R. E., 1962, Applied Clay Mineralogy, McGraw-Hill Book Co., New York, 432 p.

Hadley, J. B., and Goldsmith, R., 1963, Geology of the Eastern Great Smoky Mountains, North Carolina, and Tennessee, U.S. Geol. Surv. Prof. Paper 349 b.

Hayes, J. B., 1970, Polytypism of Chlorite in Sedimentary Rocks. Clays and Clay Minerals, V. 18, 285-306.

Henderson, G. V. 1970, The Origin of Pryophyllite Rectorite in Shales of North Central Utah. Clays and Clay Minerals. V. 18, 239-246.

Horowitz, D. H., 1971, Diagenetic Significance of Color Boundry Between Juniata and Bald Eagle Formations, Pa. J. Sed. Pet., V. 41, 1134-1144.

Hower, J.,Hurley, P. M., Pinson, W. H., and Fairburn, H. W., 1963, The Dependence of K-Ar on the Mineralogy of Various Particle Size Ranges in a Shale. Geochimica Et. Cosmochimica Acta. V. 27, 405-410.

Hower, J., 1967, Order of Mixed-Layering in Illite/Montmorillonites. Clays and Clay Minerals. V. 15, 63-74.

Hower, J., Eslinger, E. V., Hower, M. E., and Perry, E. A. 1976, Mechanism of Burial Metamorphism of Argillaceous Sediments. 1. Mineralogical and Chemical Evidence. Bull. Geol. Soc. Am. V. 87, 725-737.

Hurst, V. J., and Schlee, J. S., 1962, Ocoee Metasediments North Central Georgia, Southeast Tennessee. Annual Meeting Southeastern Section The Geol. Soc. of Am. Guidebook N. 3.

Johns, W. D., Grim, R. E., and Bradley, W. F., 1954, Quantitative Estimations of Clay Minerals by Diffraction Methods. J. Sed. Pet. V. 44, 242-251.

Karpova, G. V., 1966, Paragonite Hydromicas in Terrigenous Rocks of the Great Donets Basin, Dokl. Akad. Nauk S.S.S.R. V. 171, 443-445.

Jackson, M. L., 1956, Soil Chemical Analysis-Advanced Course, Publ. by the Author, 2nd Ed. 9th Printing, Dept. of Soil Science, Univ. of Wisconsin, Madison, Wisconsin.

Johnson, L. J., 1964, Occurance of Regularly Interstratified Chlorite-Vermiculite as a Weathering Product of Chlorite in a Soil. Am. Min. V. 49, 556-572.

Kazi, A., 1975, Quantitative Fabric Analysis of Drammen Clay Using X-Ray Diffraction Techniques. J. Sed. Pet. V. 45, 883-890.

Kerr, P. F., 1959, Optical Mineralogy. McGraw-Hill Book Co., New York, 442 p.

Khitarov, N. I., and Pugin, V. A., 1966, Behavior of Montmorrillonite Under Elevated Temperatures and Pressures. Geochem. International 3 V. 4, 621-626.

Kisch, H. J., 1966, Chlorite-illite Tonstein in High Rank Coals from Queensland, Australia; Notes on Regional Epigenic Grade and Coal Rank. Am. J. Sci. V. 264, 386-397.

Kodama, H., 1958, Mineralogical Study on Some Pyrophyllites in Japan. Mineral J. Japan, V. 2, 236-244.

Kodama, H., and Brydon, J. E., 1965, Interstratified montmorillonite-mica clays for subsoils of the prairie provences, western Canada.

Kossovskaya, A. G., and Sutov, V. D., 1958, Zonality in the Structure of Terrigene deposits in platform and geosynclinal regions. Eclogae Geol. Helv, V. 51, 656-666.

Kossovskaya, A. G., and Shutov, V. D., 1963, The Correlation of Zones of Regional Epigenesis and Metagenesis in Terrigeneous and Volcanic Rocks. Dokl. Acad. Sci. U.S.S.R. Earth Sci. Sect. V. 139, 732-736.

Kossovskaya, A. G., and Shutov, V. D., 1965, Facies of Regional and Metagenesis. Intern. Geol. Rev. V. 7, 1157-1167.

Kubler, B., 1964, Les Argiles, Indicateurs de Metamorphisme. Rev. Inst. France Petrole, V. 19, 1093-1112.

Kubler, B., 1966, La Cristallinite d'illite et les Zones Tout a' Fait Superieur du Metamorphisme. Colloque sur les Etages Tectoniquesa' la Baconniere, pp. 105-122.

Liebling, R. S., 1976, Chlorite and Mica as Indicators of Depositionak Environment and Provenance. Geol. Soc. Am. Bull. V. 87, 513-514.

Lister, J. S., and Bailey, S. W., 1967, Chlorite Polytypism; 4. Regular Two Layer Structures. Am. Min. V. 52, 1614-1631.

Lovell, J.P.B., 1972, Diagenetic Origin of Graywacke Matrix Minerals; A Discussion. Sedimentology, V. 19, 141-143.

Lucas, J., and Ataman, G., 1968, Mineralogical and Geochemical Study of Clay Mineral Transformations in the Sedimentary Triassic Jura Basin, France. Clays and Clay Minerals, Proc. Natl. Conf. Clays Clays Minerals 16th, V. 5, 365-372.

Lydka, K. 1973, Mineralogical and Petrographic Index of Clayey Rock Alteration under Epigenetic Conditions. Przeglad Geologiczn y, Vol. 21, N. 10.

Mac Ewan, D.M.C., 1956, Fourier Transform Methods for Studying X-ray Scattering form Lamellar Systems, A Direct Method for Analyzing Interstratified Mixtures. Kolloid-Z V. 149, 96-108.

Maxwell, D. T., and Hower, J., 1967, High Grade Diagenesis and Low Grade Metamorphism of Illite in the Precambrian Belt Series. Am. Min. V. 52, 843-857.

Milici, R. G., Greenberg, S. S., and Jones, C., 1966, Paragonite Bearing Phyllites in the Central Virginia Piedmont. Southeastern Geol. V. 7, 111-120.

Miyashiro, A., and Haramura, H., 1966, Sedimentation and Regional Metamorphism in the Paleozoic Geosynclinal Pile of Japan. Reprint from Bull. of the Indian Geophysical Union N. 3, 45-55.

Moore, B. C., Lalicker, C. G., and Fisher, A. G., 1952, Invertebrate Fossils. McGraw-Hill Book Co. New York 766 p.

Muffler, L. J., and White, D. E., 1969, Active Metamorphism of Upper Ceneozoic Sediments in the Salton Sea Geothermal Field and the Salton Sea Trough, Southern California. Bull. Geol. Soc. Am. V. 80, 157-180.

Ostrom, M. E., 1961, Separation of Clay Minerals from Carbonate Rocks by Using Acid. J. Sed. Pet. V. 31, 123-129.

Perry, E. and Hower, J., 1970, Burial Diagenesis in Gulf Coast Pelitic Sediments. Clays and Clay Minerals V. 18, 165-177.

Perry, E. and Hower, J., 1972, Late Stage Dehydration in Deeply Buried Pelitic Sediments. Am. Assoc. Petr. Geol. Bull. V. 56, 2013-2021.

Powers, M. C., 1959, Adjustment of Clays to Chemical Change and the Concept of Equivalence Level. Proc. Natl. Conf. Clays Clay Minerals, 6th Natl. Acad. Sci. Natl. Res. Council Publ. 309-326.

Powers, M. C., 1967, Fluid Release Mechanisms in Compacting Marine Mudrocks and their Importance in Oil Exploration: Am. Assoc. Petrol. Geol. Bull. 51, 1240-1253.

Reynolds, R. C., 1967, Interstratification Clay Systems; Calculations of the Total One-Dimensional Diffraction Function. Am. Min. V. 52, 661-672.

Reynolds, R. C., 1968, The Effect of Particle Size on Apparent Lattice Spacings, Acta. Crystallogr. A. 24, 319-320.

Reynolds, J. C., Jr., and Hower, J., 1970, The Nature of Interlayering in Mixed-Layer Illite Montmorillonites. Clays and Clay Minerals V. 18, 25-36.

Sarkissyen, S. G., 1972, Origin of Authigenic Clay Minerals and their Significance in Petroleum Geology. Sed. Geol. V. 7, 1-22.

Schultz, L. G., 1964, Quantitative Interpretation of Mineralogical Composition from X-ray and Chemical Data for the Pierre Shale. U.S. Geol. Surv. Prof. Paper 391C CL-C31.

Shirozu, H. and Bailey, S. W., 1965, Chlorite Polytypism; 3. Crystal Structure of an Orthohexagonal Iron Chlorite. Am. Min. V. 50, 868-885.

Slaughter, M. and Milne, I. H., 1960, The Formation of Chlorite-like Structures from Montmorillonite. Clays and Clay Minerals. V. 7, 114-124.

Smith, J. V., and Yoder, H. S., 1956, Studies of Mica Polymorphs. Min. Mag. V. 31, 209-235.

Teodorovich, G. I., and Konyukhov, A. I., 1970, Mixed-Layer Minerals in Sedimentary Rocks as Indicators of Depth of their Catagenetic Alteration. Dokl. Akad. Nauk. SSSR, V. 191, 194-196.

Till, R. and Spears, D. A., 1969, The Determination of Quartz in Sedimentary Rocks Using an X-ray Diffraction Method, Clays and Clay Minerals. V. 17, 323-327.

Tower, K. M., 1962, Diagenesis of Clay Minerals as a Possible Source of Silica Cement in Sedimentary Rocks, J. Sed. Pet. V. 32, 26-28.

Van Moort, J. C., 1971, A Comparative Study of the Diagenetic Alteration of Clay Minerals in Mesozoic Shales from Papau, New Guinea and Tertiary Shales form La. U.S.A. Clays and Clay Minerals, V. 19, 1-20.

Velde, B., and Hower, J., 1963, Petrological Significance of Illite and Polymorphism in Paleozoic Sedimentary Rocks, Am. Min. V. 48, 1239-1254.

Weaver, C. E., 1958, The Distribution and Identification of Mixed-Layer Clays in Sedimentary Rocks. Am. Min. V. 41, 202-221.

Weaver, C. E., 1958, The Effects and Geologic Significance of Potassium "fixation" by Expandable Clay Minerals Derived from Muscovite, Biotite, Chlorite, and Volcanic Material. Am. Min. V. 43, 839-861.

Weaver, C. E., 1958, Origin and Significance of Clay Minerals in Sedimentary Rocks. A.A.P.G., V. 42, N. 2.

Weaver, C. E., 1958, Geologic Interpretation of Argillaceous Sediments. Bull. Am. Assoc. Petrol. Geol. V. 42, 254-309.

Weaver, C. E., 1959, The Clay Petrology of Sediments. Clays and Clay Minerals, Pergamon Press, New York, 154-187.

Weaver, C. E., 1960, Possible Uses of Clay Minerals in Search for Oil. Bull. Am. Assoc. Petrol. Geol. V. 44, 1505-1518.

Weaver, C. E., 1961a Minerals of the Ouachita Structural Belt and Adjacent Foreland in the Ouachita System. Bur. Econ. Geol. Publ. 6120-147-162.

Weaver, C. E., 1961b Clay Mineralogy of the Late Cretaceous Rocks of the Washakie Basin. Wyoming Geol. Assoc. Guidebook, 16th Field Conf. 148-154.

Weaver, C. E., 1965, Potassium Content of Illite, Science, 147, 603-605.

Weaver, C. E., 1967, Potassium, Illite, and the Ocean. Geochim. et. Cosmochim. Acta. V. 31, 2181-2196.

Weaver, C. E., and Wampler, J. M., 1970, K, Ar, Illite Burial. Bull. Geol. Soc. Am. V. 81, 3423-3430.

Weaver, C. E., and Beck, K. C., and Pollard, C. O., 1971, Clay Water Diagenesis During Burial; How Mud Becomes Geniss. Geol. Soc. Am. Spec. Paper 134, 1-78.

Weaver, C. E., and Pollard, L. D., 1973, The Chemistry of Clay Minerals. Elsevier Scientific Publishing Co., New York, 213 p.

Weber, K., 1972, Notes on Determination of Illite Crystallinity. N. Jb., Miner. Mh. 267-276.

Yoder, H. S., and Eugster, H. P., 1955, Synthetic and Natural Muscovites. Geochim. et. Cosmochim. Acta. V. 8, 225-280.

Zen, E. A., 1960, Metamorphism of Lower Palezoic Rocks in the Vicinity of the Jaconic Range in West-Central Vermont. Am. Min. 45, 129-175.

Zen, E. A., 1974, Burial Metamorphism. Canadian Mineralogist. V. 12, 445-455.